STOCHASTIC PROGRAMMING APPROACH TO HYDRAULIC FRACTURE

DESIGN FOR THE LOWER TERTIARY GULF OF MEXICO

A Thesis

by

SETH PODHORETZ

Submitted to the Office of Graduate Studies of
Texas A&M University
in partial fulfillment of the requirements for the degree of

MASTER OF SCIENCE

Chair of Committee,   Robert Lane
Co-Chair of Committee, Peter Valkó
Committee Member,   Benchun Duan

Head of Department,   Daniel Hill

August 2013

Major Subject: Petroleum Engineering

ABSTRACT

In this work, we present methodologies for optimization of hydraulic fracturing design under uncertainty specifically with reference to the thick and anisotropic reservoirs in the Lower Tertiary Gulf of Mexico. In this analysis we apply a stochastic programming framework for optimization under uncertainty and apply a utility framework for risk analysis.

For a vertical well, we developed a methodology for making the strategic decisions regarding number and dimensions of hydraulic fractures in a high-cost, high-risk offshore development. Uncertainty is associated with the characteristics of the reservoir, the economics of the fracturing cost, and the fracture height growth. The method developed is applicable to vertical wells with multiple, partially penetrating fractures in an anisotropic formation. The method applies the utility framework to account for financial risk.

For a horizontal well, we developed a methodology for making the strategic decisions regarding lateral length, number and dimensions of transverse hydraulic fractures in a high-cost, high-risk offshore development, under uncertainty associated with the characteristics of the reservoir. The problem is formulated as a mixed-integer, nonlinear, stochastic program and solved by a tailored Branch and Bound algorithm. The method developed is applicable to partially penetrating horizontal wells with multiple, partially penetrating fractures in an anisotropic formation.

DEDICATION

I dedicate this work to my parents, my sisters, and all my kin.

ACKNOWLEDGEMENTS

TABLE OF CONTENTS

CHAPTER

LIST OF FIGURES

LIST OF TABLES

CHAPTER I

INTRODUCTION AND LITERATURE REVIEW

Introduction

With current world energy demand reaching all times high, operators have pushed the limits of hydrocarbon exploration and production to ever-deeper waters and increasingly more hostile environments. For publicly owned companies, the search has additional geopolitical and geographic constraints limiting the areas of production. This has led exploration departments from a large number of exploration and production companies to the deepwater Gulf of Mexico, Lower Tertiary, Paleogene, Wilcox sands.

The Wilcox formation contains upwards of 25 billion barrels of oil and by many is considered the final frontier in the Gulf (Lewis et al. 2007, Lach and Longmuir 2010). The high exploration success has led to a high degree of certainty of hydrocarbon presence (Mathur 2008). Its location under US federal waters means that geopolitical risks are minimized.

However, at water depths approaching 10,000 ft, total formation depths of 30,000 ft, and overpressured reservoirs, significant technological constraints limit the design, completion, and production of developmental wells. Furthermore, commercial production requires high wellbore productivity to balance upfront initial costs. Current industry conjecture suggests that anticipated wellbore productivities are orders of magnitude lower

than previously found in the Gulf of Mexico. A major factor of the low wellbore productivity is low permeability.

One especially attractive method for wellbore improvement in these fields is hydraulic fracturing (Dusterhoft, Strobel, and Szatny 2012). As many of the producing reservoirs in the Gulf of Mexico (GOM) are unconsolidated, high-permeability sandstones, generally requiring single zone-frac-pack completions, hydraulic fracturing for productivity in the GOM is still a new mindset (Haddad, Smith, and Moraes 2012).

 Massive hydraulic fracturing is a costly operation, particularly offshore where logistic constraints and exorbitant rig rates add significant financial risk. Cost estimates are uncertain with highly variable nonproductive time. Limited production from analogous fields coupled with monumental appraisal drilling costs result in *certain* uncertainty in key reservoir and fracture design parameters. New tools and methodologies are needed for design and optimization of hydraulic fracturing in this high-risk environment.

The objective of this work was to provide new approaches to fracture design for thick anisotropic reservoirs with uncertainty in reservoir parameters in the face of limited data and with significant financial risk as a result of reservoir depth and remoteness.

Deep-water Lower Tertiary Background

The majority of current Gulf of Mexico production comes from the Micocene trend, which has had significant appraisal and development since the mid-1990s. As the Micocene trend exploration success dwindled in the 2000s, few geologists expected to find new oil in the Gulf, especially in older sediments. However, in 2001, Shell's exploratory well Baha No. 1, located in the Alaminos Canyon Block 857, drilled through 4,500 ft of reservoir quality turbidite sands containing a 12-ft oil zone. Follow-up drilling in the Alaminos Canyon led to Wilcox discoveries of the Trident and Great White fields. Simultaneously, BHP Billiton discovered the Chinook formation in the Wilcox sands, located in Walker Ridge Block 206 (Wiltgen 2008).

These discoveries motivated continued exploration in the Lower Tertiary. To date 12 discoveries have been made out of 19 wells drilled, indicating high probability of exploration success (Mathur 2008). The established trend encompasses 34,000 square miles from Alminos Canyon, Keathley Canyon and Walker Ridge. Current geologic interpretation suggests the formations are thick turbidite sands with trap styles consisting of compressional Louann salt-cored symmetrical box folds, symmetrical salt pillows, and asymmetrical salt-cored thrust anticlines (Lewis et al. 2007).
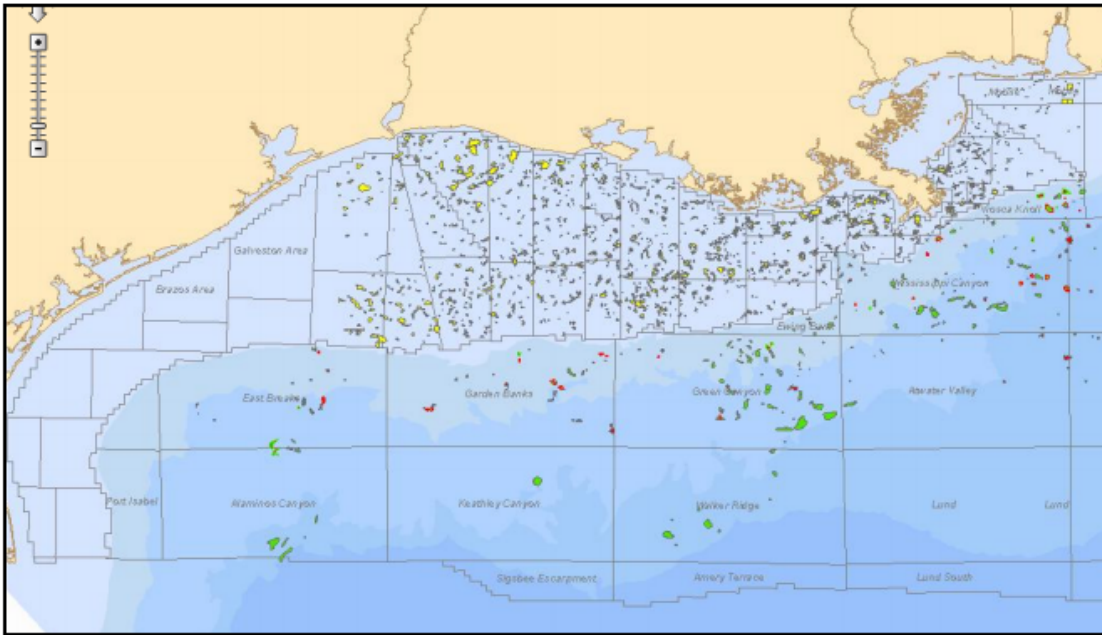
Fig. 1.1. Gulf of Mexico trend

The main technical challenges in the formations are water depth, reservoir depth, high temperatures and pressures, low permeability, and high viscosity. General reservoir properties are shown in Table 1.1 Furthermore, Fig. 1.1 shows the reservoir locations that are generally remote. Limited infrastructure exists, and lack of ultradeepwater drilling rigs presents additional operational challenges and constraints (Cunha et al. 2009).

Table 1.1 General Properties of the Lower Tertiary

Water Depth (ft)	7000-10000	Permeability (md)	5-25
Depth (ft)	25000-30000	Gravity (API)	20-30
Effective Porosity (%)	0.15-.20	GOR (cfb)	300-500
Gross (ft)	1000-1500	Viscosity (cp)	3.0-20.0
Net/Gross (%)	50	Bubble Point (psi)	1000-2000
Temperature (°F)	200-250	Formation Volume Factor (Rb/Stb)	1.1-1.2
Initial Pressure (psi)	20000-25000	Water Saturation (%)	0.2-0.3

A key feature of the trend is that the reservoirs are thick and layered with much lower

permeability than previous Gulf of Mexico Shelf and Miocene plays. Furthermore, some

formations have effectively zero vertical permeability. Many have suggested that

hydraulic fracturing may be the key to economic production (Haddad, Smith, and Moraes

2012, Dusterhoft, Strobel, and Szatny 2012, Ogier et al. 2011, Cunha et al. 2009). Given

the thickness of the reservoirs and limits on fracture height growth, partial fracture

penetration must be accounted for. This work proposes an efficient semi-analytical

method to determine productivity for partial penetration fractures in anisotropic media

using the distributed volumetric source method. The flexibility of this method and its

computational robustness will be shown to be vital for sensitivity analysis and

optimization purposes.

Currently, the most complex producing well in the lower tertiary is Petrobras's CA003

located in the Cascade formation in Walker Ridge Block 249 (Ogier et al. 2011). The

CA003 is a 17° deviated well with 3 stacked vertical hydraulic fractures. The well

encountered numerous mechanical problems during the lower completion phase, resulting

in 25 days of nonproductive time (NPT) (Ogier et al. 2011). For offshore operations, economic costs are significantly impacted by the spread rate, which is the daily cost of renting and operating a drilling rig, Currently, the spread rate is $1 million+, and combined with nearly 25 days of NPT, this easily added an additional $25 million to well costs. To date no horizontal wells have been drilled into the formations. Financial risks from NPT and hostile operating conditions are nontrivial and must be accounted for in the design phase of development.

Decisions regarding an offshore project must be made well before a significant amount of information is realized. Appraisal drilling is costly and only reveals limited information about the entirety of a reservoir. For the Lower Tertiary, the uncertainty is even greater as production data is almost nonexistent. Cost estimates carry significant risk factors as operations at these depths and pressures are novel. These obstacles present a formidable task for the completion engineer attempting to design an optimal wellbore. New tools are needed to account for the uncertainty in reservoir properties and economic risks apparent with increasing complexity of operations. This work proposes new methodologies for tackling these problems, including the application of stochastic programming for design under uncertainty and the application of utility theory to account for risk.

Research Objectives

The overall objectives of this study were:

- To develop an efficient model for optimal fracturing design for partially penetrating fractures in anisotropic and multilayer formations by applying the distributed volumetric source method.

- To develop a stochastic programing framework for fracture design under economic and reservoir uncertainty. The development included a two-stage stochastic program with simple recourse and a two-stage stochastic program with full recourse.

- To apply utility theory for risk quantification in optimization and design of fracture treatments.

- To combine the above-mentioned methods for fracture design and optimization for developmental wells in the Gulf of Mexico Lower Tertiary trend.

Literature Review

The literature review focuses on three distinct topics that are paramount to this work. The first subject is a review of hydraulic fracturing theory; the second subject is a review of the work done in stochastic modeling and optimization; and the third subject is a review of utility theory analysis pertaining to the petroleum industry.

Performance of Various Wellbore/Hydraulic Fracture Configurations

Hydraulic fracturing is a stimulation technique used to increase the productivity of a wellbore. It involves pumping high-pressure liquid carrying proppant to induce fractures into petroleum-bearing rocks. The high-pressure liquid serves to create and propagate fractures while the proppant serves to prop the induced fracture open. Hydraulic fracturing began in the petroleum industry in 1947 and is one of the most studied topics in petroleum engineering. A review of the fundamental theory is given in this section.

Prats (1961) investigated the effect of propped vertical fractures. He introduced the effective wellbore radius concept, suggesting that a larger hypothetical wellbore radius can represent the fracture. He introduced the parameter of *fracture conductivity* that is the product of fracture permeability and thickness.

Gringarten (1974) developed a mathematical models to investigate infinite conductivity and uniform flux vertical fractures in infinite and bounded reservoirs. These models present semianalytical solutions for the pressure distribution created by the fracture via Green's function.

Cinco, Samaniego, and Dominguez (1978) developed a mathematical model to investigate the transient pressure response of a finite-conductivity vertical fracture in an infinite-slab reservoir. They introduced the parameter of dimensional fracture conductivity.

Mukherjee and Economides (1991) investigated horizontal wells with transverse hydraulic fractures. They introduced the choke skin effect to account for the radial convergent flow that occurs in horizontal wells with transverse fractures.

Raghavan, Chen, and Agarwal (1997) developed a mathematical model to investigate the response of a horizontal well with multiple fractures. They presented correlations to determine long-term pressure performance and analytical procedures to evaluate pressure measurements in a horizontal well with multiple fractures.

Valko and Economides (1998) introduced the concept of the proppant number as an optimization method for designing hydraulic fracture treatments. They demonstrated that there is an optimal fracture geometry for a given reservoir and proppant mass that corresponds to a maximum gain in wellbore productivity.

Wattenbarger et al. (1998) noted that for low-permeability reservoirs, the pressure response of a fractured system may never reach pseudosteady state. They developed an analytical expression for the transient dimensionless production rate.

Romero, Valko, and Economides (2002) extended the work done by Valko and Economides (1998) to include the effect of fracture face and choke skin for optimization proposes. They used Ozkan's influence functions and a boundary element method to

calculate pseudosteady-state performance of a vertical well with a fully penetrating fracture.

Valko and Amini (2007) introduced the distributed volumetric source (DVS) method for calculating the productivity index for various well-fracture configurations including fully and partially penetrating hydraulically fractured vertical wells with uniform flux, infinite conductivity, and finite conductivity in an anisotropic homogenous reservoir. The DVS approach is an efficient method that provides the productivity index and well testing derivative in transient and pseudosteady-state flow regimes.

Uncertainty Analysis and Stochastic Modeling

Stochastic models are used when parameters in the problem data are uncertain. In the field of petroleum engineering, uncertainty is natural as it is impossible to measure or *see* the entire reservoir or to predict future costs and prices. Stochastic models carry increasing complexity and computational burden by their nature, as a large or even infinite numbers of possible outcomes can be realized from a number of uncertain variables.

Stochastic modeling in the petroleum industry dates back to the 1960s, however, it wasn't until the 1990s that stochastic modeling gained rapid popularity and usage, largely with the advent of high performance computing. This rebirth, founded by geoscientists, was mainly due to the realization that many problems such as the architecture of flow units and the spatial distribution of rock properties could not be adequately addressed without

the use of probabilistic models (Yarus and Chambers 1994). Stochastic modeling took off in the geoscience communities under the guise of *geostatistics* and is now a fundamental aspect of the field.

Throughout the past 20 years, stochastic modeling has evolved from the geosciences to the reservoir management field. Instead of simply portraying a number of possible realizations, the reservoir manager seeks to make decisions such as wellbore placement, production strategies, pipeline infrastructure, etc. under uncertainty. This highlights an often-confused distinction between stochastic models and methods (Haldorsen and Damsleth 1990): a stochastic *model* describes a statistical distribution while a *method* operates on a model.

Currently, a well-accepted model for optimization in the petroleum industry is Monte Carlo sampling. Monte Carlo sampling is the repeated random selection of variables from a distribution. For optimization purposes, the Monte Carlo method revolves around fixing design variables, random sampling of uncertain parameters, and continued iteration of each to generate probability distributions of outcomes. An important aspect of the Monte Carlo method for optimization is the initial guess of first-stage design variables. If the guess is not *good* a large number of iterations may be required to reach optimal design parameters.

A clear distinction should be made between Monte Carlo sampling and Monte Carlo sampling with optimization. Monte Carlo sampling is a statistical method for generating plausible outcomes while Monte Carlo sampling with optimization involves the same sampling method but also seeks to optimize decision variables by iterative processes.

The Monte Carlo method has been widespread in the petroleum industry for sampling and optimization purposes. Literally, thousands of papers exist in the petroleum industry on the use and application of the Monte Carlo method. Below selected reference will be given showing the breadth and popularity of the Monte Carlo method in all aspects of petroleum engineering.

Stoian (1965) outlined the fundamentals and application of the Monte Carlo method and it application to the petroleum industry. Reed (1972) applied Monte Carlo for drilling optimization. Hughes and Murphy (1988) applied the Monte Carlo method to simulate unstable miscible and immiscible flow through porous media. Dear III, Beasley, and Barr (1995) applied Monte Carlo sampling to optimize mud system design. Zhang and Srinivasan (2005) used Monte Carlo for modeling permeability variation. Kabir et al. (2007) applied Monte Carlo sampling to well count decision making under uncertainty for gas/condensate reservoirs. Dong, Holditch, and McVay (2013) applied Monte Carlo sampling for resource evaluation in shale gas reservoirs.

An alternative and less used model for optimization is the stochastic programming model. Stochastic programs are models that explicitly seek to maximize an object function subject to constraints on functions of variable randoms. The stochastic model does not require fixed inputs of first-stage parameters or random sampling of uncertainty. The stochastic program implicitly searches over the entire range of design variables to find an optimum solution honoring all constraints.

The origins of stochastic modeling date back to the work of Dantzig (1955). Currently stochastic programing has found widespread use in the finance industry, the distribution sector, the aviation industry, the agriculture industry, and so forth. Stochastic programing in the petroleum industry has largely been driven from the reservoir management perspective. Well placement optimization has been the major application of stochastic programs from the reservoir engineering discipline where uncertainties reveal themselves on the grid-block scale of the simulator. The main objectives of these programs are to optimize the exact location and number of wells for a specific reservoir. These are generally computationally expensive programs with numerous (even prohibitive) full-scale simulations required. There also has been significant work with stochastic programing in planning infrastructure for offshore developments. The objectives of these programs are to optimize the locations of production facilities, pipelines, and well locations. Generally, these programs use a simple or surrogate reservoir model as opposed to full-scale reservoir simulation. An extensive literature review for stochastic optimization is given below.

Haugland, Hallefjord, and Asheim (1988) applied a mixed-integer programming model to optimize the net present value (NPV) for an offshore oilfield development. They optimized the number of wells, the timing of the drilling program, and the production profile to meet facility capacity. They did not account for uncertainties in the reservoir or fluid parameters but did include price uncertainty in the sensitivity analysis.

Jonsbraten (1998) applied a mixed-integer stochastic program to optimize the expected NPV regarding offshore oilfield development. They extended the work of Haugland, Hallefjord, and Asheim (1988) but explicitly optimized the number of wells and location, the timing of the drilling program, the platform capacity, and the production profile under uncertain future oil prices. They directly optimized the variables for maximum expected NPV.

Goel and Grossmann (2004) applied a stochastic program to facilitate decision making for offshore gas field development. The decisions they optimized on were the location and number of wells, the location and capacity of the production platform, and the number and location of pipeline connectors. Their objective function was the expected NPV, and the uncertainties were the size and deliverability of the fields. They approached the problem from the surface/process engineering prospective and used a simple linear model to describe the reservoir.

Guyaguler and Horne (2004) addressed geological uncertainty for well placement optimization. They use a hybrid genetic algorithm (GA) to determine the optimal well locations. Their method works as follows: the GA selects a well location and numerical simulation is carried out on a random selection of selected realizations of uncertain parameters. If the selection is feasible, the GA will revisit the well location with another set of realizations. The GA revisits the location with higher resultant outcomes and determines an *apparent* optimum.

Guyaguler and Horne provide valuable insight into the problem of well placement under uncertainty by showing that the optimum location found by the algorithm never coincides with the truth-case optimum location. This is because the truth-case (deterministic) is never known. They show that the optimum location depends on the amount of risk the decision maker is willing to take. They apply utility theory to address the risk involved with different possible realizations.

Ozdogan and Horne (2006) extended upon the work of Guyaguler and Horne (2004) to address the time-dependent uncertainty for well-placement optimization. They approach the well-placement problem sequentially, using time-dependent information to improve decision making and expected NPV. They used the production profiles from initial wells to determine the location of new wells. They proposed a pseudo-history method that recursively updates history matches in an effort to better predict actual well performance.

Tarhan, Grossmann, and Goel (2009) developed a stochastic program for planning offshore oil field infrastructure under decision-dependent uncertainty. They optimized the location and capacity of the production facility, the number and drilling schedule of wells, and specific production strategies. They extended upon the work of Goel and Grossmann (2004) by including a nonlinear reservoir model that accounts for water breakthrough. They considered uncertainty in the maximum oil rate, the recoverable oil, and water-breakthrough time. They emphasized the importance of decision-dependent uncertainty or uncertainty that is realized from the decisions made.

Ettehad, Jablonowski and Lake (2011) formally introduced stochastic programming as a method to optimize offshore gas field developments under uncertainty. They applied a linear stochastic two-stage program with recourse. They used a gas-tank model with two compartments to model the reservoir. The constraints include maximum well production rate, facility capacity, and compressor power requirements. Their objective function is maximization of expected NPV. The first-stage decisions in their model include the number of wells to drill, facility capacity, and compressor power. The second-stage decisions in their model are operating conditions and production schedule. They introduced uncertainties in original gas in place and transmissibility between reservoir compartments. The uncertainties are realized after the first-stage decision has been made. Ettehad et al. compared the stochastic program to a Monte Carlo optimization scheme and noted the robustness of the stochastic solution in terms of computational efficiency and

flexibility. This appears to be the only application of a formal stochastic program with recourse in the Society of Petroleum Engineers literature.

As shown above, there is a breadth of literature concerning the well-placement problem and the infrastructure-planning problem. However, only three papers in the literature address wellbore completion/stimulation under uncertainty.

Wehunt (2006) discussed the use of probabilistic methods for predicting well performance under uncertainty. He presented tabulated values of skin and constructed a cumulative density function for different completion types. He coupled these uncertainties in reservoir parameters and used Monte Carlo sampling to probabilistically predict well productivity. He did not provide an optimization procedure but showed the use of historical values of skin for probabilistically predicting future performance.

Ouyang (2007) discussed the role of uncertainty on well performance for oil wells with different completion types. He used commercial completion software and discussed the sensitivities using different completion types. He did not offer any guidance on optimization or design under uncertainty but simply presented data on his specific case.

Birchenko et al. (2008) investigated the impact of reservoir uncertainty on horizontal well completions with inflow-control devices (ICDs) with inflow-control valves. They presented probabilistic results from different geological realizations of wells with inflow

control devices. They concluded that ICDs increase mean recovery and limit risk. However, they did not offer an optimization methodology but just presented specific data for a specific case.

As seen from the above summary, optimization of fracture design under uncertainty is still uncharted territory. This is the main motivation of this work. To approach the problem, following the style of Ettehad et al. (2011), the classical theory of stochastic programming with recourse was applied. A brief review of stochastic programming with recourse is given below.

The first stochastic program was developed by Dantzig (1955). This pioneering work set forth the basic modeling for the two-stage stochastic program with recourse. He provided a framework to optimize decisions made in a number of stages with each decision stage dependent on the last and ending with a random outcome. This work provided a procedural formulation to solve linear programs containing stochastic input. The motivation of this work was to optimize the allocation of a carrier fleet to meet anticipated but uncertain demands.

Raiffa and Schlaifer (1961) developed the concepts of *opportunity loss* and the *expected value of perfect information* in decision theory analysis. Opportunity loss is quantification of the consequences of an action made without perfect knowledge of a future outcome. It explicitly measures the value of a suboptimal decision made before a specific realization

of a future outcome and the optimal decision concerning the exact future outcome. They

extend this work to determine the expected value of perfect information or the worth of

complete information regarding a future outcome. This is the value a decision maker

would pay for complete information about a specific future realization.

Madansky (1960) and Mangasarian and Rosen (1964) expanded Raiffa's (1961) work by

providing the bounds of the expected value of perfect information for stochastic linear and

nonlinear programs respectively. This information provides the potential worth of more

accurate predictions of future outcomes and is a useful measure when deciding if more

data gathering is worthwhile.

Birge (1982) noted that, in certain situations, it is impossible to gain further information

about the future. He introduced a new measure, *the value of the stochastic solution,* which

is the value of solving the more complex stochastic solution versus the simpler mean-

value solution. The mean-value problem uses the expected value of an uncertain variable

in a sole deterministic program. He demonstrated by Jenson's (1906) inequality that the

solution obtained by the stochastic program is always equal to the solution obtained from

the mean-value program.

The expected value of perfect information and the value of the stochastic solution are the

fundamental motivations for the use of stochastic programming. The values have direct

application to the petroleum industry. The expected value of perfect information may be

used when determining if further appraisal drilling or more core sampling is warranted. The value of the stochastic solution demonstrates that using averages or expected values for modeling and design purposes may result in suboptimal design. For example, as will be shown in this work, the use of an average permeability as opposed to a distribution of permeability for fracture design will result in a suboptimal design when uncertainty exists.

The stochastic program with recourse will be used extensively in this work as applied to fracture and wellbore design under reservoir and economic uncertainties.

In decision analysis a common optimization variable is the expected NPV. However, as noted by many, expected NPV in itself does not capture the inherent risk (Campbell, Campbell, and Brown 1999, Begg, Bratvold, and Campbell 2001, Guyaguler and Horne 2004, Newendorp 1978, Esmaiel and Heeremans 2006). An alternate metric for optimization is *utility*, which is a quantitative measure of the decisions makers' comparative preference to different asset values.

The numerical concept of utility was introduced by von Neumann and Morgenstern (1944) in their pioneering work and brought into the petroleum industry by Newendorp (1967). The utility function represents a quantitative description of the decision maker's preference. The motivation of utility theory is in the fact that different decisions may have the same expected value but possibly radically different ranges in regard to the possibility

20

of different outcomes. A literature review of the applications of utility theory in the petroleum literature is given below.

Newendorp and Root (1967) introduced utility theory to quantify the risk inherent with different drilling investments. They demonstrated that decision makers have different levels of tolerance for profits and losses. He directly applied utility theory to account for the difference level of risk decisions makers were willing to take for deciding when to drill, not drill, or farm out.

Cozzolino (1977) reinforced the concepts of utility shown by Newendorp and Root (1967) in the language of von Neumann and Morgenstern. He investigated the use of the exponential utility function again with application for drilling investments. He also introduced the risk-aversion criteria first shown in the mathematical literature by Pratt (1964).

Harrison (1982) applied utility theory for decisions regarding fishing operations. He applied probabilistic distributions for the expected utilities of successful and unsuccessful fishing operations. He used a linear utility function for the expected cost relationship and derived distributions from historical data on fishing operations.

Walls (1995) provided a thorough overview of corporate risk tolerance and capital allocation. He investigated risk tolerance levels and provided a holistic approach to capital

budgeting decision. He highlighted inadequacies of solely using decision metrics such as the NPV and internal rate of return. He discussed the use of an exponential utility as a consistent measure of value for varying investments.

Guyaguler and Horne (2004) applied utility theory in the optimization of well placement under geological uncertainty. They used a theoretical exponential utility function with regards to expected NPV. They showed multiple optimum locations based on the decision makers' preference to risk.

Yu et al. (2011) applied utility theory for quantitative decision analysis regarding optimal drilling practices. They formulated a multivariate utility function to account for economics, environmental impacts, perception, and safety of the drilling process. They developed an approach to optimize drilling technology selection for numerous preferences associated with a range of attributes. This work encompassed various industry and government sources, indicating increasing interest in the applications of utility to the oil and gas industry.

Utility theory has been applied to various applications in the petroleum industry from drilling to well placement. The theory is well accepted in the industry with dedicated chapters in numerous texts [Newendorp (1978) , Mian (2011)]. However, the theory has never been directly applied to completion design or-specifically-to fracture design. This work is intended to fill the gap.

CHAPTER II

THEORY AND BASIC CONCEPTS

Darcy's Law

The fundamental equation governing fluid flow through porous media is Darcy's (1856) law, which states that the flux is proportional in magnitude to the pressure gradient of the potential field.

$$\mathbf{v} = \frac{k\rho}{\mu}\nabla\Phi \quad\text{...}\quad (2.1)$$

where k is the permeability, ρ is the fluid density, μ is the fluid viscosity, and Φ is the flow potential. The flow potential is defined as the work required to transfer a unit mass of liquid from rest to standard state in porous media.

$$\nabla\Phi = \int_{p'}^{p}\bar{v}dp + gz + \frac{\bar{u}^2}{2}\quad\text{...}\quad (2.2)$$

where $\bar{v}$ is the specific volume, g is the gravitational constant, z is the height (above datum), p is pressure, and $\bar{u}$ is the average microscopic velocity. Neglecting the kinetic and gravitational energy term for an incompressible fluid, Darcy's law can be written as Eq. 2.3.

$$\mathbf{v} = \frac{k\rho}{\mu}\nabla p \quad\text{...}\quad (2.3)$$

The Diffusivity Equation

The 3-dimensional mass balance in vector notation yields

$$\nabla \cdot (\rho\mathbf{v}) = \frac{\partial(\phi\rho)}{\partial t}\quad\text{...}\quad (2.4)$$

where ϕ is porosity and t is time. The equation of state for a slightly compressible fluid is given by

$$\rho = \rho_0[1 + c(p - p_0)] \quad\text{..}\quad (2.5)$$

where c is compressibility.

For anisotropic media the permeability will be different in each direction. The hydraulic diffusivity η can be expressed as

$$\eta_i = \frac{k_i}{\phi c_T \mu}, \quad\text{..}\quad (2.6)$$

where $i = x, y,$ and z and c_T is the total system compressibility.

Combining Eq. 2.4 with Darcy's law and ignoring higher-order nonlinear terms, the diffusivity equation for slightly compressible fluids in Cartesian coordinates is defined as

$$\frac{\partial p}{\partial t} = \eta_x \frac{\partial^2 p}{\partial x^2} + \eta_y \frac{\partial^2 p}{\partial y^2} + \eta_z \frac{\partial^2 p}{\partial z^2} \quad\text{..}\quad (2.7)$$

The Distributed Volumetric Source Method

The distributed volumetric source is a flexible method to solve the diffusivity equation. In this method it is assumed that the source is box-shaped:

$$\frac{\partial p}{\partial t} = \eta_x \frac{\partial^2 p}{\partial x^2} + \eta_y \frac{\partial^2 p}{\partial y^2} + \eta_z \frac{\partial^2 p}{\partial z^2} + \frac{Q(x,y,z,t)}{\phi c_t} \quad\text{..}\quad (2.8)$$

$$Q(x,y,z,t) = U(t - t_0)\frac{q(t-t_0)}{\phi\, c_t}[U(x - cx - dx) - U(x - cx + dx)][U(y - $$

$$cy - dy) - U(y - cy + dy)][U(z - cz - dz) - U(z - cz + dz)] \quad\text{......................}\quad (2.9)$$

where U is the Heaviside function and δ is the Dirac delta function.

This mathematical formulation is formidable due to the added nonlinearity in the source term. However, as first shown by Valko and Amini (2007), the 3-dimensional pressure response can be represented as product of three 1-dimensional pressure responses via the Newman (1936) principle.

$$p_{\delta D}(x_D, y_D, z_D, t_D) = X(x_D, t_D)Y(x_D, t_D)Z(z_D, t_D) \ \dots\dots\dots\dots\dots\dots\dots\dots\dots \ (2.10)$$

This method, termed distributed volumetric sources, adds greater flexibility in problem characterization, allowing for increasingly complex source and parameter descriptions. Pertinent to the petroleum-engineering field, the DVS method can be used to calculate fully and partially penetrating hydraulically vertical and horizontal fractured wells with uniform flux, infinite conductivity, and finite conductivity at any position in an anisotropic homogenous reservoir. Fig. 2.1 is a schematics of the DVS model.
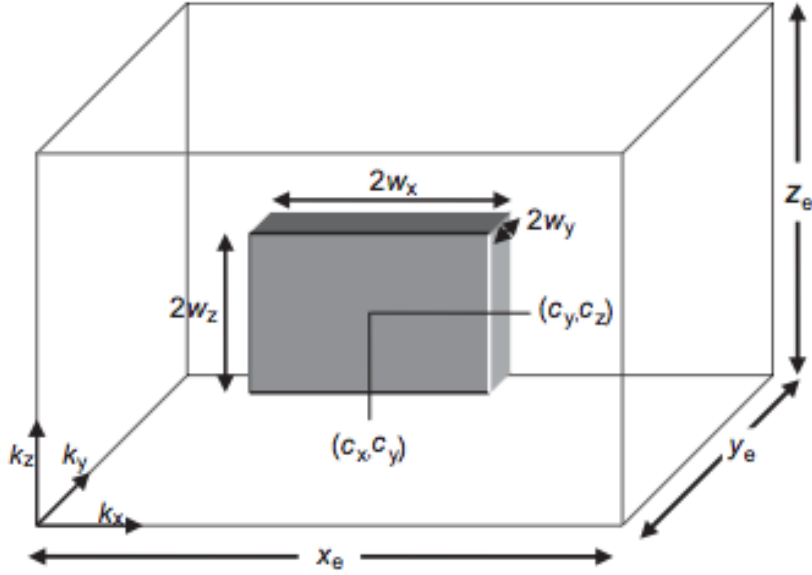
Fig. 2.1. Schematics of the DVS Method

In a similar manner, Thambynayagam (2011) solved the diffusivity equation with an explicit sink term by applying successive Fourier and Laplace transforms. Thambynayagam *nearly* solves the same problem proposed by Valkó and Amini, but only considers 1-dimensional and 2-dimensional sources. His closest representation of a volumetric source is his case of a rectangular (planer) source. For 2-dimentional sources located at $(x_0, y_1, z_1), (x_0, y_2, z_1), (x_0, y_1, z_2), (x_0, y_2, z_2)$, the solution for a continuous source is given by:

$$p =$$

$$\frac{U(t-t_0)}{\phi \, c_t \, a \, b \, c} \int_0^{t-t_0} q(t - t_0 - \tau) \left\{ \Theta_3 \left(\frac{\pi(x-x_0)}{2a}, e^{-\left(\frac{\pi}{a}\right)^2 \eta_x \tau} \right) + \right.$$

$$\left. \Theta_3 \left(\frac{\pi(x+x_0)}{2a}, e^{-\left(\frac{\pi}{a}\right)^2 \eta_x \tau} \right) \right\} \left\{ \Theta_3^{\int} \left(\frac{\pi(y-y_{01})}{2b}, e^{-\left(\frac{\pi}{b}\right)^2 \eta_y \tau} \right) + \Theta_3^{\int} \left(\frac{\pi(y+y_{01})}{2b}, e^{-\left(\frac{\pi}{b}\right)^2 \eta_y \tau} \right) + \right.$$

$$\Theta_3^{\int}\left(\frac{\pi(y-y_{02})}{2b},e^{-(\frac{\pi}{b})^2\eta_y\tau}\right)+$$

$$\Theta_3^{\int}\left(\frac{\pi(y+y_{02})}{2b},e^{-(\frac{\pi}{b})^2\eta_y\tau}\right)\}\{\Theta_3^{\int}\left(\frac{\pi(z-z_{01})}{2d},e^{-(\frac{\pi}{d})^2\eta_z\tau}\right)+$$

$$\Theta_3^{\int}\left(\frac{\pi(z+z_{01})}{2d},e^{-(\frac{\pi}{d})^2\eta_z\tau}\right)+\Theta_3^{\int}\left(\frac{\pi(z-z_{02})}{2d},e^{-(\frac{\pi}{d})^2\eta_z\tau}\right)+$$

$$\Theta_3^{\int}\left(\frac{\pi(z+z_{02})}{2d},e^{-(\frac{\pi}{d})^2\eta_z\tau}\right)\}d\tau \quad\text{...}\quad (2.11)$$

where Θ_3 is the elliptical theta function of the third kind and $\Theta_3^{\int}$ is the integral of the

elliptical theta function of the third kind. Thambynayagam defined the elliptic theta

functions as piecewise functions of two time series.

$$\Theta_3\left(\pi x, e^{-\pi^2 t}\right)=\begin{cases}1+2\sum_{n=1}^{\infty}e^{-n^2\pi^2 t}\cos(2n\pi x), & e^{-\pi^2 t}>\frac{1}{\pi}\\ \frac{1}{\sqrt{\pi x}}\sum_{n=-\infty}^{\infty}e^{-\frac{(x+n)^2}{t}}, & e^{-\pi^2 t}>\frac{1}{\pi}\end{cases} \quad\text{............}\quad (2.12)$$

He extended this solution to determine the spatial average pressure of the source by

integrating over the source area $[(y_{02}-y_{01})(z_{02}-z_{01})]$.

$$p_{ave}=$$

$$\frac{8U(t-t_0)bd}{\phi\, c_t\, a}\int_0^{t-t_0}q(t-t_0-\tau)\left\{\Theta_3\left(\frac{\pi(x-x_0)}{2a},e^{-(\frac{\pi}{a})^2\eta_x\tau}\right)+\right.$$

$$\Theta_3\left(\frac{\pi(x+x_0)}{2a},e^{-(\frac{\pi}{a})^2\eta_x\tau}\right)\}\,\{\Theta_3^{\int\int}\left(\frac{\pi(y-y_{01})}{2b},e^{-(\frac{\pi}{b})^2\eta_y\tau}\right)+$$

$$\Theta_3^{\int\int}\left(\frac{\pi(y+y_{01})}{2b},e^{-(\frac{\pi}{b})^2\eta_y\tau}\right)+\Theta_3^{\int\int}\left(\frac{\pi(y-y_{02})}{2b},e^{-(\frac{\pi}{b})^2\eta_y\tau}\right)+$$

$$\Theta_3^{\int\int}\left(\frac{\pi(y+y_{02})}{2b},e^{-(\frac{\pi}{b})^2\eta_y\tau}\right)\}\{\Theta_3^{\int\int}\left(\frac{\pi(z-z_{01})}{2d},e^{-(\frac{\pi}{d})^2\eta_z\tau}\right)+$$

$$\Theta_3^{\iint}\left(\frac{\pi(z+z_{01})}{2d}, e^{-\left(\frac{\pi}{d}\right)^2 \eta_z \tau}\right) + \Theta_3^{\iint}\left(\frac{\pi(z-z_{02})}{2d}, e^{-\left(\frac{\pi}{d}\right)^2 \eta_z \tau}\right) +$$

$$\Theta_3^{\iint}\left(\frac{\pi(z+z_{02})}{2d}, e^{-\left(\frac{\pi}{d}\right)^2 \eta_z \tau}\right)\} d\tau \quad\text{...}\quad (2.13)$$

where $\Theta_3^{\iint}$ is the second integral of the elliptical theta function of the third kind

The strength in Thambynayagam's methods is his use of two time series in the elliptical theta function. Solving the solution in this piecewise manor will allow the series to converge faster than in the previous Valkó and Amini formulation, in which a sole time series is used. Furthermore, the introduction of the special average pressure as opposed to a point pressure offers a possibly better representation of the physical situation.

The solution of the DVS method yields the transient and pseudosteady-state dimensionless pressure and the dimensionless pressure derivative, which are the foundations of petroleum engineering.

For purposes of this work the DVS, takes the form given below.

$$L = \sqrt{x_e y_e} \quad K = \sqrt{k_x k_y} \quad\text{..}\quad (2.14)$$

$$t_D = \frac{k}{\phi\, c_T\, \mu\, L^2} \quad\text{...}\quad (2.15)$$

$$p_D = \frac{2\,\pi\, kh}{\mu\, q}\,(p - p_{\text{ini}}) \quad\text{..}\quad (2.16)$$

$$J_D = \frac{\mu}{2\,\pi\,kh} \frac{q}{(p_{\text{ave}} - p_{wf})} \quad\text{...}\quad (2.17)$$

Productivity Index

The performance of a wellbore is precisely described by the productivity index, which is

the ratio of the flow rate to the pressure drawdown.

$$J = \frac{q}{\overline{p_r} - p_{wf}} = \frac{2\,\pi\,kh}{\alpha_1 B\mu} J_D \quad\text{..}\quad (2.18)$$

The dimensionless productivity index J_D is a function of dimensionless pressure and time.

(Ramey and Cobb 1971).

$$J_D = \frac{1}{p_d - 2\pi t_D} \quad\text{...}\quad (2.19)$$

In boundary-dominated flow, the dimensionless productivity index will become time

invariant. For a vertical well in boundary-dominated flow, the productivity index is given

as

$$J_D = \frac{1}{\ln\left(\frac{r_e}{r_w}\right) - .75 + s} \quad\text{..}\quad (2.20)$$

For a hydraulically fractured well, the dimensionless productivity index will depend on

the fracture conductivity and the penetration ratio:

$$C_{fd} = \frac{k_f\, w_{\text{ave}}}{k\, x_f} \quad\text{..}\quad (2.21)$$

$$Ix = 2\frac{x_f}{x_e} \quad \text{...} \quad (2.22)$$

where C_{fd} is dimensionless conductivity, k_f is proppant pack permeability under in-situ stress, w_{ave} is the fracture width, x_f is the fracture half length, and x_e is the side length of rectangular reservoir.

Valko and Economides (1998) have shown that the optimal performance of a fracture solely depends on the proppant number, which is a ratio of the flow capacity of the fracture to the flow capacity of the reservoir.

$$N_{prop} = I_x^2 C_{fd} = 2\frac{k_f}{k}\frac{V_{prop}}{V_{res}} = 4\frac{k_f}{k}\frac{x_f wh}{x_e y_e h} = \frac{1}{A_r}I_x^2 C_{fd} \quad \text{.....................................} \quad (2.23)$$

For a given proppant number, a single fracture geometry will correspond to optimal productivity. This concept applies to fully and partial penetrating fractures.

Generally, the calculation of J_D for a fractured well is a daunting task except for certain cases in which the fracture receives uniform flux from the reservoir or has infinite conductivity. For these situations, analytical calculations of J_D are possible. When the fracture has finite conductivity, rigorous calculations of J_D must apply numerical discretization schemes to capture the varying strength of flow along the fracture. One such method is the boundary element method given by Romero, Valko, and Economides (2002) However, analytical approximations for finite conductivity fractures have been

developed to avoid the arduous numerical computations. The first approximation given by

Prats (1961) is the equivalent wellbore radius concept. In the approximation, the fracture

is treated as a larger wellbore.

$$r'_w = r_w e^{-s_f} \quad \text{...} \quad (2.24)$$

where s_f is the fracture skin. Cinco, Samaniego, and Dominguez (1978) applied this

concept to directly relate the fracture skin to fracture conductivity. While Cinco,

Samaniego, and Dominguez (1978) presented only graphical results, Meyer and Jacot

(2005) presented simple analytical calculations for determining the equivalent wellbore

radius.

$$r'_w = \frac{x_f}{\frac{\pi}{c_{fd}}+2}. \quad \text{...} \quad (2.25)$$

For a horizontal well with a transverse hydraulic fracture, the convergent radial flow to

the wellbore will cause an additional pressure drop inside the fracture. This pressure drop

can be approximated by a choke skin given by Mukherjee and Economides (1991)

$$s_c = \left(\frac{kh}{k_f w}\right)\left[\ln\left(\frac{h}{2r_w}\right) - \frac{\pi}{2}\right]. \quad \text{...} \quad (2.26)$$

The Material Balance

The material balance is the fundamental tool of reservoir engineering which relates the underground withdrawal of fluids to pressure drop inside the formation. The model relates the expansion of reservoir fluid, the expansion of reservoir rock, and water influx to the production. Ignoring water influx, the material balance can be expressed as

$$\frac{d\bar{p}}{dt} = \frac{qB}{\phi A h c_T}$$ .... (2.27)

Coupling the material balance with an inflow performance relationship (determined from the dimensionless productivity index) will yield a production forecast. It should be emphasized that the material balance considers the reservoir in entirety as a tank. In this form it does not account for reservoir compartmentalization or heterogeneity.

For this work in designing wellbore completions for the Lower Tertiary, using a simple reservoir representation is logical. Many of these reservoirs have only had exploratory and limited appraisal drilling. Serious uncertainties exist in reservoir extent and heterogeneity. More importantly, a thick layer of allochtonous salt covers nearly 90% percent of the trend. From an exploration standpoint, even with WAz (wide azimuth seismic) mapping, individual sandstone reservoirs below this salt layer are nearly impossible (Lewis et al. 2007). This vastly inhibits the accuracy of upscaling well-log properties for full-field numerical reservoir simulation.

Stochastic Models

Stochastic models are used in optimization problems involving uncertainty. The goal of a stochastic program is find a feasible solution that maximizes the expected value of a random variable (or variables). There are numerous types of stochastic programs including the classical two-stage stochastic linear programs with recourse, block separable or multistate recourse programs, and chance-constrained programs. The importance of a stochastic program is exemplified by two quantities: the expected value of perfect information (EVPI) and the value of the stochastic solution (VSS) (Raiffa and Schlaifer 1961, Birge 1982). The EVPI measures the value of knowing the future (or uncertain parameters) with certainty while the VSS assesses the value of solving the more complex stochastic program with distribution as inputs over the simpler deterministic problem with single-valued input parameters (Birge and Louveaux 2011). The importance of the value of information (VOI) can be quantified through these quantities and can be used in the decision-making process. Bratvold, Bickel, and Lohne (2009) give an excellent overview of the VOI used in the oil and gas industry.

Two Stage Stochastic Program with Recourse

The general model of the linear two-stage program with recourse was first given by Dantzig (1955).

$$\min z(x, \xi) = c^T x + E_\xi [\min Q(x, \xi(\omega))]$$

$$\text{s.t.} \ Ax = b$$

$$Wy(\omega) = h(\omega) - T(\omega)$$

$$x \geq 0, y(\omega) \geq 0. \ \text{..} \ (2.28)$$

where

$$Q(x, \xi(\omega)) = \min \{q(\omega)^T y | Wy(\omega) = h(\omega) - T(\omega)x, y \geq 0\} \quad \text{...............} \quad (2.29)$$

In the above formulations the vector x is the first-stage decisions. These are the decisions that must be made without full information on the random event. The y vector is the second-stage (recourse) decisions, which are made after a realization of ξ has occurred. ξ is the vector representing a random realization of the uncertainty in data contained in $\xi(q, T, W, h)$ and ω is a random event. Mathematical expectation E_ξ for discrete sets is defined as

$$E_\xi[Q(x, \xi)] = \sum_{n=1}^{N} p_n Q(x, \xi_n). \quad \text{...} \quad (2.30)$$

where p_n is the probability mass associated with realization ξ_n.

When ξ is a continuous variable, analytical solutions for Eq. 2.30 are rare except for simple cases(Shapiro, Dentcheva, and Ruszczyński 2009). However, for the case when the random vector ξ is a discrete set or can be numerically discretized, Eq. 2.30 can be readily solved by standard techniques. When Eq. 2.30 is satisfied, the stochastic problem can be transformed into a larger deterministic problem. This formulation is known as the deterministic equivalent program (DEP) (Birge and Louveaux 2011;Shapiro et al. 2009).

The original model given by Dantzig defines the linear stochastic program. This concept

can be extended to the general stochastic program (Mangasarian and Rosen 1964,

Mangasarian 1964).

$$\min f^1(x) + E_\xi Q(x,\xi). \quad \text{...} \quad (2.31)$$

$$s.t \quad g_i^1(x) > 0, i = 1 \dots, \overline{m}_1. \quad \text{...} \quad (2.32)$$

$$Q(x,\xi) = \inf f^2[x, y(\omega)]. \quad \text{...} \quad (2.34)$$

The general nonlinear stochastic program is harder to solve and computationally more

expensive but is able to capture a broader spectrum of problems.

For the purposes of this work, the nonlinear stochastic program was used with the

constraint of convexity in the objective function and constraints. This will ensure that the

Karush-Kuhn-Tucker conditions are met and local optimums are the global optimum.

Furthermore, by invoking convexity, the Jensen (1906) inequality applies and will have

profound impacts on the optimal solution.

$$\varphi(E[X] \le E[\varphi(X)]. \quad \text{...} \quad (2.35)$$

In fact, Jensen's inequality will demand that the solution of the stochastic program will

always be greater than or equal to the solution of the deterministic mean value problem.

The Value of the Stochastic Solution

The solution of the two-stage recourse problem can be written as:

$$RP = \min_x E_\xi\, Q(x, \xi).$$ .... (2.36)

If it is possible to remove all uncertainty in input variables and future outcomes, the two-stage recourse problem can be reduced to a deterministic optimization problem. The optimal design could be readily achieved in this certain situation. This information is the expected value of perfect information (EVPI) and it measures the amount the uncertainty in the data is worth. It is the price a decision maker would pay for perfect information. The EVPI can be calculated by the difference between the so-called *wait-and-see* and *here-and-now* solution (the RP solution). (Madansky 1960). The wait -and-see solution is given by

$$WS = E_\xi[\min z(x, \xi)] = E_\xi Q(\bar{x}(\xi), \xi) \, ,$$ .... (2.37)

where $\bar{x}(\xi)$ is an optimal solution and $z(\bar{x}(\xi), \xi)$ is the optimal objective value to all to scenarios of $\min c^T x + E_\xi Q(x, \xi)$. The wait-and-see solution represents the optimal solution under which perfect information is known. The EVPI is defined as

$$EVPI = RP - WS.$$ .... (2.38)

Instead of solving the recourse problem, it is possible to replace all random variables by their expected values and solve the resulting mean value problem (Eq. 2.39). Although

easier to implement, this approach will not in general lead to the optimal solution of the stochastic program (Madansky 1960).

$$EV = \min z(x, \bar{\bar{\xi}}). \quad \text{..} \quad (2.39)$$

The expected result of using the EV solution over all realizations can be determined:

$$EVV = E_\xi\{z([(\bar{x}, \bar{\xi}), \xi)])\} . \quad \text{..} \quad (2.40)$$

The value of the stochastic program as opposed to the deterministic program can be quantified through the EVV solution and the RP. This value represents the cost of ignoring the uncertainty and using a mean value in decision parameters. The value of the stochastic solution is

$$VSS = EVV - RP. \quad \text{..} \quad (2.41)$$

For the case of the convex stochastic program, Mangasarian (1964) has shown by Jensen's inequality that the wait-and-see solution is always better than the recourse solution, which is always better than the expected value of mean value solution.

$$WS \leq RP \leq EEV. \quad \text{...} \quad (2.42)$$

Note that in the above discussion as in classical literature, the objective function is represented as cost and the optimization goal is to minimize the cost. For this work the objective function was a reward and the goal was to maximize the reward. This can be expressed as the dual problem, and thus all the mentioned theory holds.

Remarks on Stochastic Programming

The term *recourse* means that decisions are made after uncertainty is revealed. In this case a set of decisions x is made in the first stage where uncertainty exits. At some point later, a realization of random event $\xi(\omega)$ occurs, the second-stage data $q(\omega)$ $h(\omega)$ and $T(\omega)$ are revealed, and a recourse action $y(\omega)$ is taken. In full recourse, $y(\omega)$s are decisions that are made to optimize the current realization, which is deterministic optimization in itself. For the case where the recourse matrix W is fixed, the problem is said to have fixed recourse.

In certain situations, the second-stage decisions are automatic (Birge and Louveaux 2011). In these cases, the $y(\omega)$s take the form of penalties incurred from the first stage. This recourse is deemed *simple recourse*. The objective in this case is to select a first-stage decision that will minimize the penalties incurred in the second (Hansotia 1980). In fact, simple recourse is defined if the state vector in each period is uniquely determined once all previous decisions and random vectors are known (Everitt and Ziemba 1979).

Since the stochastic program objective function is an expectation, it is possible to directly extend the optimization to account for variability in the outcome. One method is to formulate the objective function as a variance instead of an expected value. The variance of set is defined as:

$$V(Y) = E[Y - E(Y)]^2]$$ .... (2.43)

The new objective function can take the form of

$$\min z(x, \xi) = V_\xi[Q(x, \xi(\omega))] \quad \text{..} \quad (2.44)$$

This will minimize the variance between the expected outcomes and the tightly bound actual solution. However, this function does not explicitly maximize expected value and may be unsatisfactory. Considering expected value and variance, an alternate objective function can be formulated:

$$\max z(x, \xi) = (1 - \alpha)E_\xi[Q(x, \xi(\omega))] - \alpha V_\xi[Q(x, \xi(\omega))] \quad \text{...................} \quad (2.45)$$

where α is a weighting factor on the variance of the set.

Although this formulation is robust, it does not capture the *preference* or risk of expected outcome. To explicitly account for risk, a utility function can be used.

$$\max z(x, \xi) = E_\xi[u(Q(x, \xi(\omega)))] \quad \text{...} \quad (2.46)$$

This formulation can be used to directly maximize expected value while accounting for risk between possible outcomes. The fundamentals of utility theory are discussed below.

Utility Theory

Mathematically utility is defined as:

$$u: X \to \mathbb{R} \; L_1 < L_2 \text{ implies } u(L_1) \le u(L_2) \quad \text{...................................} \quad (2.47)$$

where u is utility and L is a lottery composed of a set of payoff and associated probabilities (McKenna 1986). This states that a higher utility will be associated with a higher function value and a lower utility will be associated with a lower function value. Although the absolute utility will always be higher for higher function value in comparison to a lower function value, the derivative or marginal utility will be different. Pratt (1964) introduced the risk aversion function to quantify the degree of aversion to uncertainty in the utility function.

$$r(x) = -\frac{u''(x)}{u'(x)} \quad\text{...} \quad (2.48)$$

In a situation under uncertainty, the expected utility can be defined in a way similar to expected monetary value (Cozzolino 1977):

$$E\{u(x + \tilde{z})\} = \int u(x + z)f(z)dz \quad\text{...} \quad (2.49)$$

where $E\{u(x + \tilde{z})\}$ is the expected utility for asset x with utility u , risk $\tilde{z}$, and probability density function $f(z)$, which can be continuous or discrete.

For situations involving uncertainty a useful concept when discussing utility is the *certainty equivalent* (CE or cash equivalent) and *risk premium* (RP). For a decision maker with assets x, there is a risk premium $\pi(x, \tilde{z})$ such that the decision maker would be indifferent to receiving risk $\tilde{z}$ or a nonrandom event $E(\tilde{z})$- $\pi(x, \tilde{z})$ (Pratt 1964). This value is the cash equivalent

$$\pi_a(x, \tilde{z}) = E(\tilde{z}) - \pi(x, \tilde{z}) \, t \quad\text{...} \quad (2.50)$$

The cash equivalent is the no-risk certain amount of cash the decision maker is willing to exchange for a gamble—essentially the cash value of the decision under uncertainty. The risk premium is the value that a decision maker would give up for a nonrandom outcome as opposed to a random outcome (Newendorp and Schuyler 2000).

Utility functions are useful in representing different risk attitudes. Three general cases of risk are conservative, neutral, and aggressive. The utility of a decision is represented by eqn. 2.51 which shows how levels of indifference between alternative

$$U(x) = U(x_1)I + U(x_2)(I - 1) \dots\dots\dots\dots\dots\dots\dots\dots\dots\dots\dots\dots\dots\dots \quad (2.51)$$

where x is a decision, x_1 is a *good* alternative, x_2 is a *poor* alternative, and I is indifference between alternatives. The definition of *good* and *poor* in the above formulation are determined by the relative risk of each alternative. In this sense, a conservative risk profile would have an indifference value $I = 0$,while an aggressive risk profile would have an indifference value $I = 1$.

By incorporating risk via the utility function, more consistent and logical decisions can be made.

Risk Neutral

Risk neutral is defined as an attitude that indifferent to amount of capital at risk. The risk-neutral utility curve is a linear line with unity slope. A risk-neutral decision maker will have the same policy of an expected monetary-value decision maker. A risk-neutral attitude may result when an event is repeatable and the absolute monetary value of the outcome is smaller than the total net worth. The risk neutral utility will be used as a baseline for comparison to other risk profiles. The risk-aversion function is 0, implying no risk aversion, which is consistent with the above definition.

Risk Conservative

The risk-conservative (or risk-averse) attitude represents the willingness to take a certain payoff over a probabilistic payoff with possibly higher expected value; that is, a risk-averse person would take a certain \$0.5 or less in a game where there is a 50:50 chance of obtaining \$1.00. Interestingly, the risk-conservative utility can take different mathematical forms with unique meanings. On such form suggested by Schuyler (2001) is the exponential utility function.

$$u(x) = r\left(1 - e^{-\frac{x}{r}}\right) \dotfill (2.52)$$

Applying Eq. 2.48,

$$r(x) = -\frac{u''(x)}{u'(x)} = \frac{\frac{e^{-\frac{x}{r}}}{r}}{e^{-\frac{x}{r}}} = \frac{1}{r} = c \dotfill (2.53)$$

Eq. 2.52 shows a constant level of risk aversion regardless of the amount of total assets. Alternatively, it has been suggested that the level of risk aversion should decrease as total assets increase. A utility function of this form is the logarithmic form:

$$u(x) = r \ln (1 + x) \quad\text{..} \quad (2.54)$$

Applying equation Eq. 2.48,

$$r(x) = -\frac{u''(x)}{u'(x)} = \frac{1}{1+x} \quad\text{..} \quad (2.55)$$

Eq. 2.53 shows the risk-aversion level decreasing (risk tolerance increases) with increasing asset value. Although the graphs have similar shapes, the two forms indicate significant different economical implications.

Risk-Aggressive Utility Curve

The risk-aggressive profile is an attitude of the gambler. The gambler represents an attitude that would to take a probabilistic chance with a lower expected value but a chance to obtain a higher value than a certain payoff; that is, a risk-aggressive person would prefer to play a game with a 50:50 chance of winning \$1.00 than to take a certain \$0.5. This risk-aggressive behavior is not common in business practice as it has long-term negative expected value; however, some short-term decisions may be made using a risk-aggressive utility. A cubic equation may be used to represent the risk-aggressive attitude.

$$u(x) = x^3 + x \quad\text{..} \quad (2.56)$$

The risk-aversion coefficient is

$$r(x) = -\frac{u''(x)}{u'(x)} = -\frac{6x}{1+3x^2} \quad\text{.. (2.57)}$$

The risk-aversion coefficient is negative and decreasing with total wealth. This implies the risk seeker is willing to take more risk at lower total asset value.

The above-mentioned utility curves (Fig. 2.2) apply to positive asset values. For negative asset values, the utility curves can be constructed in the same way but may be piecewise as the preference to negative values may be significantly different from those to positive asset values.
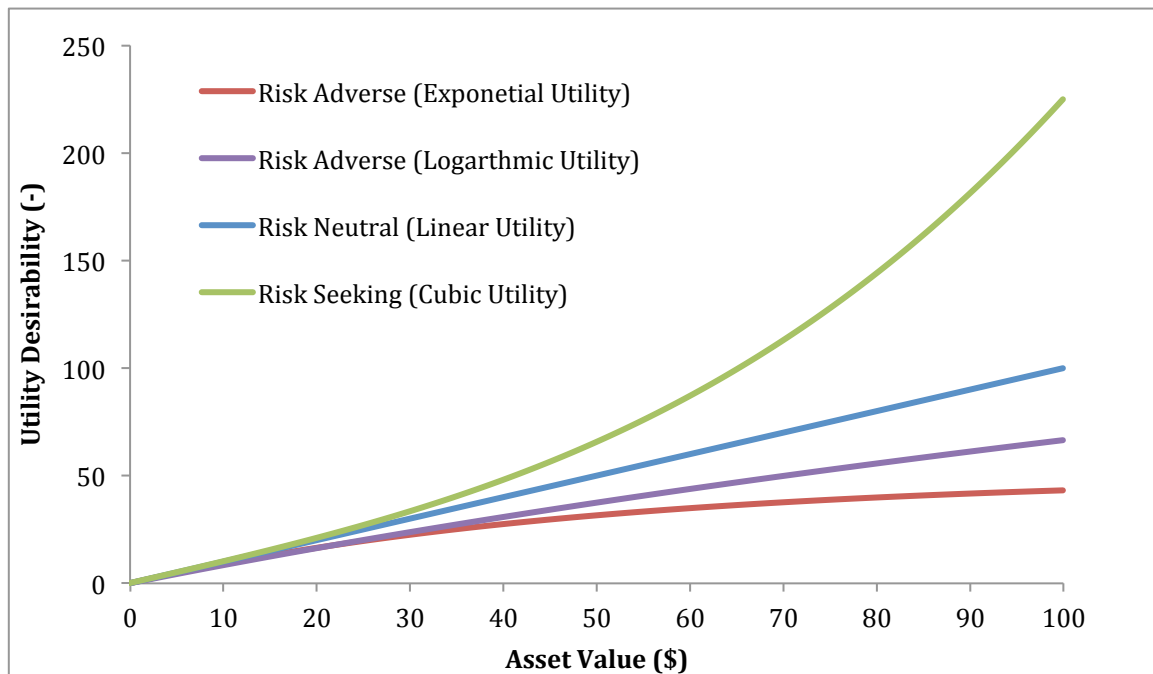
Fig. 2.2. Utility curves for selected risk profiles

For purposes of this work, the utility used was marginal utility as opposed to cardinal utility. *Marginal utility* is defined in such a way that the utility value does not have significant physical or economic meaning; it can only be used for comparative purposes. *Cardinal utility* implies that the actual value of the utility is numerical and can be used as direct measure of the transformed variable.

It must be stressed that the application of utility theory is nontrivial for offshore production and development. Given the extreme cost of developments and relatively small number of wells drilled, each and every decision requires extensive planning. Purely statistical approaches without accounting for risk are unacceptable in this environment: utility *must* be considered.

CHAPTER III

MODEL DEVOLOPMENT AND DETERMINISTIC OPTIMIZATION

Distributed Volumetric Source Method Update

Combining the distributed volumetric source method of Valkó and Amini (2007) with

Thambynaygam's (2011) spatial average and a two-series representation of the elliptic

theta function, Valkó (2013) developed a new formulation of the DVS method:

$$p = \frac{U(t-t_0)}{\phi\, c_t\, a\, b\, c} \int_0^{t-t_0} q(t - t_0 - \tau) L_1 L_2 L_3 d\tau \quad \dots\dots\dots\dots\dots\dots\dots\dots\dots \quad (3.1)$$

where

$$L_i = \frac{\Theta_3^{\iint} \left[\frac{i_{01}}{i_D}, \frac{i_{02}}{i_D}, \frac{\eta_i}{i_D^2}t\right]}{\frac{(i_{02}-i_{01})^2}{i_D}} =$$

$$\Theta_3^{\iint} \left(\frac{\pi(i_{02}-i_{01})}{i_D}, e^{-(\frac{\pi}{i_D})^2 \eta_i \tau}\right) + \Theta_3^{\iint} \left(\frac{\pi(i_{02}+i_{01})}{i_D}, e^{-(\frac{\pi}{i_D})^2 \eta_i \tau}\right) + \frac{1}{2}\left\{\Theta_3^{\iint} \left(\frac{\pi z_{02}}{i_D}, e^{-(\frac{\pi}{i_D})^2 \eta_i \tau}\right) + \right.$$

$$\left(\frac{\pi z_{01}}{i_D}, e^{-(\frac{\pi}{i_D})^2 \eta_i \tau}\right)\right\} \text{ and } i = x, y, z \quad \dots\dots\dots\dots\dots\dots\dots\dots \quad (3.2)$$

To further improve algorithmic speed, an additional time cut is added to the elliptic theta

function. This additional time cut is a simplification of the infinite series at large

dimensionless time values.

$$\Theta_3\left(\pi x, e^{-\pi^2 t}\right) = \begin{cases} 1 + 2\sum_{n=1}^{\infty} e^{-n^2\pi^2 t} \cos(2n\pi x), & e^{-\pi^2 t} > \frac{1}{\pi} \\ \frac{1}{\sqrt{\pi t}}\sum_{n=-\infty}^{\infty} e^{-\frac{(x+n)^2}{t}}, & e^{-\pi^2 t} < \frac{1}{\pi} \\ 1 & e^{-\pi^2 t} > \frac{9}{\pi} \end{cases} \quad \dots\dots \quad (3.3)$$

This formulation allows for an efficient and accurate calculation of the transient and pseudosteady productivity indices for a *uniform flux* source term. This implies the solution will be valid for uniform flux vertical and horizontal wells and fractures. For the case when the source does not exhibit uniform flux (such as a finite-conductivity fracture), the solution will require modification. Although the DVS method can rigorously be used to calculate the finite-conductivity fracture as shown by Amini and Valkó (2010), it requires numerical discretization of the source to capture the unknown strengths of flow along the fracture. These large matrix computations vastly reduce the computational efficiency of the method. To capture the inherent finite-conductivity, approximate *equivalent flux sources* are used.

Distributed Volumetric Source Comparison

For consistency in the modified DVS method, we compared the new formulation to classical solutions including a uniform flux vertical well in the center of a square reservoir, a uniform flux vertical well in an irregularly shaped drainage area, and a uniform flux fracture in the center of a square drainage area.

Fully Penetrating Vertical Well

Fig. 3.1 shows excellent agreement between the cylindrical source solution and the DVS

method for a vertical well in the center of a square drainage area.
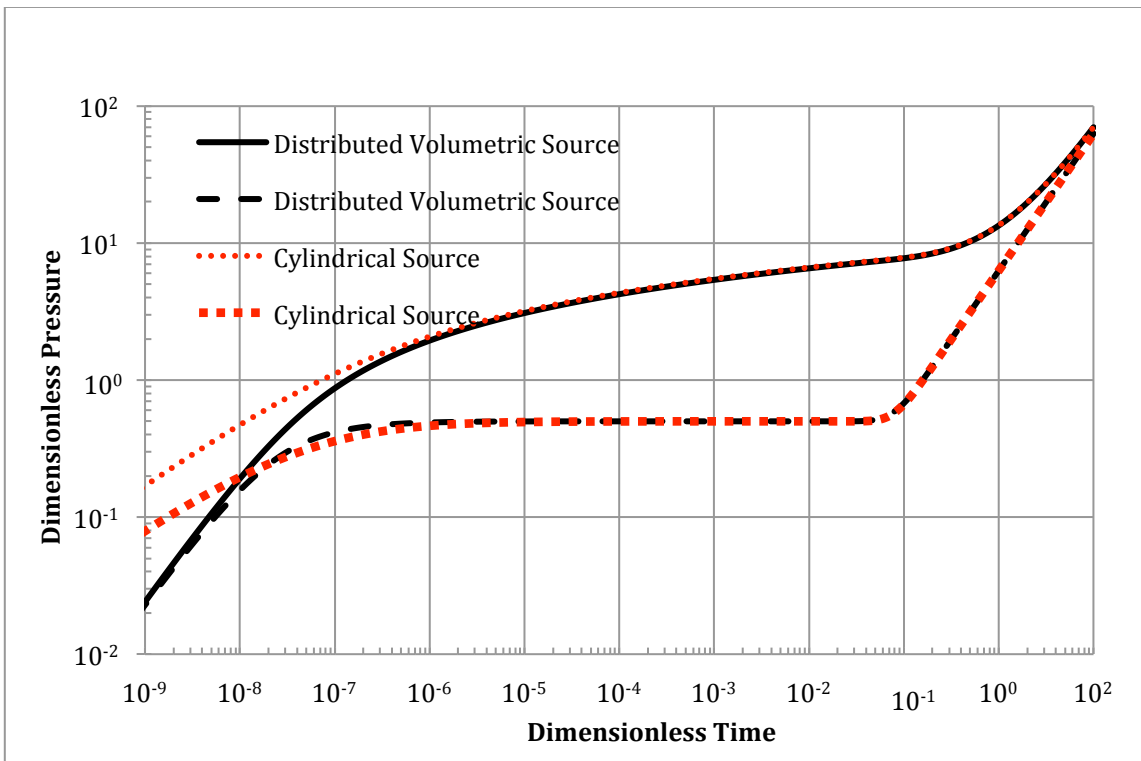
Fig. 3.1. Vertical well, center of square reservoir

The early time discrepancy reflects the fact that the DVS method considers area in the

source to have flow potential, whereas the cylindrical-source method does not. This minor

discrepancy is negligible for all practical purposes. It should be noted for computational

purposes the DVS method vastly outperforms the cylindrical source method, which

requires numerical inversion. For using Mathematica 9 on MacBook Pro 2.5 GHz Intel

Core i5, the computational times are summarized below.

Table 3.1. Cylindrical Source and DVS Computational Time Comparison

Method	Cylindrical Source w/ Gaver,Wynn-Rho Inversion	Distributed Volumetric Source
Time (seconds)	664	3.01

Fully Penetrating Vertical Well in Irregular Drainage Area

Fig. 3.2 shows excellent agreement for wells in irregular drainage areas.
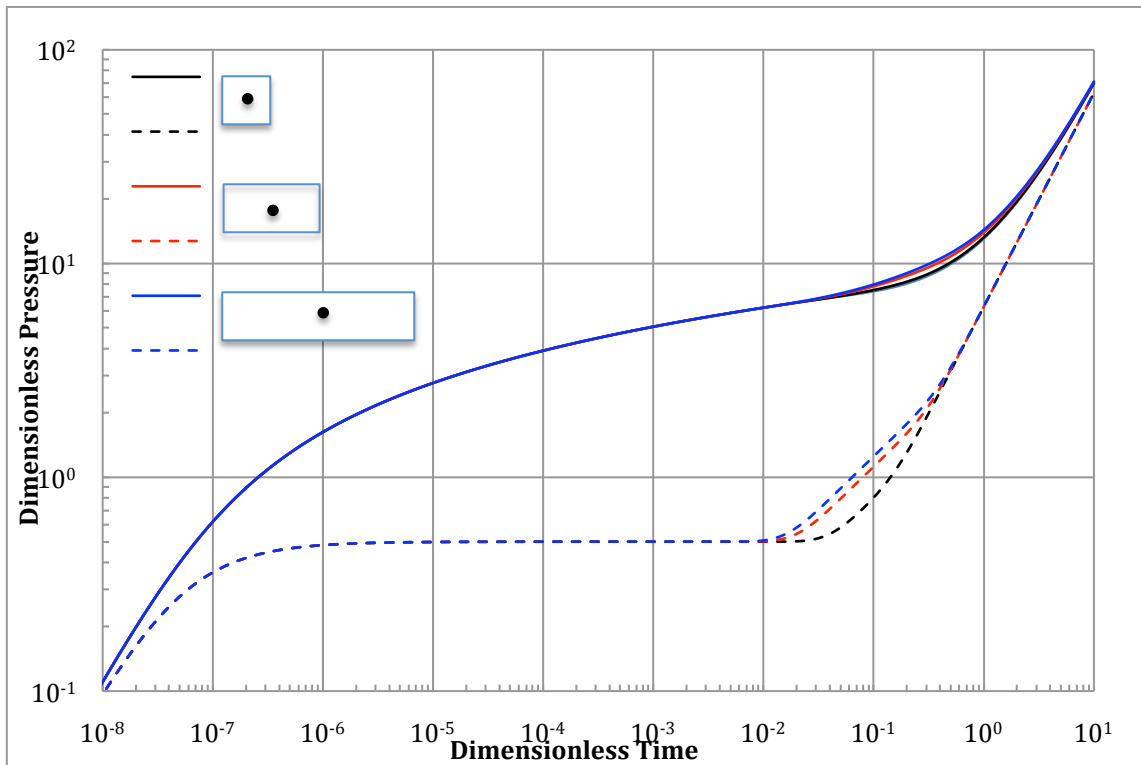
Fig. 3.2 Vertical well, irregular drainage area
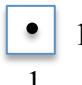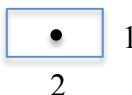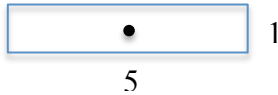
For a fully penetrating well in an irregular-shaped drainage area, it is common to compute the Dietz (1965) shape factor.

$$C_a = \frac{4A}{r_w^2} e^{-\gamma - \frac{2}{J_D}}$$ .... (3.4)

where γ is the Eulergamma constant ≈ 0.577.

Table 3.2 shows the DVS method is in excellent agreement with the classical solutions.

Table 3.2. Dietz Shape Factors

Drainage Shape	Dietz Shape Factor	DVS Shape Factor
	30.882	30.865
	21.836	21.820
	5.379	5.374
	2.361	2.357

Uniform Flux Vertical Fracture

Fig. 3.3 shows excellent agreement between the DVS method and the classical Gringarten solution.
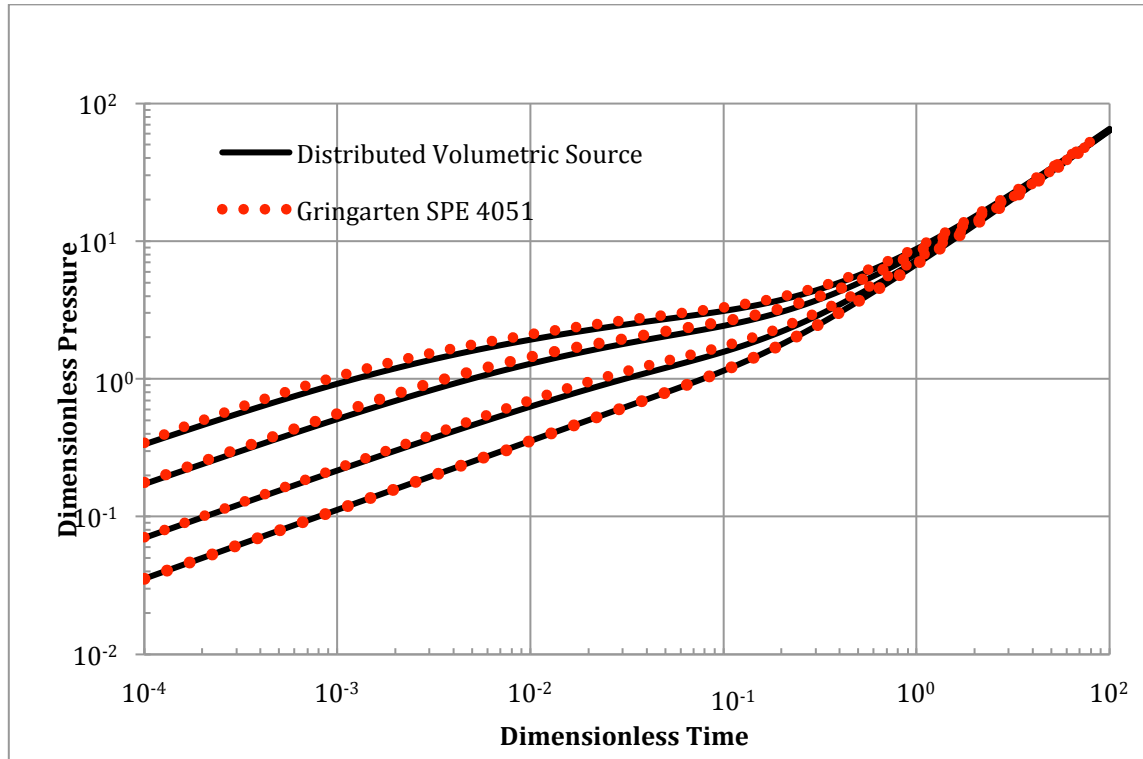
Fig. 3.3 Uniform flux, vertical facture

Furthermore, the updated DVS method computationally outperforms the original DVS method proposed by Valko and Amini (2007).

Table 3.3. DVS Computational Time Comparison

Method	Distributed Volumetric Source (Valko and Amini 2007).	Distributed Volumetric Source Updated
Time (seconds)	84.73	4.49

Finite Conductivity Fracture Approximation

To account for fracture finite conductivity, the dimensionless productivity is modified by

Eq. 3.5:

$$J_D = \cfrac{1}{\cfrac{1}{J_{D,\text{Uniform Flux}}}+\alpha_1 \ln} \quad \text{..} \quad (3.5)$$

where α_1 is a constant from a least-squares fit from the known dimensionless productivity

index. This approximation is validated against the known values of dimensionless

productivity index given by Valko and Economides (1998).

Fig. 3.4 shows the approximation is valid for proppant numbers less than 1. Using this

method the finite conductivity fracture productivity index can be directly calculated from

the uniform flux fracture solution in a computationally robust manor.
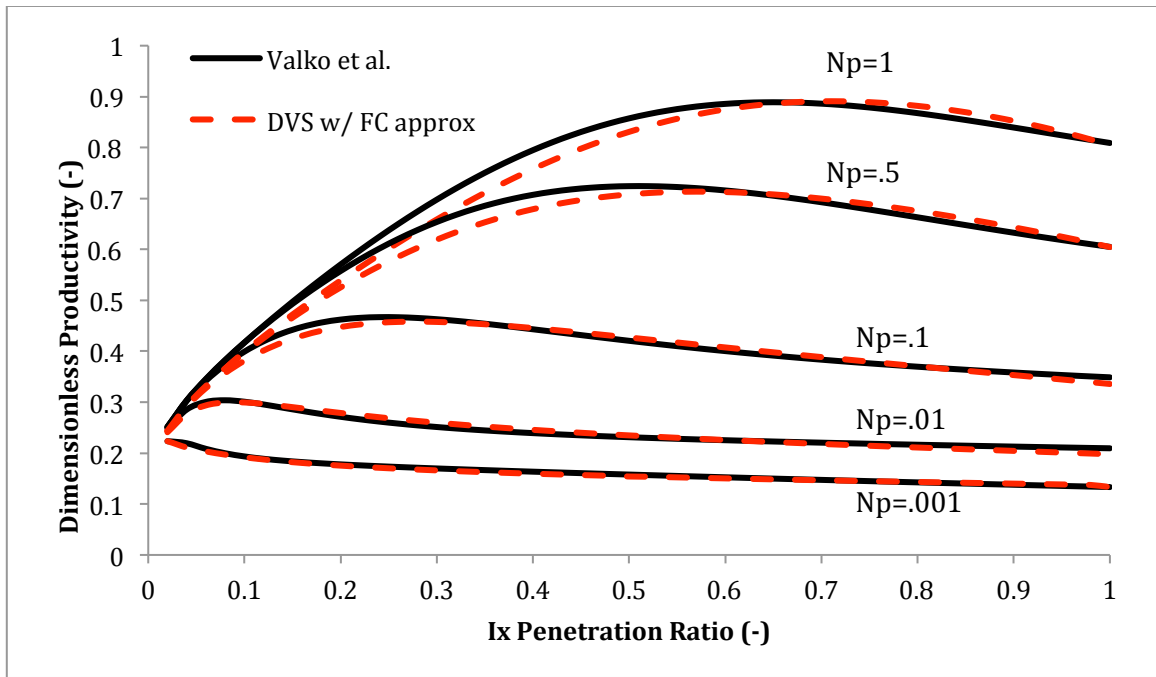
Fig. 3.4 Vertical fracture, dimensionless productivity

Proppant Allocation in Multilayer Reservoirs

As noted before, some Lower Tertiary formations are multilayered stacked sands with varying fluid and reservoir quality. An example is the Cascade formation, which is composed of the Wilcox 1 & Wilcox 2 with permeability and height 25 md, 400 ft, and <10 md, 600 ft, respectively (Haddad, Smith, and Moraes 2012).

For a well completed in multiple layers without pressure communication, the productivity index can be determined from a summation of the inflows.

$$q_t = q_1 + q_2 \ldots + q_n$$ .... (3.6)

For a constant drawdown and the fluid properties, the total productivity index is given by Eq. 3.7.

$$J = \frac{q}{\overline{p}_r - p_{wf}} = \frac{2\,\pi}{B_o\mu}\left(k_1 h_1 J_{d1} + k_2 h_2 J_{d2} \dots + k_n h_n J_{dN}\right) t \ \text{..............................} \quad (3.7)$$

where $k_n h_n J_{dN}$ are the permeability, height, and dimensionless productivity of each layer.

The question poised is how to deviate a fixed amount of proppant in a vertical well with multiple completion zones for maximum wellbore performance. Assuming the zones do not have pressure communication and are fractured separately, each layer will have a separate proppant number ($N_{prop1}, N_{prop2\dots}N_{propN}$) depending on the permeability, height, and proppant allotted. For maximization of total productivity, the two-layer system with constant fluid properties the optimization is written as Eq. 3.8

$$\text{maximize } \frac{2\,\pi}{B_o\mu}\left(k_1 h_1 J_{d1}(p_1) + k_2 h_2 J_{d2}(p_2)\right)$$

$$p_1 + p_2 = 1$$

$$0 < p_1 < 1 \quad 0 < p_2 < 1 \ \text{...} \quad (3.8)$$

Assuming full fracture height penetration, the dimensionless productivity can be readily calculated by the DVS method with the finite-conductivity approximation.

By treating the proppant allocation percent p_1 as a discrete variable and enumerating, an optimal solution is found: the optimum placement of proppant occurs when the proppant number of each layer is equal.

$$N_{\text{prop1}} = N_{\text{prop2}} = N_{\text{prop}N} \quad\text{...}\quad (3.9)$$

The result of this is that a majority of the proppant is allotted to the layer with the largest permeability × height product. It also signifies that the each layer will have the same half-length but different widths. The layers will have the same dimensionless productivity indices but different absolute productivity indices. Analytically, the percent of total proppant allotted to each layer for a two-layer system can be found by Eqs. 3.10 to 3.12.

$$\frac{N_{\text{prop1}}}{N_{\text{prop2}}} = 1 \quad\text{..}\quad (3.10)$$

$$\frac{k_1 h_1}{k_2 h_2} = \frac{p_1}{p_2} \quad\text{..}\quad (3.11)$$

$$p_1 + p_2 = 1 \quad\text{...}\quad (3.12)$$

where $\boldsymbol{p_1}$ and $\boldsymbol{p_2}$ are the percentage of proppant allotted to each layer respectively. Fig. 3.5 shows the productivity index as a function of the ratio of proppant numbers for different productivity × height ratios.
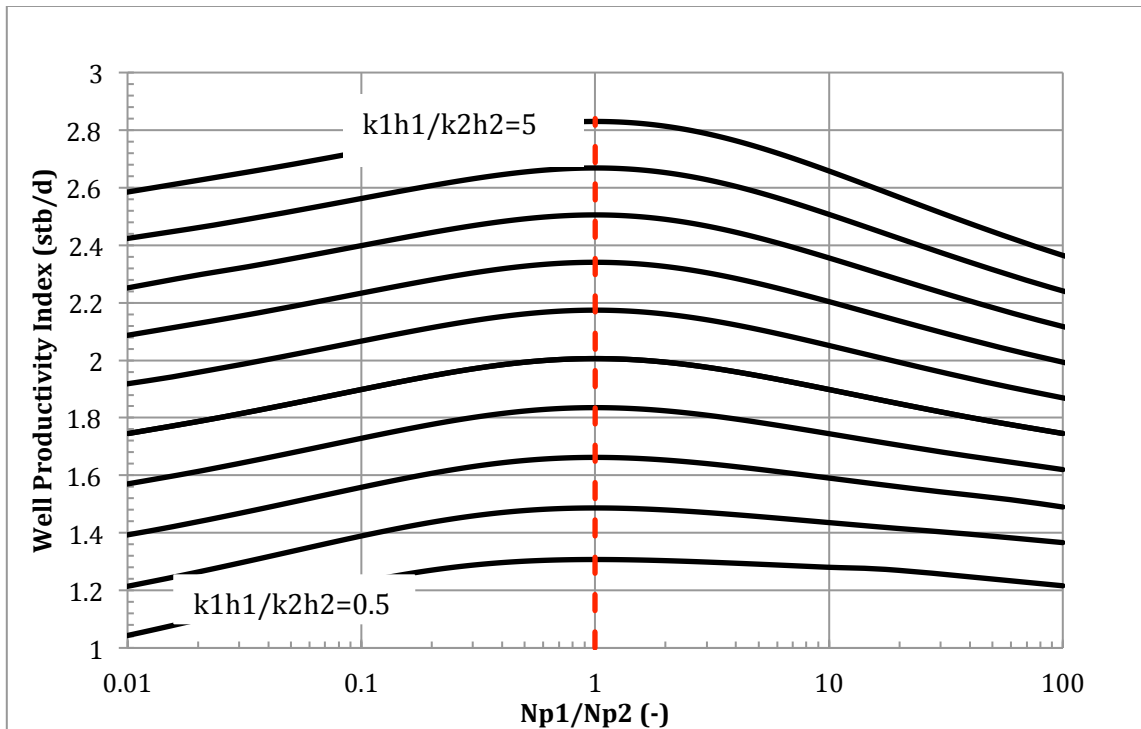
Fig. 3.5 Productivity index vs. ratio of proppant numbers

Table 3.4 Multilayer System Properties

RESERVOIR AND FLUID	PROPPANT
$A = 500$ acre	$M_p = 1,000,000$ lbm
$B_o = 1.1$	$k_f = 100,000$ md
$\mu = 5\ cp$	$\phi = .3$

The results can be generalized for an *N*-layer system. This analytical solution avoids the

use of expensive numerical optimization.

$$
\begin{vmatrix}
\dfrac{1}{k_1 h_1} & \dfrac{1}{k_2 h_2} & & & \\[2ex]
 & \dfrac{1}{k_2 h_2} & \dfrac{1}{k_3 h_3} & & \\[2ex]
 & & \ddots & \ddots & \\[2ex]
 & & & \dfrac{1}{k_{n-1} h_n} & \dfrac{1}{k_n h_n} \\[2ex]
1 & 1 & 1 & 1 & 1
\end{vmatrix}
\begin{vmatrix}
p_1 \\ p_2 \\ \vdots \\ p_{n-1} \\ p_n
\end{vmatrix}
=
\begin{vmatrix}
0 \\ 0 \\ \vdots \\ 0 \\ 1
\end{vmatrix}
$$

This result maximizes the productivity of a wellbore from an inflow performance mindset. It optimizes the production rate but does not account for possibly different oil-in-place and reservoir drive mechanisms.

CHAPTER IV

STOCHASTIC OPTIMIZATION

Fracture Design Under Uncertainty

In the following example, the distributed volumetric source method is applied in a two-stage recourse optimization where the vertical permeability is uncertain. This example will illustrate the expected value of the perfect information and the value of the stochastic solution.

Partial Penetrating Fracture with Anisotropy Uncertainty

The DVS method (Fig 4.1) is well-suited to calculate partially penetrating fractures in anisotropic media. This method is used to optimize fracture dimensions in a constrained system. In this example the uniform flux solution is used for simplicity and efficiency. The constraint on the system is that of constant fracture area (as the width is trivial for the uniform flux fracture). The fluid viscosity, porosity, and total compressibility of the system remain constant. The example goes through the step-step the optimization process, applying the stochastic method.
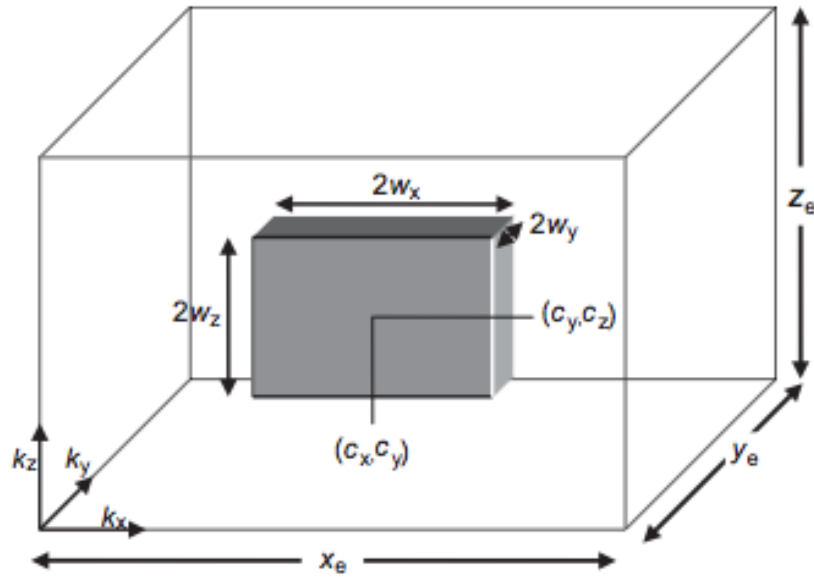
Fig. 4.1. DVS schematic

The first problem is approached as a deterministic nonlinear program. The objective is to maximize dimensionless productivity by varying w_x and w_z while keeping the product $w_x w_z$ constant. The fracture is located in the center of the reservoir, so $cx = \frac{1}{2}$, $cy = \frac{1}{2}$, and $cz = \frac{1}{2}$. The reservoir is box-shaped with $x_e = y_e = 10\ z_e$ For this problem, it is convenient to introduce a dimensionless term ctz, which is a factor representing the time it takes in a given direction to reach the boundary wall.

$$ctz = \frac{k_z}{k_x}\frac{x_e^2}{z_e^2} \quad \text{..} \quad (4.1)$$

In case of reservoir anisotropy in the vertical direction with $\frac{k_z}{k_x} = \frac{1}{100}$ and $k_x = k_y$,

$$ctz = \frac{1}{100}\frac{10^2}{1} = 1 \quad \text{..} \quad (4.2)$$

Note that for constant reservoir dimensions, variations in ctz can be used to represent

different anisotropy ratios. The optimization problem can mathematically be described as

$$\max J_D(w_x, ctz)$$

$$w_x w_z = C$$

$$0 < w_x < \frac{1}{2}, 0 < w_z < \frac{1}{2} \quad\text{..}\quad (4.3)$$

For an arbitrary constant $= \frac{1}{8}$, the optimal dimensions and dimensionless productivity are

given in Table 4.1.

Table 4.1 Optimal Fracture Dimensions and Productivity For Partially Penetrating Fracture

ctz	$w_{x,opt}$	$w_{z,opt}$	$J_{D,opt}$
1	.35	.25	1.14

Instead of representing the value of anisotropy with a single value, a set of values is used

$\{ctz_1, ctz_2, \ldots ctz_n\}$. For simplicity, we assume in this case only three different

permeability realizations $\{ctz_1, ctz_2, ctz_3\}$. For each case it is possible to optimize in a

similar manner as shown above.
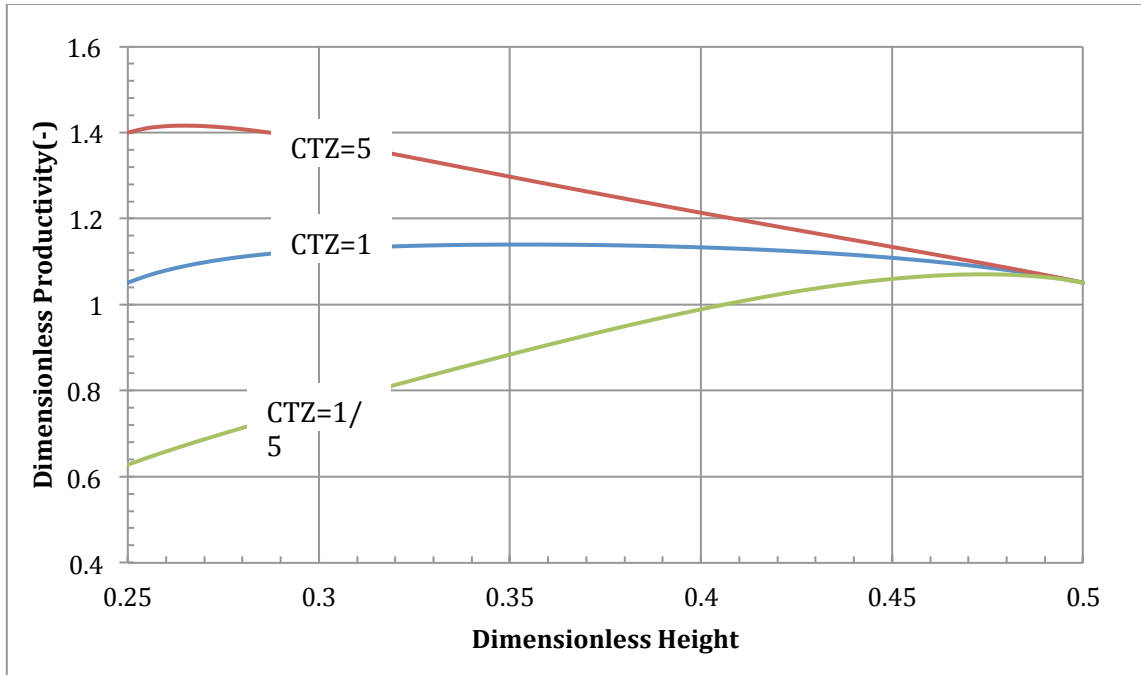
Fig. 4.2. Dimensionless height versus dimensionless productivity for different anisotropy ratios

Table 4.2 Optimal Fracture Dimensions and Productivity for Different Anisotropy Ratios

CTZ	$w_{x,opt}$	$w_{z,opt}$	$J_{D,opt}$
1	.35	.35	1.14
5	.48	.26	1.41
1/5	.27	.47	1.07

Table 4.2 shows the optimal dimensions for each case in the above-mentioned situation. It is apparent that in the case of higher vertical permeability, the optimal solution favors more horizontal penetration as more flow is realized in the vertical direction. In the case of lower vertical permeability, the optimal favors almost full-fracture-height penetration because the flow is minimal in the vertical direction. Note the sensitivity changes in optimal design dimensions for the different permeabilities.

61

By the above analysis, it is readily achievable to optimize the fracture dimension for any given anisotropy ratio. These designs were determined with a single certain value for anisotropy. Now, assume that the three values of anisotropy $\{ctz_1, ctz_2, \dots ctz_n\}$ have associated probabilities $\{p_1, p_2, \dots p_n\}$ and it is only possible to identify the actual anisotropy after the fracture has been placed. For this uncertain situation, the permeability realization $ctz(\omega)$ will be a function of a random vector ω. The objective function is now defined as $J_D(w_x, ctz(\omega))$ and will now depend on the specific realization of vertical anisotropy. The optimization is to determine what fracture dimensions will maximize the expectation E_{ctz} over all of the realizations. The problem takes the form of a stochastic program with simple recourse.

$$\max E_{ctz}[J_D(w_x, ctz(\omega))]$$

$$w_x w_z = C$$

$$0 < w_x < \frac{1}{2}, 0 < w_z < 1/2 \quad\text{..} \quad (4.4)$$

For this discrete case, the expectation decomposes to a finite series.

$$E_{ctz}[J_D(w_x, ctz(\omega))] = \sum_{i=1}^{n} J_D(w_x, ctz(\omega_i)) \, p(\omega_i) \quad\text{..............................} \quad (4.5)$$

Under this uncertain scenario, a new optimum is found.

$$w_{x,\text{opt}} = 0.32 \text{ and } w_{z,\text{opt}} = 0.39$$

Table 4.3. EVPI: Optimal Fracture Dimensions and Productivity

CTZ	1	5	1/5	$Expected$
J_D	1.13	1.22	.98	1.11

This is the solution to the stochastic program given in Table 4.3, which maximizes long-term (expected) productivity.
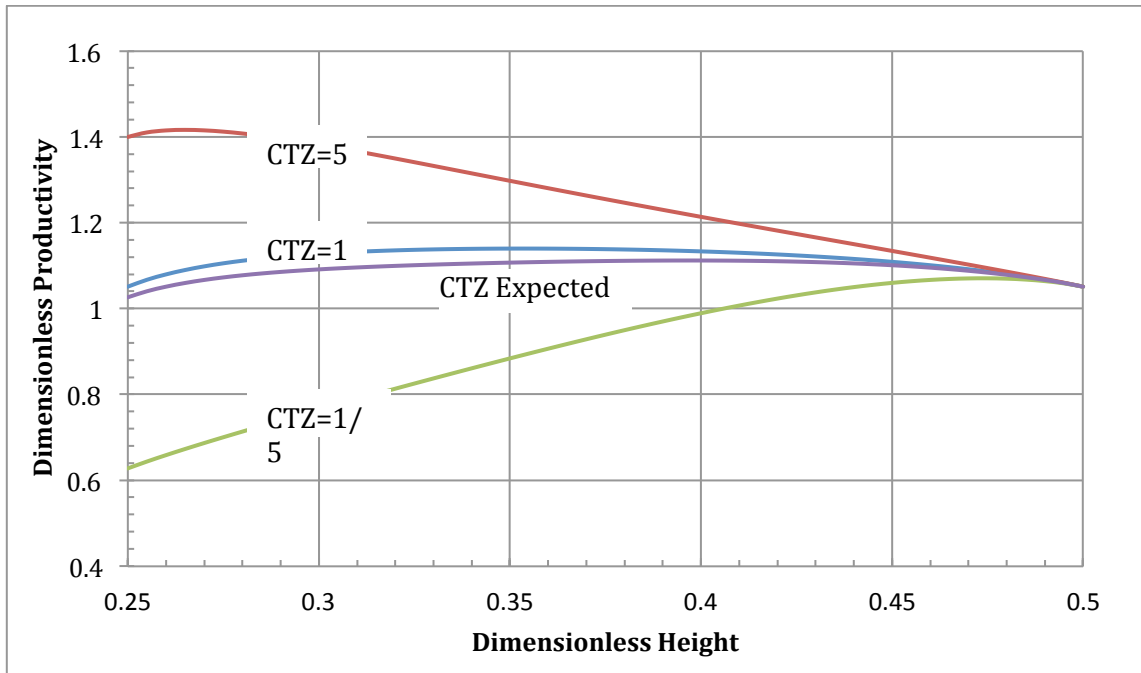
Fig. 4.3. Stochastic solution: dimensionless height versus dimensionless productivity

A metric to judge the stochastic solution against is the solution given by perfect information. This case would represent the expected value of productivity given a set of anisotropy realizations with associated probabilities, but for any given well the exact permeability is known. The concept is easily conceptualized in a reservoir where many wells are to be drilled in the formation. For each well the anisotropy is a random realization of the set but is known, and an optimum design can be implemented. The expected productivity would be the expected value of the 3 deterministic cases. Using the above values,

$$E[J_D] = (1.14\,)\frac{1}{3} + (1.41)\frac{1}{3} + (1.07)\frac{1}{3} = 1.20 \quad \text{..} \quad (4.6)$$

This quantity is known as the wait-and-see solution and represents the maximum

achievable expected productivity if all uncertainty is removed. The difference between

this value and the solution to the stochastic solution is the expected value of perfect

information.

$$EVPI = 1.20 - 1.11 = 0.09 \quad \text{..} \quad (4.7)$$

This is the measure of the worth of uncertainty in terms of dimensionless productivity.

Generally (although not in this example), the EVPI can be expressed as a monetary

amount and is a metric that can be used to warrant additional data gathering.

An alternative yet unfortunate approach to the stochastic program that is sometimes

implemented is to solve the deterministic program with a mean value of the random

variable. In this formulation, a weighted average anisotropy is used to and solve a single

optimization problem. The problem is termed the mean value problem.

$$\max J_D(w_x, \overline{ctz})$$

$$w_x w_z = C$$

$$0 < w_x < \frac{1}{2}, 0 < w_z < 1/2$$

$$\overline{ctz} = \sum_{i=1}^{n} ctz(\omega_i)\, p(\omega_i) \quad \text{..............................} \quad (4.8)$$

For this case,

$$\overline{ctz} = (1)\frac{1}{3} + (5)\frac{1}{3} + \left(\frac{1}{5}\right)\frac{1}{3} = 2.06 \quad \text{............................} \quad (4.9)$$

For this situation a new optimal design is found:

$$w_{x,opt} = .28 \; and \; w_{z,opt} = .45$$

Table 4.4 Mean Value Solution: Optimal Fracture Dimensions and Productivity

CTZ	1	5	1/5	$Expected$
J_D	1.10	1.267	.87	1.08

As a direct result of Jensen's inequality, the expected productivity from the mean value

solution is always less than or equal to the stochastic solution. The difference is the value

of the stochastic solution. In this case,

$$VSS = 1.11 - 1.08 = 0.03 \; \text{..} \quad (4.10)$$

This number represents the expected gain in productivity for design under uncertainty

rather than deterministically. Interesting insight comes from the ranges of possible

solutions for different design criteria as shown in Table 4.5.

Table 4.5 Summary of Stochastic Optimization

w_x	w_z		$J_D(CTZ = 1)$	$J_D(CTZ = 5)$	$J_D(CTZ = 1/5)$	$J_D(Expected)$
.35	.35	$(CTZ = 1)_{opt}$	1.14	1.29	.89	1.10
.48	.26	$(CTZ = 5)_{opt}$	1.08	1.41	.67	1.05
.27	.47	$(CTZ = 1/5)_{opt}$	1.08	1.09	1.07	1.08
.32	.39	$E[J_D(w_x, ctz(\omega))]$	1.13	1.22	.98	1.11
.28	.45	$(\overline{CTZ})_{opt}$	1.10	1.26	.87	1.08

There is a significant physical meaning of the optimal design from the stochastic solution.

From the base case, there is a greater absolute change in productivity realizing lower

permeability than higher permeability. In other words, there is a gain in productivity when

permeability is higher, but this gain does not offset the loss in productivity when the lower permeability state is realized.

At first glance it might seem that geometric average of the vertical permeability ratio, $CTZ = 1$, results in an expected value (1.10) that is close to the stochastic optimization solution expected value (1.11). While this is true, a closer look at the range of the productivity indices reveals that the stochastic solution has much tighter bounds. In the worst case—$CTZ = 1/5$—the stochastic solution design yields a productivity of 0.98 while the geometric average design yields a productivity of 0.89, which is significantly worse. Of course, in the case where $CTZ = 1$, the geometric average design yields a better productivity of 1.13 versus 1.14. In the best-case $= 5$, the geometric average design yields a higher productivity—1.26 versus 1.22 from the stochastic solution. This observation highlights the importance of variability and risk.

For a repeatable decision, the solution to the stochastic analysis will result in long-term higher expected profits. However, as discussed above, for any single decision there will be a single outcome. Even when designing for the optimal long-term performance, there will be inherent variability of each exact outcome. *This is the definition of risk*. A decision maker may only be able to make a decision once, and using purely expected values of the objective variable may not yield satisfactory results. To resolve this issue as introduced above, utility theory is applied.

For this hypothetical situation, it is assumed that there is a *threshold* dimensionless productivity that must be met. For productivity above this level, the marginal gain in utility will diminish. For productivity below this level, the marginal loss in utility will be exacerbated. This risk profile can be precisely accounted for in modified exponential utility function.

$$u(J_d) = r\left(1 + e^{-\frac{(J_d - J_{dth})}{r}}\right) + J_{dth} \quad \dots\dots\dots\dots\dots\dots\dots\dots\dots\dots\dots\dots\dots\dots \quad (4.11)$$

where r is a coefficient reflecting the decision makers' risk level, and J_{dth} is the threshold dimensionless productivity.

The optimization problem can be set as before with a modification of the objective function.

$$\max E_{ctz}[u(J_D(w_x, ctz(\omega)))]$$

$$w_x w_z = C$$

$$0 < w_x < \frac{1}{2}, 0 < w_z < \frac{1}{2} \quad \dots\dots\dots\dots\dots\dots\dots\dots\dots\dots\dots\dots\dots\dots \quad (4.12)$$

In this formulation the goal is to maximize the expected utility. It must be stressed again that the utility does not have physical meaning; it is a measure for comparative purposes.

1.4
1.3
1.2
1.1
1
0.9
0.8
0.7
0.6
0.5
0.4

CTZ=5

CTZ=1

CTZ Expected

CTZ=1/5

Utility

0.25   0.3   0.35   0.4   0.45   0.5

Dimensionless Height
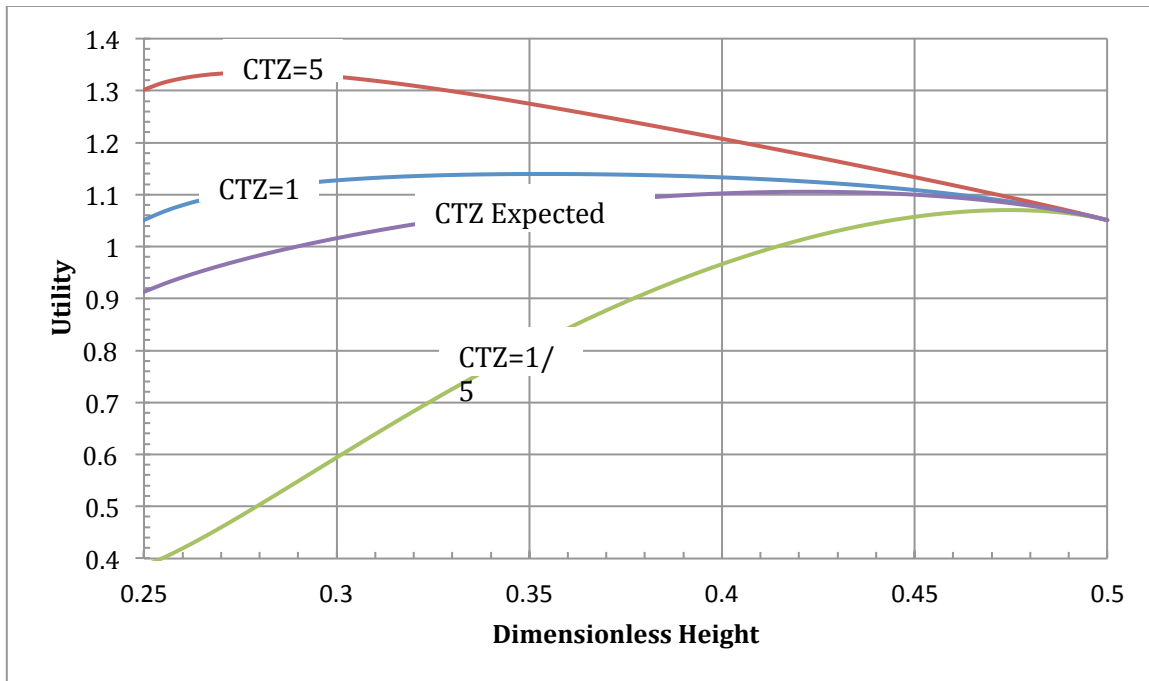
Fig. 4.4. Dimensionless height versus utility for different anisotropy ratios

Table 4.6. Summary of Stochastic Optimization with Utility

w_x	w_z		$u(CTZ=1)$	$u(CTZ=5)$	$u(CTZ=1/5)$	$u(expected)$
.35	.35	$(CTZ=1)_{opt}$	1.14	1.27	.82	1.08
.48	.26	$(CTZ=5)_{opt}$	1.09	1.33	.43	.95
.27	.47	$(CTZ=1/5)_{opt}$	1.09	1.10	1.07	1.08
.29	.42	$E[u(J_D(w_x,ctz(\omega)))]_{opt}$	1.12	1.17	1.01	1.10

Table 4.6 gives the stochastic program summary for the utility objective function. The

optimal dimensions are shifted closer to the worst-case optimum. This is directly a result

of the utility function by definition, which discounts lower productivity at a greater rate

than productivity above the threshold. In essence, the happiness gained from realizing a

good situation is lower than the loss realized in a bad situation. This behavior occurs due

to the risk conservative profile that puts greater weight on the worst-case scenario. By

68

using the utility formulation, risk can be directly quantified and accounted for in

optimization purposes.

At times, an exact utility function is difficult to formulate if the risk preference is

unknown. An alternate optimization method that does not account explicitly for risk but

solely variability in the outcome maximizes the expected outcome minus the variance of

the outcomes.

For this hypothetical case an optimization, is formulated by Eq. 4.13:

$$\max[(1-r)E_{ctz}[J_D(w_x, ctz(\omega))] - rV(J_D(w_x, ctz(\omega)))]$$

$$w_x w_z = C$$

$$0 < w_x < \frac{1}{2}, 0 < w_z < \frac{1}{2} \quad \text{..} \quad (4.13)$$

where r is a coefficient reflecting the weighting of variance. Higher r will reduce the

variability while lower values will increase the variability. For $r = 1$, the solution will

solely minimize the variance, and for $r = 0$, the solution will solely maximize the

expected value.

Table 4.7 Summary of Stochastic Optimization with Variance

r	w_x	w_z	$J_D(CTZ = 1)$	$J_D(CTZ = 5)$	$J_D(CTZ = 1/5)$	$J_D(Expected)$
0	.32	.39	1.13	1.22	.98	1.11
.5	.29	.43	1.12	1.17	1.03	1.10
1	.25	.49	1.05	1.05	1.05	1.05

Table 4.7 shows that increasing the weighting factor on variance reduces the range of

possible outcomes at the cost of expected value. This analysis can be used to directly

account for variability when utility is unknown.

CHAPTER V

HYDRAULIC FRACTURE OPTIMIZATION: VERTICAL WELLS

Fracture design for the Lower Tertiary will predominantly revolve around determining the optimal number of stages for a vertical well. In our investigation, reservoir uncertainty was manifested in the vertical permeability. Economic uncertainty existed in the total cost of the fracture treatment, which depended on the number of stages. Design uncertainties included fracture height growth. This was represented as a two-stage stochastic program with simple recourse.

Background

For the deterministic optimization, the optimal number of stages for a vertical well is determined for a constant set of economic and physical parameters. The objective functions were (1) net-present-value and (2) utility. The premise of this problem was to find the optimum trade-off between the number of fracture stages, fracture half length, width, and vertical penetration. Mathematically, we dealt with an integer nonlinear programming problem, as the number of stages could not take on non-integer values.

Constraints

The main constraint in this optimization was fracture height growth. For a vertical well in a relatively thick homogenous formation, a radial (penny-shaped) fracture can be

expected. This implies an aspect of ratio of 1 where the total fracture length (two half-lengths) equals the fracture height.

$$w_x = w_z \quad\text{..} \quad (5.1)$$

However, in lieu of this assumption, data from completion of the Cascade well given by Haddad, Smith, and Moraes (2012) in Fig 5.1, shows an aspect ratio of 2 where the fracture half-length equals the fracture height.
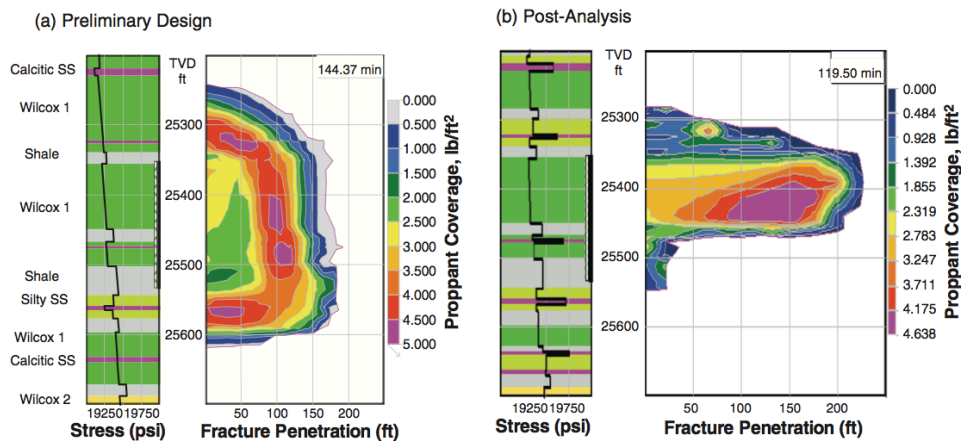
Fig. 5.1. Actual and planned fracture height growth (Haddad 2012)

This implies

$$\frac{1}{2}w_x = w_z \quad\text{..} \quad (5.2)$$

This data shows a designed fracture geometry of $x_f \approx 150$ ft and $h_f \approx 300$ ft while the post-treatment analysis shows $x_f \approx 200$ ft and $h_f \approx 200$ ft. The uncertainty in fracture

72

height growth in a highly anisotropic formation has profound implications on wellbore productivity. Therefore, in the following example we focus on the uncertainty in height growth and vertical permeability.

Reservoir Inputs

The deterministic inputs for the formation, wellbore, and operations are given in Table 5.1.

Table 5.1. Lower Tertiary Properties

Depth (ft)	30000	Gravity (API)	22
Well Spacing (acre)	500	GOR (cfb)	400
Gross (ft)	1500	Viscosity (cp)	5
Net/Gross (%)	50	Bubblepoint (psi)	2500
Effective Porosity (%)	.18	Formation Volume Factor (Rb/Stb)	1.1
Water Saturation (%)	0.25	Initial Pressure (psi)	20000
Horizontal Permeability (md)	5 md	Drawdown (psi)	5000

The formation depth, oil gravity, and gas/oil ratio will significantly impact the reservoir abandonment pressure. From preliminary analysis, the vertical lift requirement results in a reservoir abandonment pressure of 12,000 psi.

An important characteristic is the rather high drawdown of 5,000 psi. Generally, this drawdown is much higher than operators applied previously in the Gulf of Mexico Miocene and Outer Shelf plays. However, it is consistent with recent public well tests (Fig. 5.2).

FIELD	OPER	LEASE	WELL	API NO	PROD INT	DATE	TYPE	METHOD	SIBHP	PRODUCT	TEST HRS	CHOKE
WATER VOL	SI PRSS	GOR	B S & W	FLOW TB PRSS	OIL RATE	GAS RATE		WATER RATE	API GRAV	GAS SPGR		GAS DISP
WR206	01207	G16970	CA003	608124003800	S01 04/02/2012		POT	FL		O	24	11
	245		.89	7643	4763	1168		43	24.2	.846		
WR206	01207	G16970	CA003	608124003800	S01 06/10/2012		SEM	FL				136
	11120	165	.21	3208	6535	1080		14	24.3			
WR206	01207	G16970	CA003	608124003800	S01 12/04/2012		SEM	FL				136
	7337	207	.41	3247	3641	755		15	24.6			

Fig. 5.2. Results of public well tests (BOEM)

Furthermore, the drawdown assumption is consistent with Dusterhoft, Strobel, and Szatny (2012) analysis of the Lower Tertiary.

The stochastic reservoir inputs for this analysis were vertical permeability and fracture height growth. They are given in Table 5.2 .For simplicity, uniform distribution was used to demonstrate the value of stochastic programing.

Table 5.2 Probabilistic Inputs for Stochastic Optimization

Horizontal to Vertical Permeability Ratio (k_h/k_v)	Probability
1	.25
10	.25
100	.25
1000	.25
Fracture Height Aspect Ratio	Probability
1	.5
2	.5

At first glance, the horizontal to vertical permeability ratio of 1,000 may seem unrealistic, but according to Haddad, Smith, and Moraes (2012) and Ogier et al. (2011) there is effectively zero vertical permeability in the Cascade/Chinook field.

Preliminary Analysis: Fractured Vertical Well Performance

Before proceeding with the optimization, it is enlightening to highlight some subtle yet important outcomes of fracture performance in a thick anisotropic reservoir with partial vertical penetration.

Effect of Partial Height Penetration and Vertical Anisotropy:

Dimensionless Time and Dimensionless Productivity

The effect of partial height penetration on dimensionless productivity for different anisotropy ratios is displayed in the graphs below (Figs. 5.3 to 5.6). The transient behavior is considered because situations with low vertical permeability and limited fracture height penetration do not reach pseudosteady-state behavior at the generally accepted $t_{DA} \approx 0.1$.
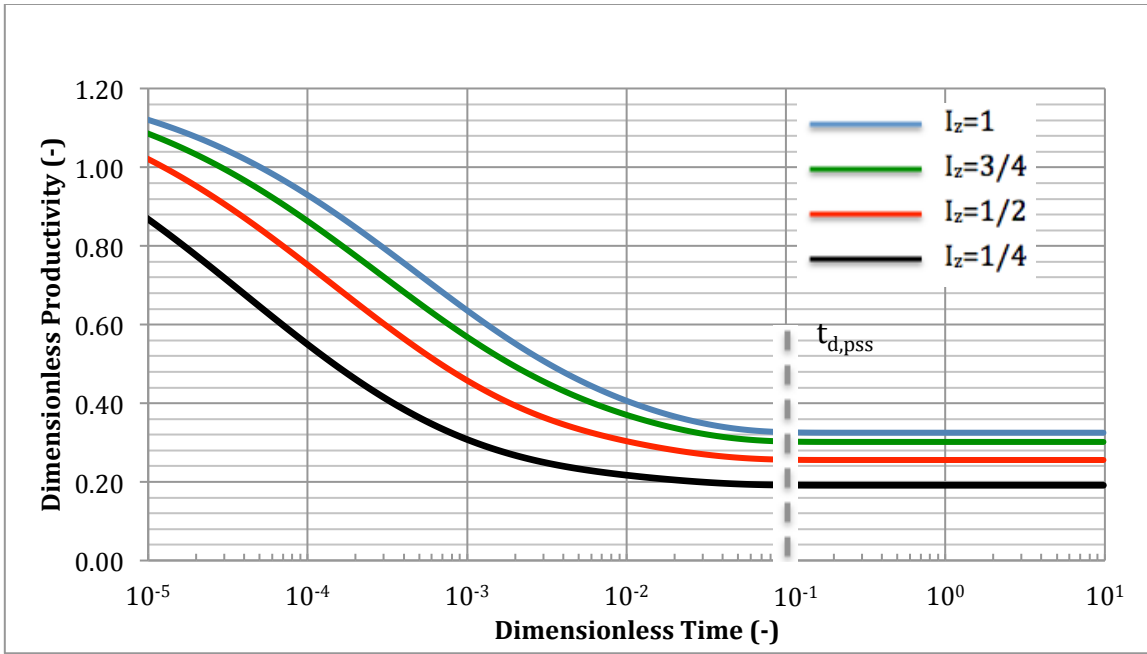
Fig. 5.3. Dimensionless productivity for *Ix*=1/8 and *kz=kh*
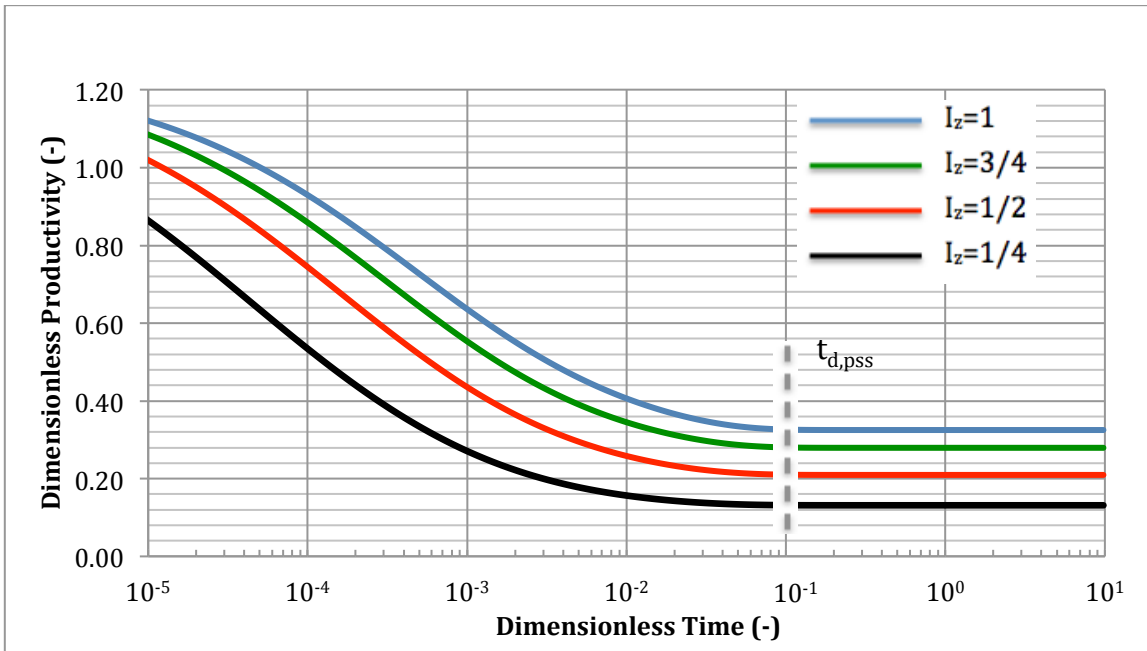
Fig.5.4. Dimensionless productivity for *Ix*=1/8 and *kz=kh*/10
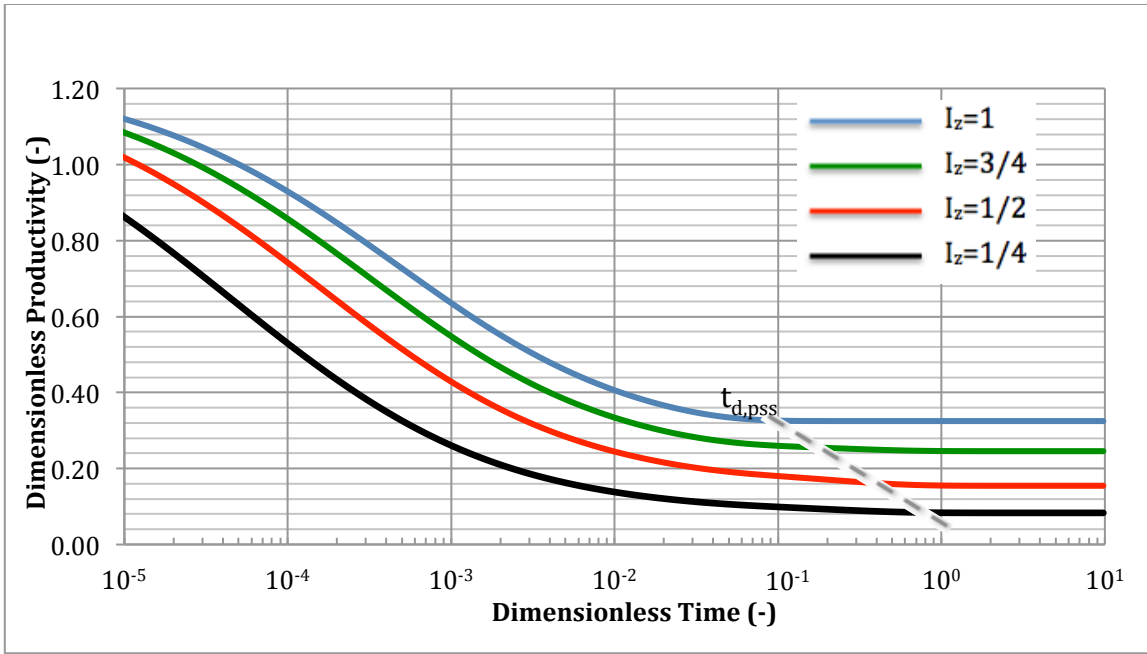
Fig. 5.5. Dimensionless productivity for *Ix*=1/8 and *kz*=*kh*/100
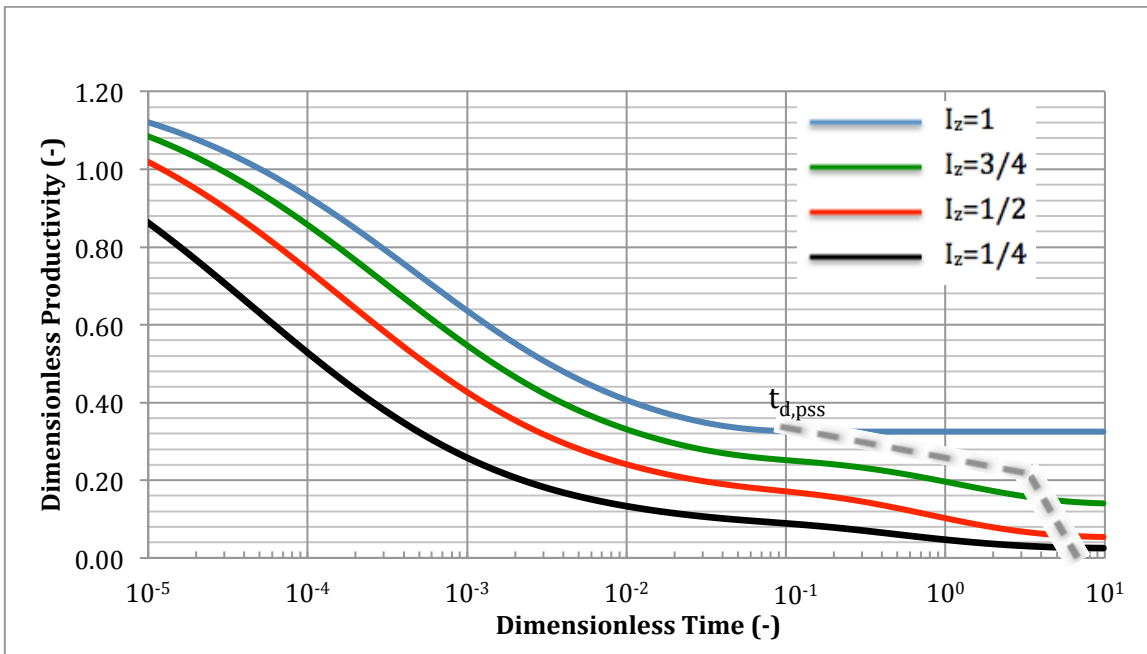
Fig. 5.6. Dimensionless productivity for *Ix*=1/8 and *kz*=*kh*/1000

As expected, the dimensionless productivity in the transient and pseudosteady state are vastly reduced with decreasing vertical permeability and vertical penetration ratio. For the cases of k_h/k_v=1 and k_h/k_v=10, pseudosteady state is reached at the expected $t_{DA} \approx 0.1$. However, as the anisotropy increases to k_h/k_v=100 and k_h/k_v=1,000, pseudosteady state is not reached at $t_{DA} \approx 0.1$ but at a later time, depending on the exact conditions.

An interesting condition is shown in Fig. 5.5 with anisotropy of k_h/k_v=1,000—distinct curvature at late dimensionless time that cannot be seen in the other figures. This phenomenon represents the boundary effects on productivity, in which the horizontal boundaries are felt much sooner than the vertical boundary. This behavior is exhibited for the other situations but is too rapid to see with relativity low values of anisotropy.

The importance of including the transient behavior of the dimensionless productivity cannot be deemed trivial. Using only the pseudosteady-state productivity will underestimate wellbore performance at early absolute times for high levels of anisotropy and low vertical fracture penetration. For subsequent optimization purposes, when considering the risk and cost of additional stages, disregarding the transient behavior could incorrectly bias the design, forcing more vertical penetration when in reality it may not be needed.

Effect of Partial Penetration Vertical Anisotropy and Fracture Growth

Assuming that fracture height growth follows a prescribed aspect ratio, it may be impossible to achieve the optimal dimensionless productivity given by unified fracture design. Assuming a fixed aspect ratio, the fracture height is intrinsically linked to the half-length and subsequently average width. For a partially penetrating fracture height, this leads to comprises between fracture height, half-length, and width that are dependent on the horizontal and vertical permeability. The effect of finite conductivity in the fracture directly competes against the effect of partial height penetration in the reservoir. This leads to an interesting result for fractures with low proppant numbers, in which the optimal dimensions do not occur at full penetration. Graphs of height penetration following an aspect ratio of 2 ($x_f = h_f$) versus dimensionless productivity are presented in Figs. 5.7 to 5.9 below.
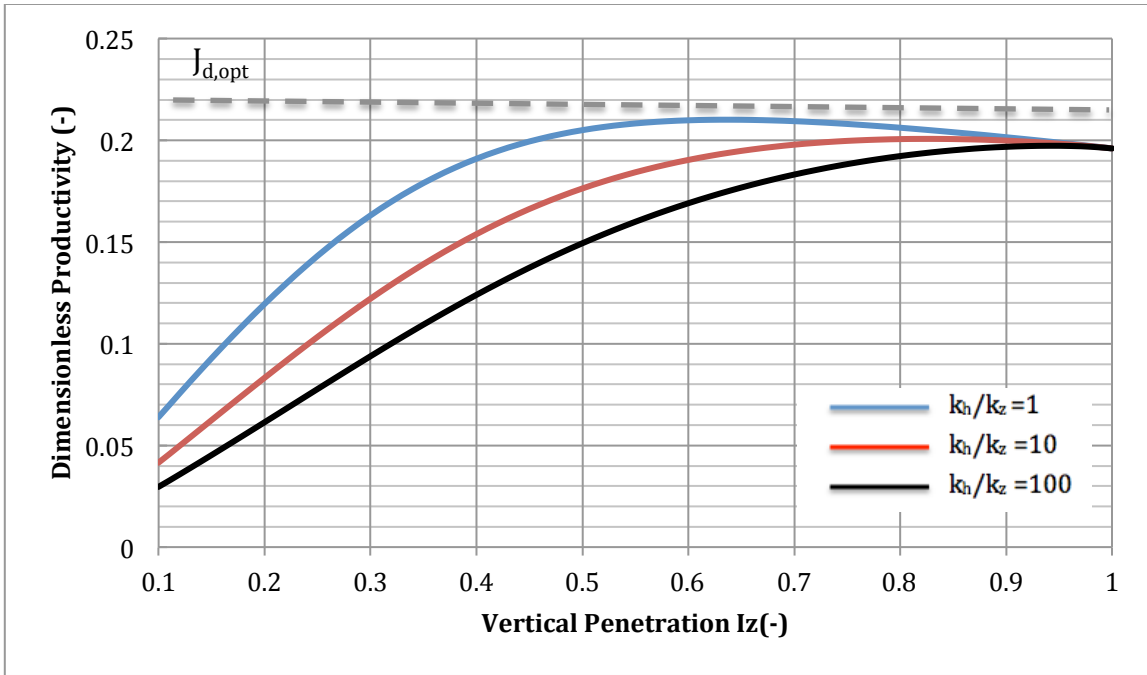
Fig. 5.7. Dimensionless productivity versus height penetration for *N*prop=0.001
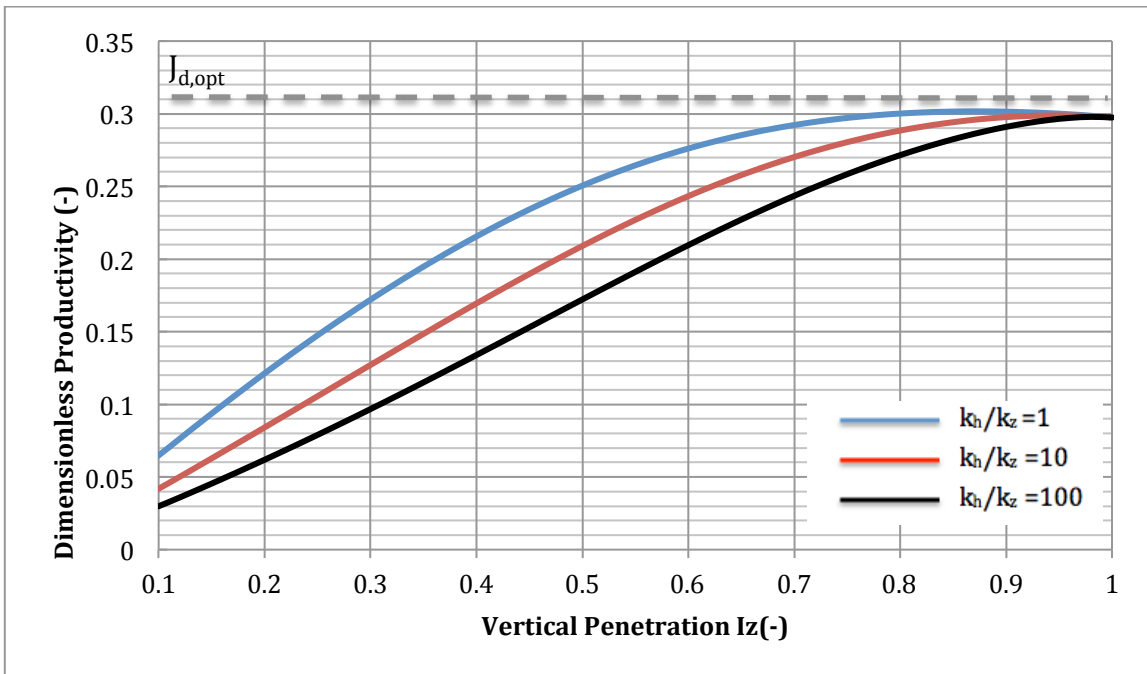
Fig. 5.8. Dimensionless productivity versus height penetration for *N*prop=0.01
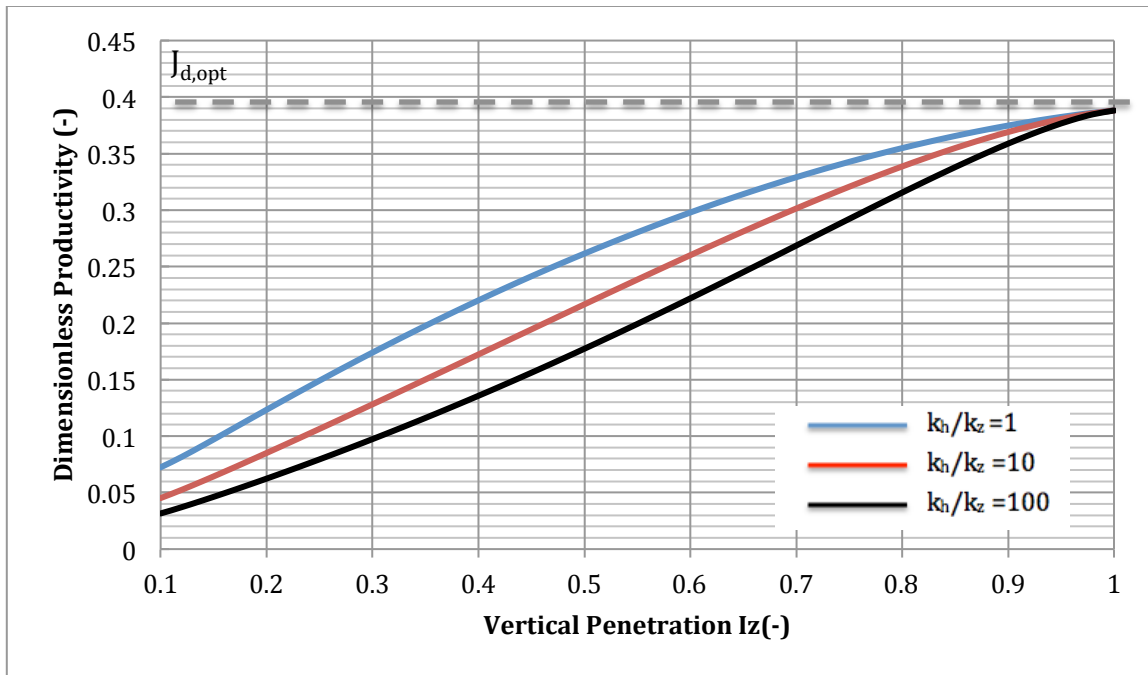
Fig. 5.9. Dimensionless productivity versus height penetration for Nprop=0.1

For N_{prop}=0.001 and k_h/k_v=1, a curious result occurs: the optimal productivity occurs at partially penetrating fracture height. However, as the proppant number and/or the anisotropy increases, the optimal productivity *always* occurs at full vertical penetration. Furthermore, due to the aspect ratio constraint, the optimal productivity may occur at dimensionless fracture conductivities less than 1.6 (the lower bound on optimum C_{fD} in case of full vertical penetration.)

An outcome to note from this analysis is the confirmation of maximum dimensionless productivity given by unified fracture design (UFD). Even with horizontal permeability that equals vertical permeability, the optimal dimensionless productivity cannot exceed that given by UFD.

Risk Analysis

Offshore applications are subject to significant risk due to the hostile operating environment and extreme financial costs involved. Although hydraulic fracturing for productivity is common onshore with financial risks well understood, the same cannot be said for the offshore environment. For a complete analysis of the benefits of hydraulic fracturing, specific offshore risks must be accounted for.

In comparison to the entire cost of drilling and completing an offshore well, the proppant cost is nearly insignificant. However, the risk associated with fracturing is paramount as any nonproductive time could result in millions of dollars. Ogier et al. (2011) outlined numerous completion-related problems related to multistage single fracturing in the Lower Tertiary: premature opening of the monitoring sleeve, a stuck service tool, a leak in the sump, and excessive erosion in the crossover tool. Fig. 5.10 gives a breakdown of the completion times related to each stage of the fracture process.

Lower Completion Time, days						
	Well A			Well B		
Task	Trouble Free	NPT	Total	Trouble Free	NPT	Total
TCP Perforate	3.2	0.5	3.7	3.4	0.1	3.5
De-burr	2.7	0.0	2.7	2.3	0.0	2.3
Make up tools at surface	0.9	0.1	1.0	1.4	0.0	1.4
Run in hole and set packers	2.0	0.0	2.0	2.2	3.9	6.1
Stimulate lower zone	2.1	1.6	3.7	1.5	0.1	1.6
Stimulate middle zone	2.0	20.8	22.8	1.4	2.3	3.7
Stimulate upper zone	1.6	0.0	1.6	1.8	2.2	4.0
Trip out of hole and tear down tools	0.9	0.0	0.9	0.9	0.0	0.9
Top-Off jobs – lower & middle zones	---	---	---	0.0	4.1	4.1
Cleanout trip	0.0	1.8	1.8	---	---	---
Run and set intermediate assembly & POOH	4.1	0.1	4.2	2.8	0.1	2.9
TOTAL	19.5	24.9	44.4	17.7	12.8	30.5

Fig. 5.10. Deepwater lower completion time analysis (from Ogier 2011)

For future analysis and forecasting, the above data were used to calibrate a Markov

Chains of nonproductive time. A Markov chain is formerly defined as

$$Pr(X_{n+1} = x | X_1 = x_1, X_2 = x_2, \dots, X_n = x_n) = Pr(X_{n+1} = x | X_n = x_n) \dots\dots\dots\dots (5.3)$$

The Markov chain represents an independent transition from one to state to next. The

transition does not depend on the previous states, only on the current state. Using the

above data and assuming a lognormal distribution. a series of Markov chains was

generated to predict nonproductive time associated with fracturing additional stages. The

Markov chain of non-productive-time versus number of fractures stages is given in Fig

5.11
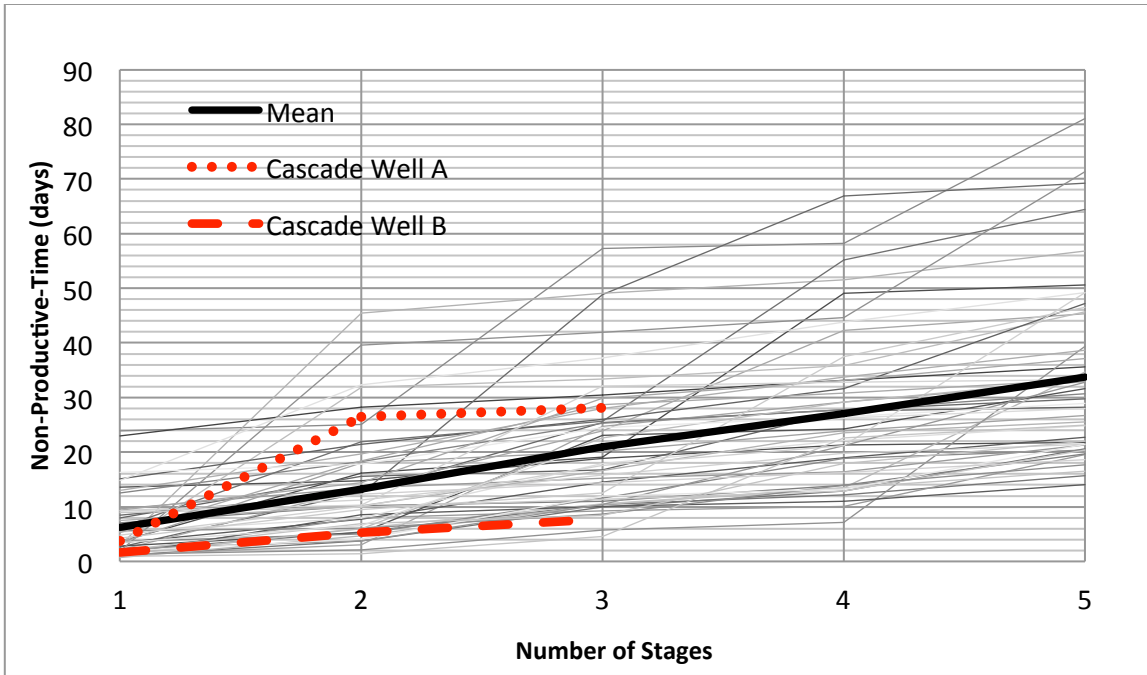
Fig. 5.11. Markov chain representation of NPT versus number of stages

These realizations were used to generate probability density curves representing the time associated with fracturing additional stages. The probability density plots are given in Fig. 5.12.
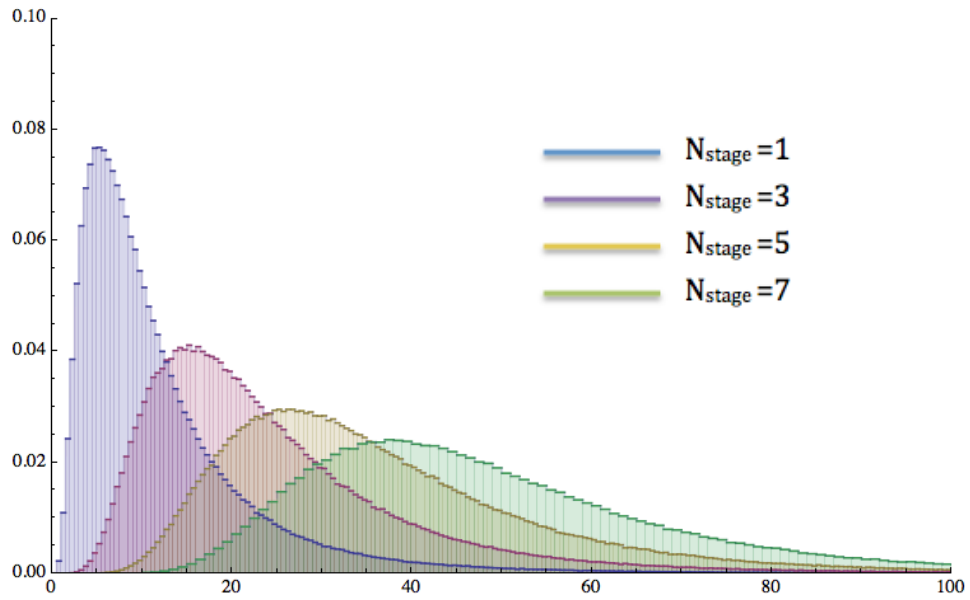
Fig. 5.12. Fracture time versus number of stages

These results can be used in determining the expected value and variation of possible

times associated with fracturing additional stages.

Deterministic Optimization Results

As mentioned above, the objective was to determine the optimal number of stages to fracture for a vertical well in an anisotropic formation subject to fracture height constraints. The objective function was the maximization of NPV and the number of stages were the decision variable. For this optimization, a maximum of 1 million lb of 30/60 buaxite proppant were available. This constraint is consistent with current mechanical integrity standards of the completion equipment. A schematics of the optimization procedure is given in Fig. 5. 13.

The trade off in the optimization is the fracture half-length and the total fracture height at any given stage. Since each individual fracture height is directly linked to the fracture half-length (via the aspect ratio), increasing the number of stages directly affects the overall vertical penetration.

$$H_{\text{total}} = N_{\text{stage}} h_f \quad \text{.. (5.4)}$$

In effect, increasing the number of stages will simply bypass the aspect ratio constraint and allow for a more theoretically optimal design.
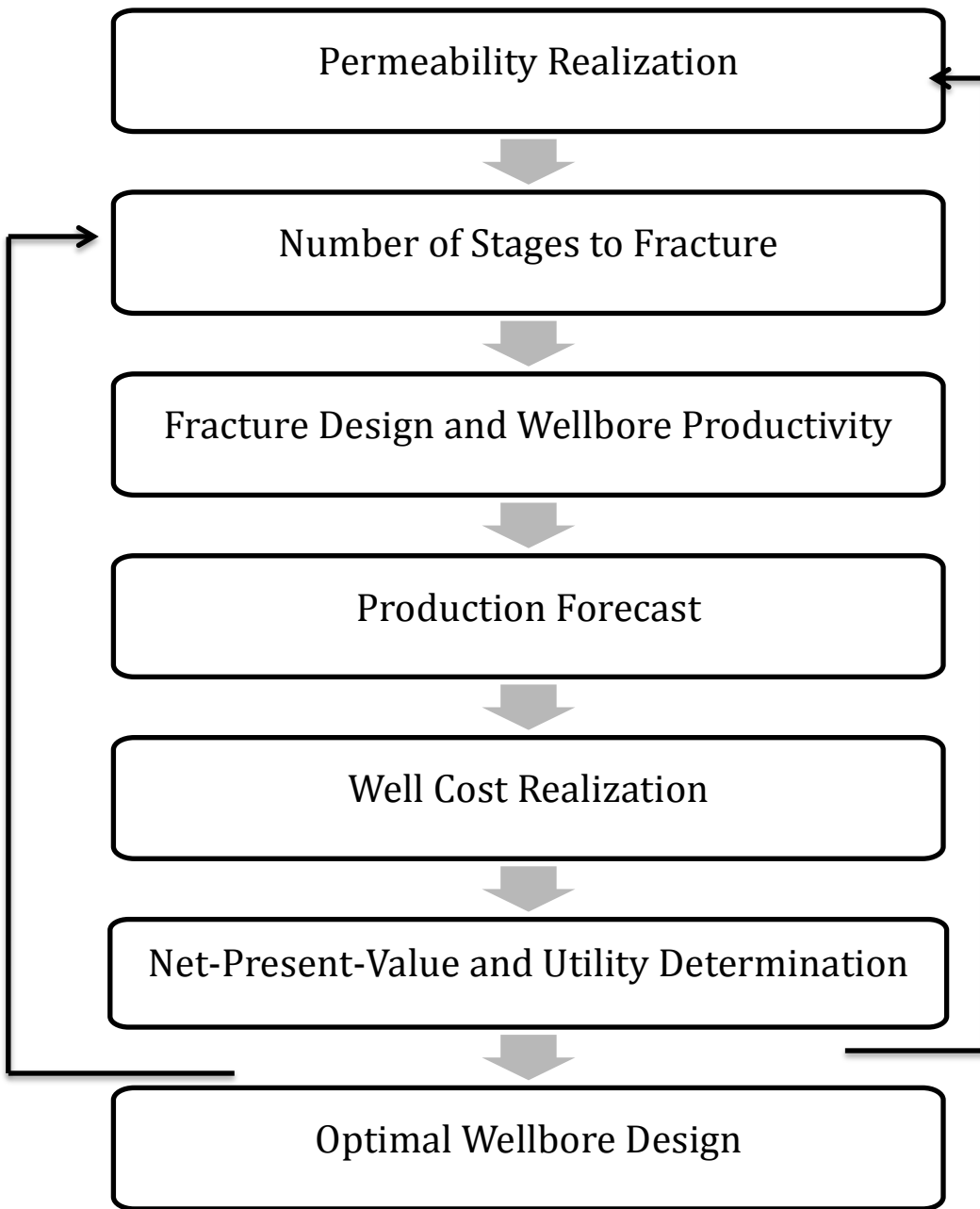
Fig. 5.13. Optimization procedure

Aspect Ratio 1

The first situation investigated is for an aspect ratio of 1 ($2\ x_f = h_f$). The NPV and

dimensionless productivity are graphed in Figs. 5.14 and 5.15. Tables 5.3 to 5.4 show the

fracture dimensions, dimensionless parameters, and NPV at each stage.

Fig. 5.14. NPV versus number of stages to fracture for *Ar*=1

Fig. 5.15. Dimensionless productivity versus number of stages to fracture for *Ar*=1

Table 5.3. Optimization Results *Ar*=1: Fracture Properties

# of Fracture	Half Length (ft)	Average Width (in.)	Fracture Height (ft)	Total Height (ft)
1	337	0.079	337	337
2	238	0.079	238	476
3	194	0.079	194	583
4	168	0.079	168	673
5	143	0.801	143	749
6	125	0.0956	125	750
7	109	0.111	109	750

Table 5.4. Optimization Results *Ar*=1: Fracture Conductivity, Vertical, and Horizontal Penetration Ratio

# of Fracture	Dimensionless Conductivity (C_{fd})	Horizontal Penetration Ratio (I_x)	Vertical Penetration Ratio (I_z)
1	0.39	0.144	0.44
2	0.55	0.102	0.63
3	0.68	0.083	0.77
4	0.78	0.072	0.89
5	0.89	0.064	0.99
6	1.27	0.053	1
7	1.71	0.046	1

Table 5.5. Optimization Results *Ar*=1: NPV

# of Fracture	NPV(mm$) k_h/k_v=1	NPV(mm$) k_h/k_v=10	NPV(mm$) k_h/k_v=100	NPV(mm$) k_h/k_v=1000
1	62	18	-33	-73
2	**87**	63	35	3
3	85	**76**	61	45
4	77	75	**70**	64
5	68	68	68	**68**
6	57	57	57	57
7	45	45	45	45

Table 5.7 shows that for different levels of reservoir anisotropy there are distinct optimal numbers of stages to fracture. For k_h/k_v=1, the optimal number of stage is 2; for k_h/k_v=10, the optimal number of stages is 3; for k_h/k_v=100, the optimal number of stages is 4; for k_h/k_v=1,000, the optimal number of stages is 5. As the anisotropy increases, the number of stages increases, the fracture half-length decreases, and the individual fracture height decreases while the net fractured height penetration increases. Furthermore, the fracture widths remain constant until the entire pay is fractured. This result is consistent with the preliminary analysis given in Figs. 5.7 to 5.9. For moderate proppant numbers, with any

level of anisotropy the optimal design always favors more vertical penetration. Since vertical penetration is directly linked to half-length until the entire formation is penetrated vertically, the width and corresponding fracture conductivity are comprised .

Aspect Ratio 2

The next situation investigated was for an aspect ratio of 2. The NPV and dimensionless productivity were graphed in Figs. 5.16 and 5.17. Tables 5.6 to 5.8 show the fracture dimensions at each stage, dimensionless parameters, and NPV at each stage.
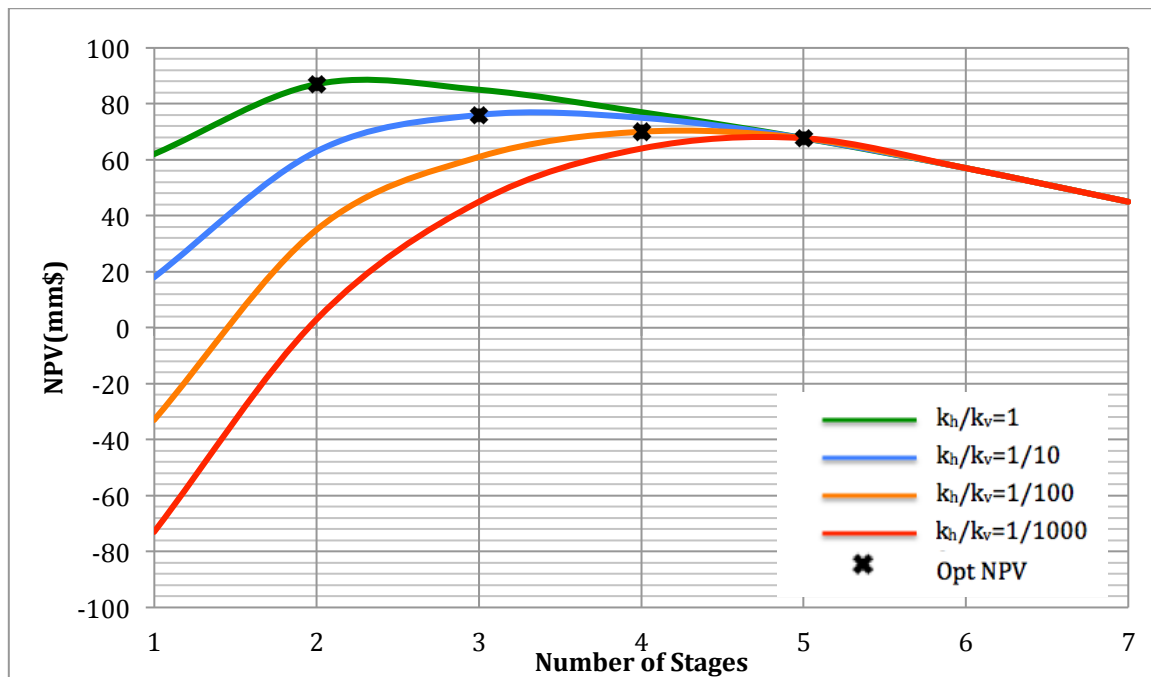

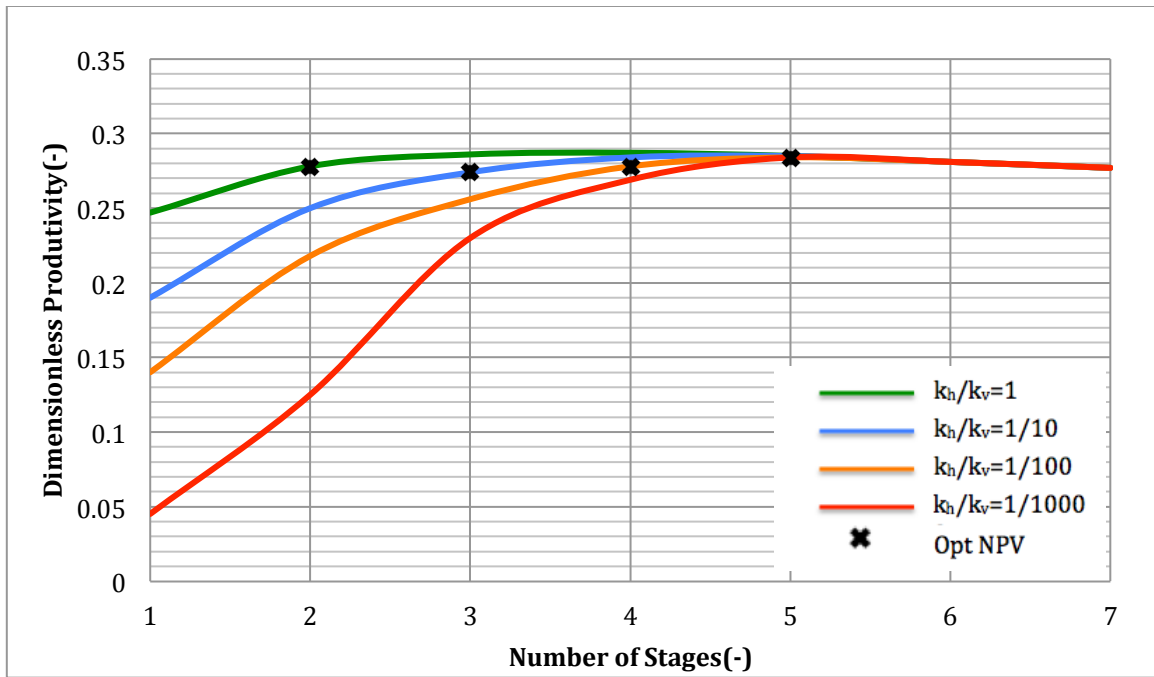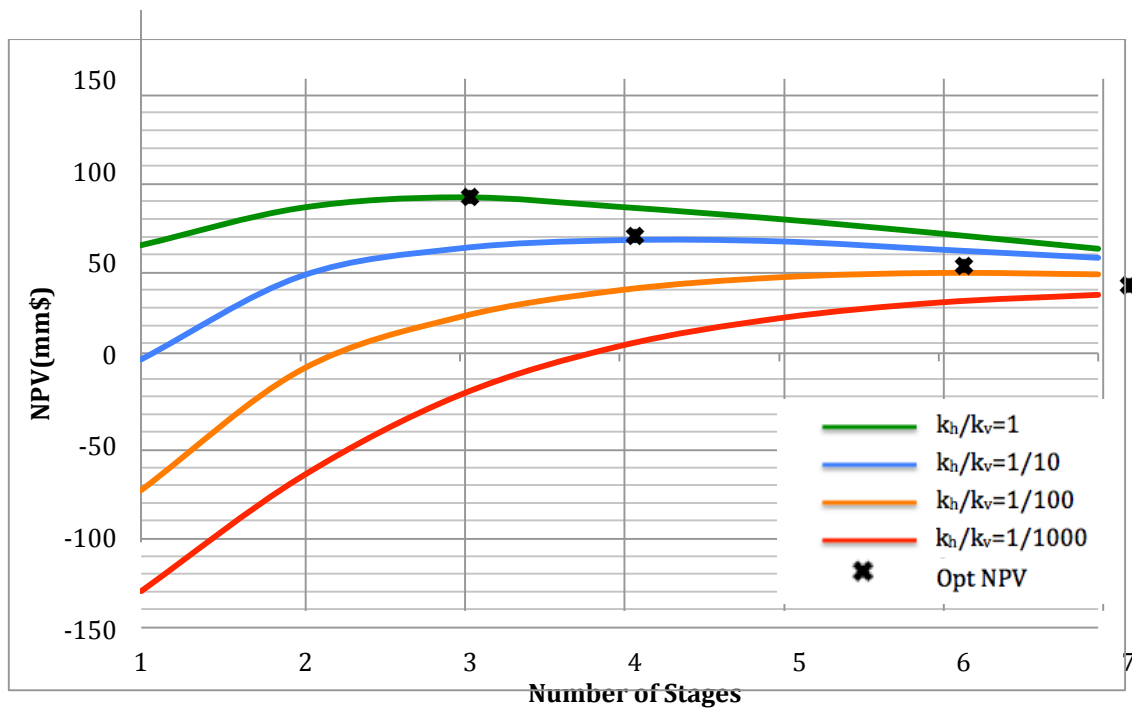**Fig. 5.16. NPV versus number of stages to fracture for *Ar*=2**
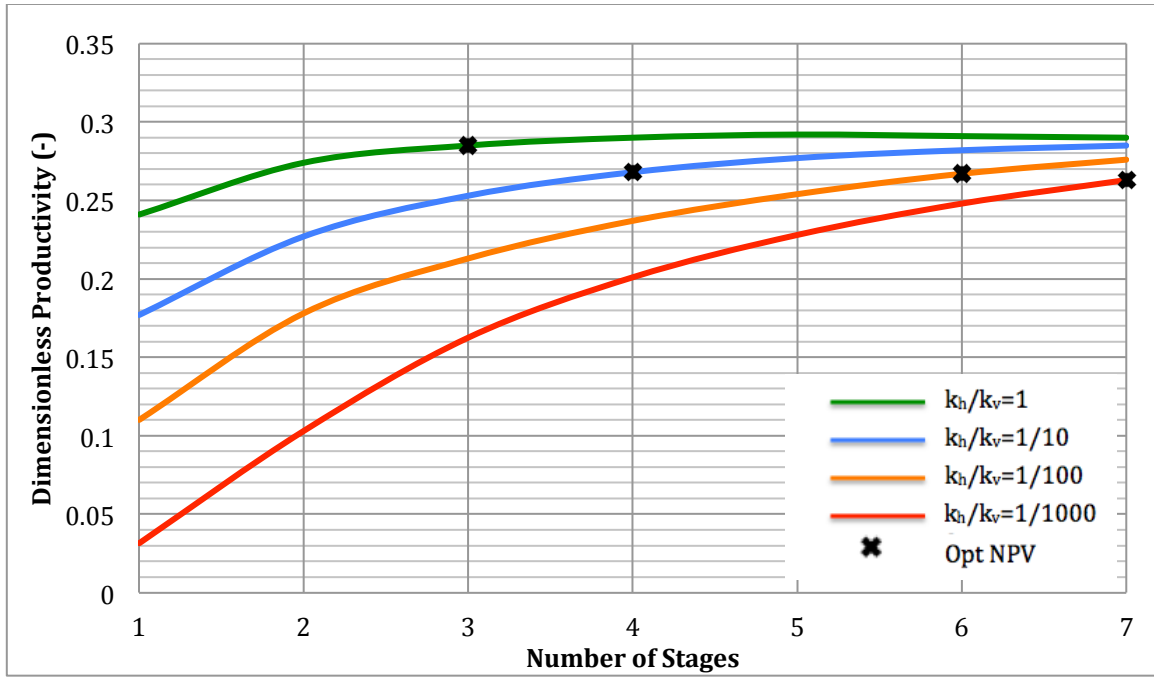
Fig. 5.17. Dimensionless Productivity versus Number of Stages to Fracture for *Ar*=2

Table 5.6. Optimization Results: *Ar*=2: Fracture Properties

# of Fracture	Half Length (ft)	Average Width (in.)	Fracture Height (ft)	Total Height (ft)
1	476	0.079	238	238
2	336	0.079	168	336
3	274	0.079	137	411
4	238	0.079	119	476
5	212	0.079	106	530
6	194	0.079	97	582
7	179	0.079	89	623

92

Table 5.7. Optimization Results *Ar*=2: Fracture Conductivity, Vertical, and Horizontal Penetration Ratio

# of Fracture	Dimensionless Conductivity (C_{fd})	Horizontal Penetration Ratio (I_x)	Vertical Penetration Ratio (I_z)
1	0.277	0.203	0.31
2	0.3982	0.144	0.448
3	0.4812	0.12	0.55
4	0.555	0.1	0.63
5	0.621	0.091	0.71
6	0.68	0.083	0.77
7	0.735	0.077	0.839

Table 5.8. Optimization Results *Ar*=2: NPV

# of Fracture	NPV (mm$) k_h/k_v=1	NPV (mm$) k_h/k_v=10	NPV (mm$) k_h/k_v=100	NPV (mm$) k_h/k_v=1000
1	58.9	-3.35	-75	-130
2	84.54	43.44	-7.26	-65.84
3	**85.29**	59.19	22.8	-19.4
4	80.58	**63.8**	37.85	8.1
5	73.73	63.135	45.12	23.8
6	65.66	58.52	**47.6**	32.65
7	57	53.86	46.8	**37**

For each level of reservoir anisotropy, there is a distinct optimal number of stages. For

k_h/k_v=1, the optimal number of stages is 3; for k_h/k_v=10, the optimal number of stages is 4;

for k_h/k_v=100, the optimal number of stages is 6; for k_h/k_v=1,000 the optimal number of

stages is 7. The results differ significantly from the previous case in which the aspect ratio

was 1. For an aspect ratio of 2, the fracture propagates more in the horizontal direction

than in the vertical direction. This impacts total wellbore performance as it takes more

stages to cover the entire interval. In fact, even after 7 stages the overall vertical

penetration is significantly less than unity. The optimal design calls for more fracture stages to achieve satisfactory vertical coverage.

For this aspect ratio, the effect of anisotropy is much more severe. Due to the limited height penetration for a single fracture, more stages are needed, increasing costs and decreasing NPV.

Stochastic Optimization Reservoir Uncertainty

Above we summarized the deterministic optimization for different ratios of vertical to horizontal permeability. The next step in the analysis was to consider the ratio of vertical permeability uncertain. For simplicity, we characterized the uncertainty with a discrete distribution of probabilities (Table 5.4). Again, two different cases of aspect ratios were considered.

Aspect Ratio 1

Fig. 5.18 shows the NPV for different vertical permeability as well as the expected NPV. Table 5.9 lists the NPV for each stage.
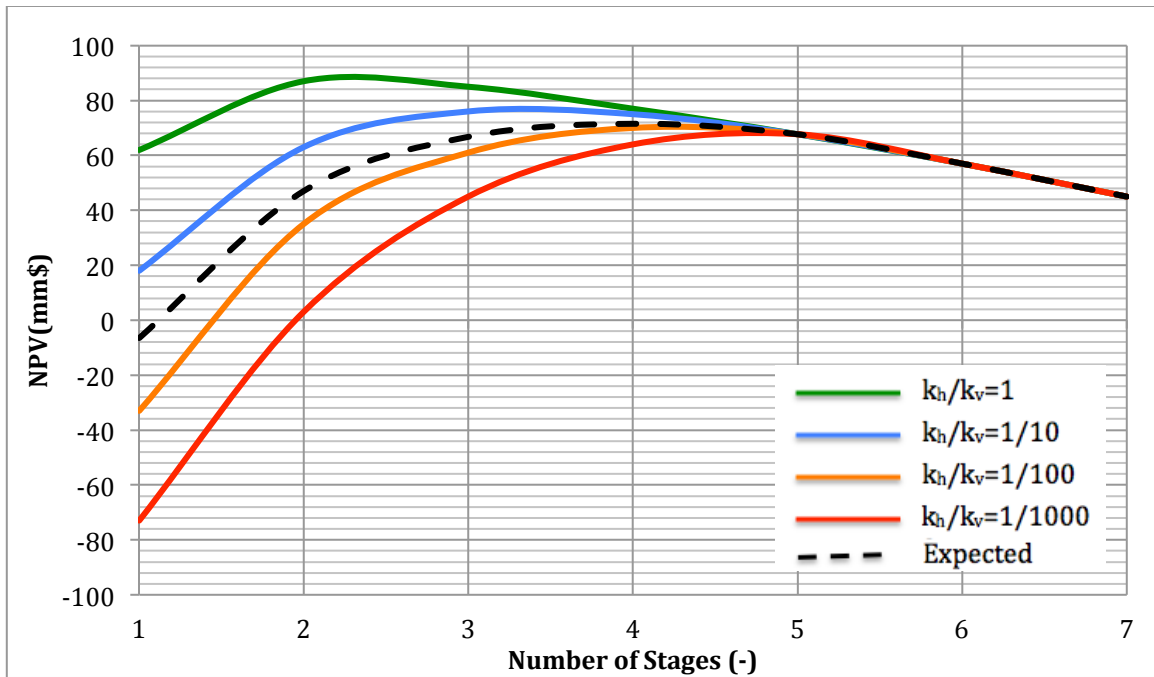
Figure 5.18 Expected NPV versus number of stages to fracture for *Ar*=1

Table 5.9. Expected Net Present Results *Ar*=1

# of Fracture	Expected NPV (mm$)
1	-6.5
2	47
3	66.75
4	**71.5**
5	67.7
6	57
7	45

Recalling the deterministic results, each realization of permeability had an optimal number of stages. For k_h/k_v=1, the optimal number of stages is 2; for k_h/k_v=10, the optimal number of stages is 3; for k_h/k_v=100, the optimal number of stages is 4; for k_h/k_v=1,000,

the optimal number of stages is 5. Now, considering the uncertainty in each realization, the optimal number of stages is 4.

Aspect Ratio 2

Fig. 5.19 shows the NPV and the corresponding expected NPV for various vertical permeabilities . Table 5.10 lists the NPV for each stage.
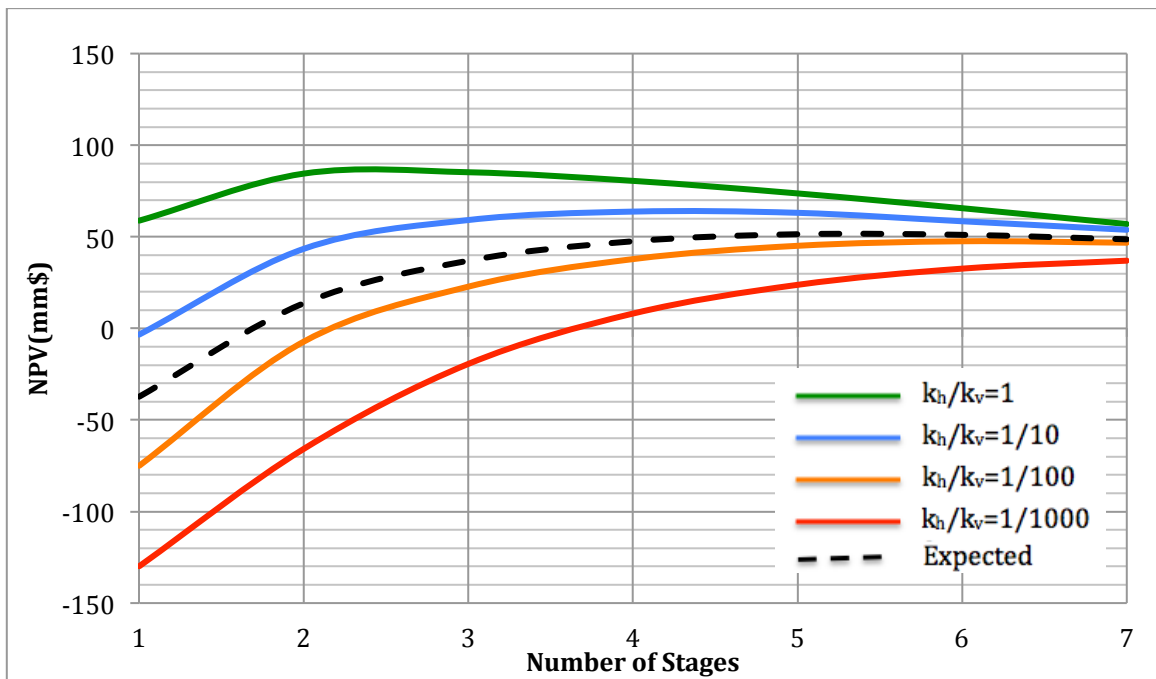
Fig. 5.19. Expected NPV versus number of stages to fracture for *Ar*=2

Table 5.10 Expected NPV s Results: *Ar*=2

# of Fracture	Expected NPV (mm$)
1	-37.36
2	13.72
3	36.97
4	47.58
5	51.50
6	51.10
7	48.66

In the deterministic case, each realization of permeability had an optimal number of stages. For k_h/k_v=1, the optimal number of stage is 3; for k_h/k_v=10, the optimal number of stages is 4; for k_h/k_v=100, the optimal number of stages is 6; for k_h/k_v=1,000, the optimal number of stages is 7. Now, considering the uncertainty in each realization, the new optimal number of stages is 5 .

As expected, when considering uncertainty the actual optimal number of stages falls in between the best- and worst-case scenarios. However, in the above analysis the expected NPV was used as an objective function. Even when designing for an expected outcome, only one single realization will occur, so designing 6 stages could result in any one of 4 possible NPV outcomes {73,63,45,23}. For nonrepeatable situations, or when certain targets must be met, it may be warranted to impose a conservative risk profile. This can be systematically achieved by applying the utility formulation.

For this case, a dimensionless modified exponential utility function is appropriate:

$$u(x) = r\left(1 - e^{-\frac{x}{r}}\right) \dots\dots\dots\dots\dots\dots\dots\dots\dots\dots\dots\dots\dots\dots\dots (5.5)$$

The utility is dimensionless and monotonic. The actual value has no physical or economic meaning; its use is restricted for comparative purposes.

Returning to the aspect ratio of 2, Fig. 5.20 and Table 5.11 show the effect of incorporating utility with a "very conservative" risk profile (r=50).
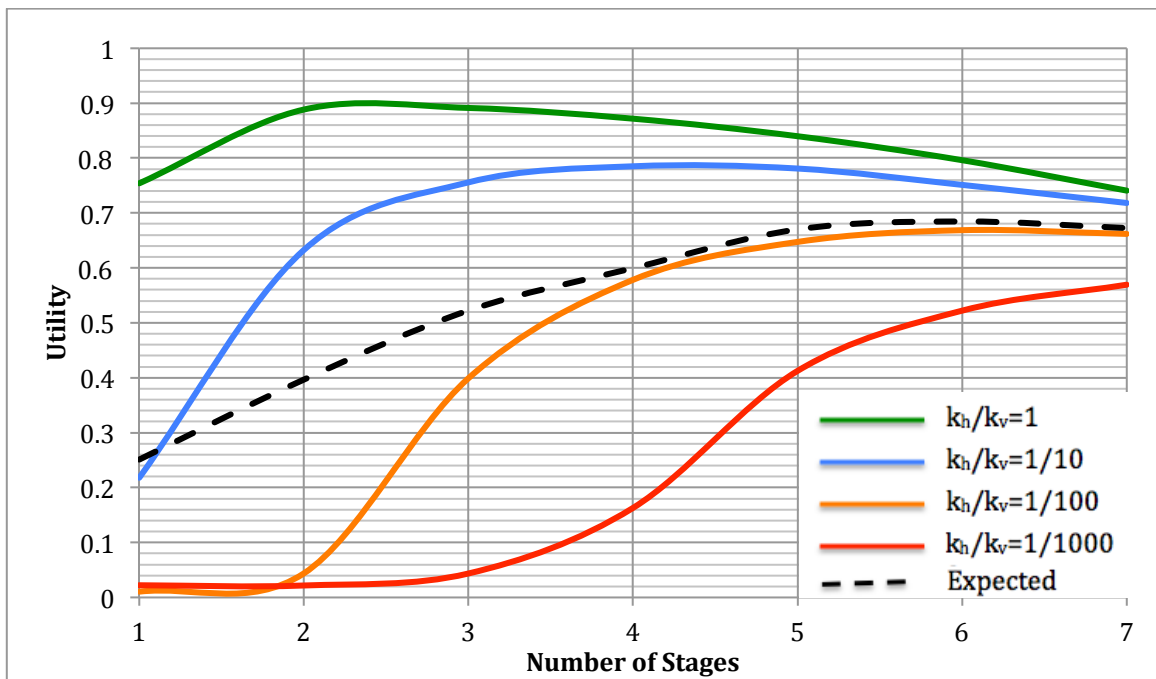
Fig. 5.20. Very conservative utility versus number of stages to fracture for *Ar*=2

98

Table 5.11 Optimization Results *Ar*=**2: Reservoir Uncertainty, Very Conservative Utility**

# of Fracture	Utility k_h/k_v=1	Utility k_h/k_v=10	Utility k_h/k_v=100	Utility k_h/k_v=1000	Utility Expected
1	0.75	0.22	0.01	0.02	0.25
2	0.88	0.63	0.04	0.03	0.40
3	**0.89**	0.76	0.40	0.04	0.52
4	0.87	**0.79**	0.58	0.16	0.60
5	0.84	0.78	0.65	0.41	0.67
6	0.80	0.75	**0.67**	0.52	**0.68**
7	0.74	0.72	0.66	**0.57**	0.67

Applying the conservative profile determines the optimal utility for each realization. The optimal number of stages will be *not* different from the case when the NPV was the objective function. For k_h/k_v=1, the optimal number of stages is 3; for k_h/k_v=10, the optimal number of stages is 4; for k_h/k_v=100, the optimal number of stages is 6; for k_h/k_v=1,000, the optimal number of stages is 7. This is expected, as the optimization is still deterministic at this point.

However, when applying uncertainty, the expected utility results in a different number of stages. For the conservative risk profile, the optimal number of stages is 6. In effect, the conservative utility reduces the number of stages and hence the overall risk, while maintaining reasonable expected NPV.

Fig. 5.21 and Table 5.12 show the effect on the less-risk-conservative profile (r=500).
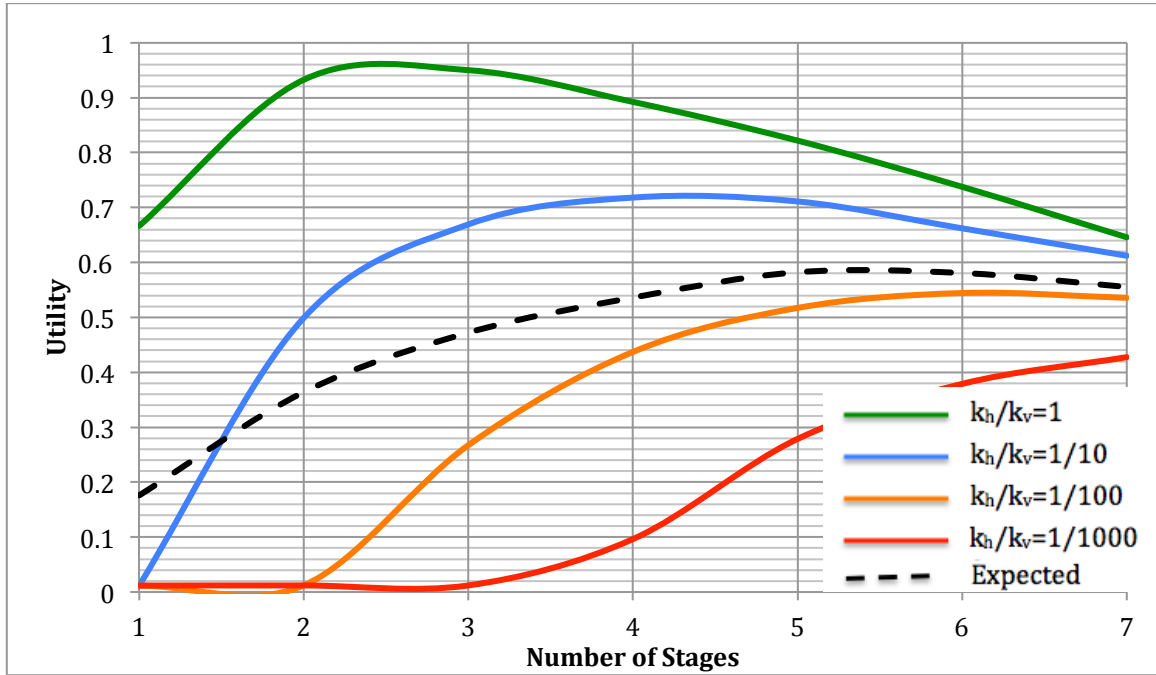
Fig. 5.21. Less conservative utility versus number of stages to fracture for *Ar*=2

Table 5.12. Optimization Results *Ar*=1: Reservoir Uncertainty, Conservative Utility

# of Fracture	Utility k_h/k_v=1	Utility k_h/k_v=10	Utility k_h/k_v=100	Utility k_h/k_v=1000	Utility Expected
1	0.67	0.01	0.01	0.01	0.18
2	0.93	0.50	0.01	0.01	0.36
3	**0.95**	0.67	0.27	0.01	0.47
4	0.89	**0.72**	0.44	0.10	0.54
5	0.82	0.71	0.52	0.28	**0.59**
6	0.74	0.66	**0.54**	**0.38**	0.58
7	0.65	0.61	0.54	0.43	0.56

By applying a less-risk-conservative profile, the outcome is the same as that of the NPV optimization. This illustrates the flexibility of the utility function: direct levels of risk can be assigned in many different ways, and it is possible to be moderately risk conservative, but not overly conservative (effectively leaving the NPV optimization decision unchanged).

Stochastic Optimization Cost Uncertainty

The Markov chains and probability density function generated above give an excellent quantification of the risk associated with increasing the number of stages in the fracturing operation. In the previous optimization, the NPV was determined by the expected value of the associated number of stages. However, similar to the discussion before, using the expected value does not account for associated risk. In order to directly quantify the risk, the utility function was applied.

Fig. 5.22 and Table 5.13 show the utility per stage associated with the completion cost risk.
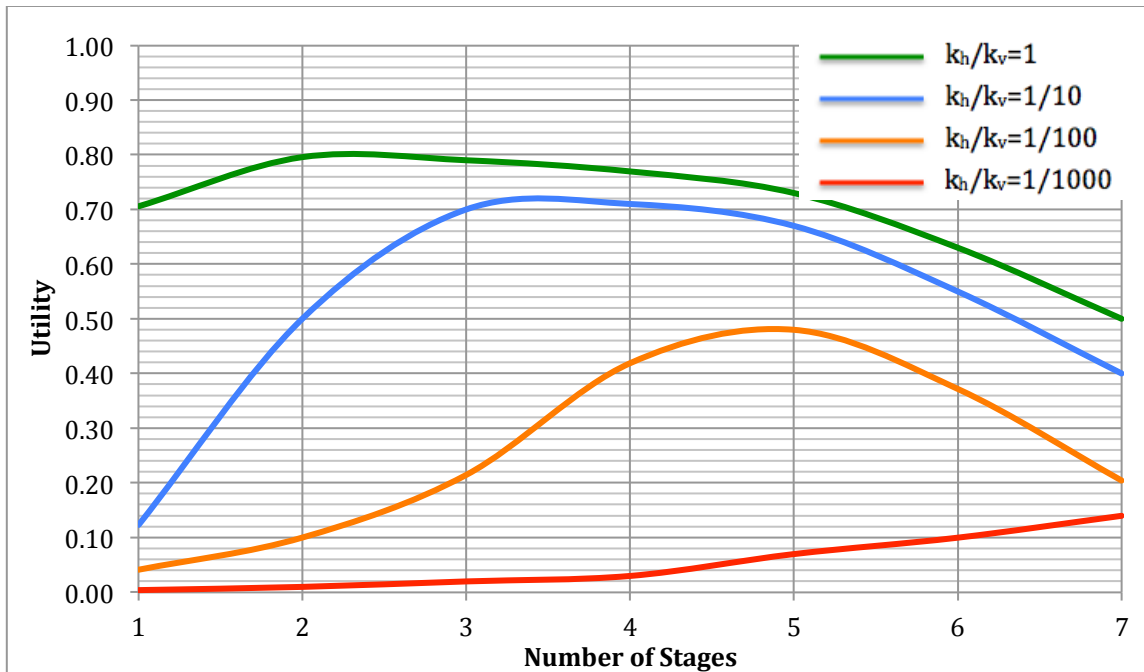
Fig. 5.22. Cost Uncertainty Utility Versus Number of Stages to Fracture for Ar=2

Table 5.13 Optimization Results *Ar*=2: Cost Uncertainty Utility

# of Fracture	Utility $k_h/k_v=1$	Utility $k_h/k_v=10$	Utility $k_h/k_v=100$	Utility $k_h/k_v=1000$
1	0.71	0.12	0.04	0.00
2	**0.80**	0.50	0.08	0.01
3	0.79	**0.71**	0.21	0.01
4	0.77	0.70	0.42	0.02
5	0.70	0.65	**0.44**	0.04
6	0.60	0.53	0.37	0.08
7	0.45	0.36	0.20	**0.12**

In considering the completion cost uncertainty, the optimal utility generally results in a

lower number of fractures. This is the case for $k_h/k_v=1$, $k_h/k_v=10$, and $k_h/k_v=100$, in

which each individual optimum number of stages is less than the optimum given by the

NPV criteria. Logically this is intuitive: as the number of stages increases, the risk increases; and in order to limit risk, we must limit the number of stages. However, for k_h/k_v=1,000, the optimum number of stages is still 7, the same as in the case of expected NPV optimization. This can be understood if we recall that there are such significant losses in wellbore productivity at lower fracture penetration for that anisotropy level, and that even with reduced risk tolerance, the best decision is to fracture "as much as possible."

Stochastic Optimization: Reservoir and Cost Uncertainty

In the above examples the uncertainty had a profound effect on decision-making. In considering reservoir risk (vertical permeability variation), risk analysis favored more fracture stages to ensure maximum penetration. In considering economic risk (nonproductive completion time), risk analysis favored fewer fracture stages to minimize high costs. For the next analysis, reservoir and cost uncertainty were considered simultaneously. Firstly, we graphed the effect of the fracturing cost and reservoir uncertainty on NPV. Figs. 5.23 and 5.24 show the effects for aspect ratios of 2 and 1 respectively.
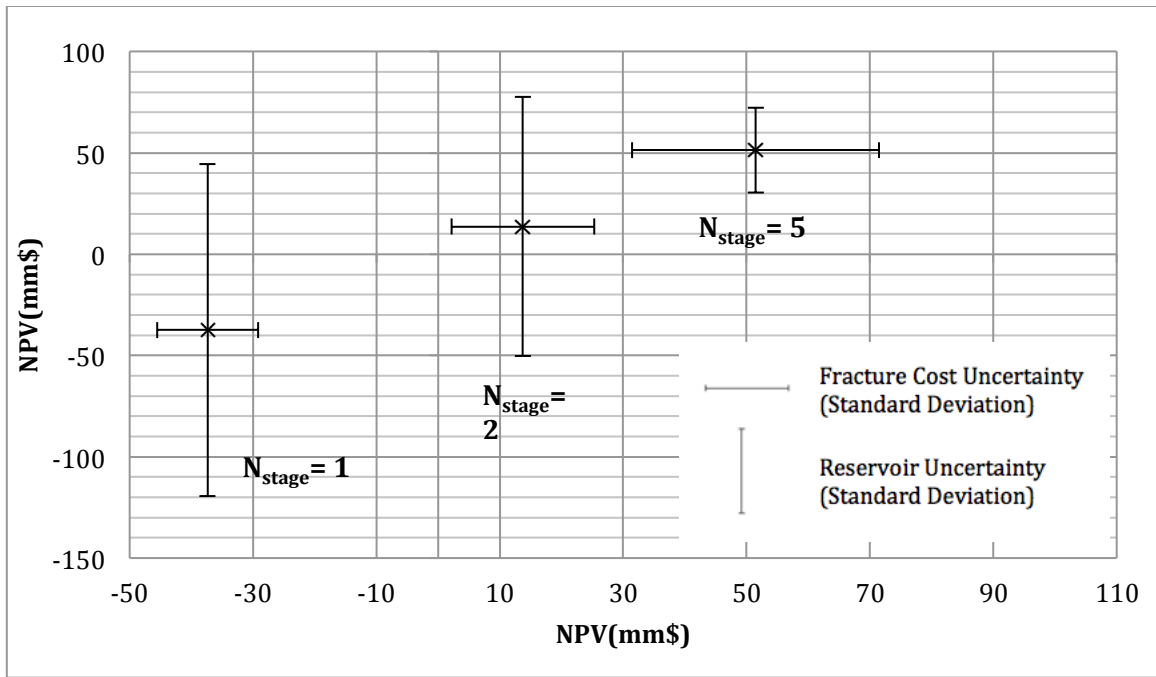
Fig. 5.23. Facture Cost uncertainty versus reservoir uncertainty *Ar*=2
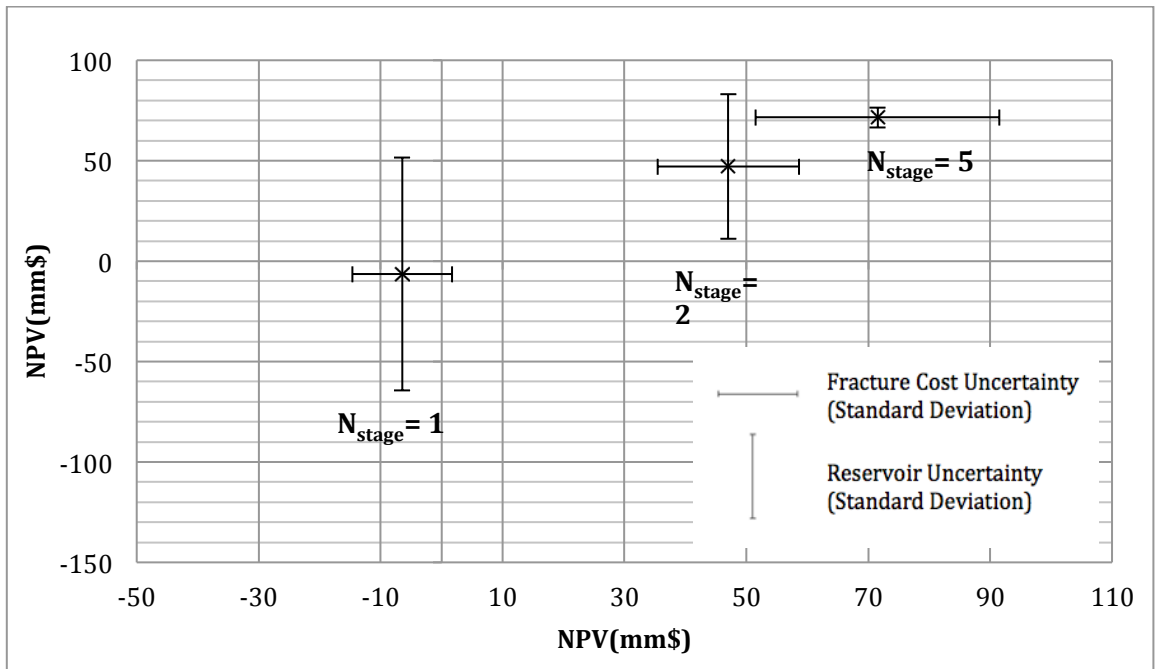
Fig. 5.24. Facture cost uncertainty versus reservoir uncertainty *Ar*=1

As seen, with a low number of stages the fracture cost risk is minimal but the reservoir risk is high. As the number of stages increases, the fracturing risk increases while the reservoir risk decreases. If the reservoir risk is calculated solely with respect to variation in vertical permeability (as in our case), the risk can be entirely eliminated when the entire zone is fractured (Fig 5.24). For any given situation, the optimal solution will depend on the range of uncertainties associated with each risk.

Using the previous example, for an aspect ratio =2 and conservative risk profile r=20, the expected utilities is given in Fig. 5.25 and Table 5.14.
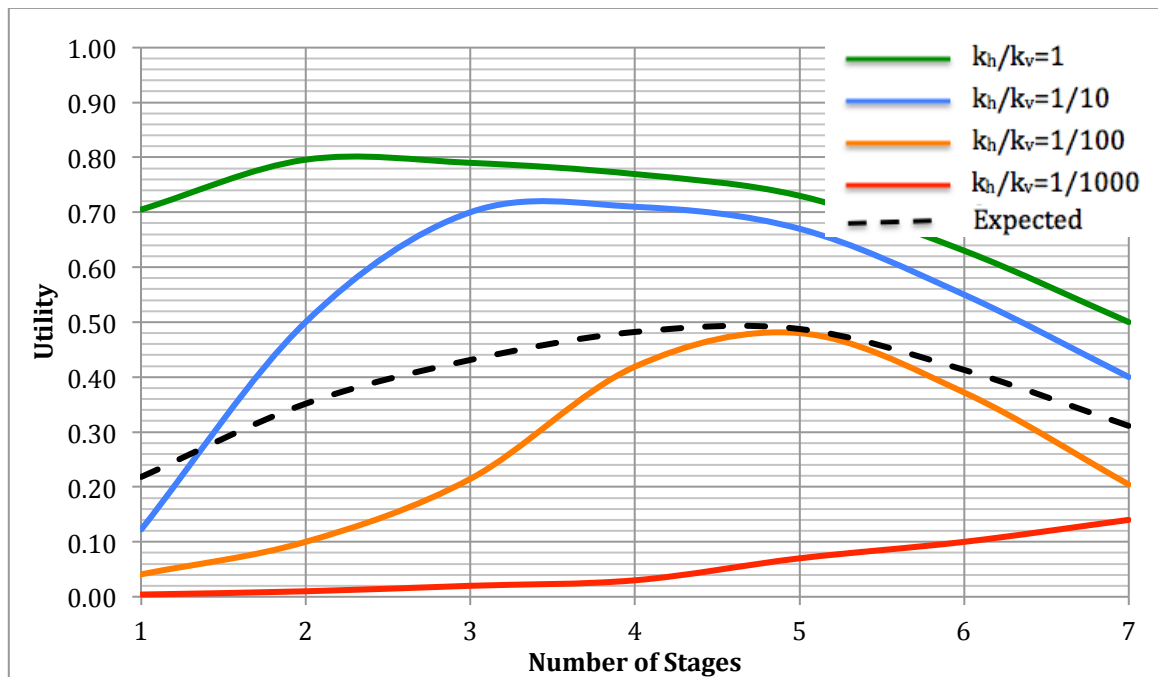
Fig. 5.25. Reservoir and cost uncertainty utility versus number of stages to fracture for Ar=2

Table 5.14. Optimization Results *Ar*=2: Reservoir and Cost Uncertainty Utility

# of Fracture	Utility $k_h/k_v=1$	Utility $k_h/k_v=10$	Utility $k_h/k_v=100$	Utility $k_h/k_v=1000$	Utility Expected
1	0.71	0.12	0.04	0.00	0.22
2	**0.80**	0.50	0.08	0.01	0.35
3	0.79	**0.71**	0.21	0.01	0.43
4	0.77	0.70	0.42	0.02	0.48
5	0.70	0.65	**0.44**	0.04	**0.49**
6	0.60	0.53	0.37	0.08	0.40
7	0.45	0.36	0.20	**0.12**	0.29

Considering both reservoir and completion cost uncertainty, a new optimum was found at 5 stages. Not surprisingly, this is a further compromise: the optimum number of stages is generally higher than the one considering only the operational cost risk, but generally lower than the one considering only the reservoir risk.

Stochastic Optimization: Fracture Height Uncertainty

The final case considered fracture height uncertainty as well as reservoir uncertainty. For this case, height growth follows an aspect ratio of either 1 or 2. Figs. 5.26 and Tables 5.15-5.16 show the expected NPV for each aspect ratio realization and the conditional expectation for all permeability realizations.
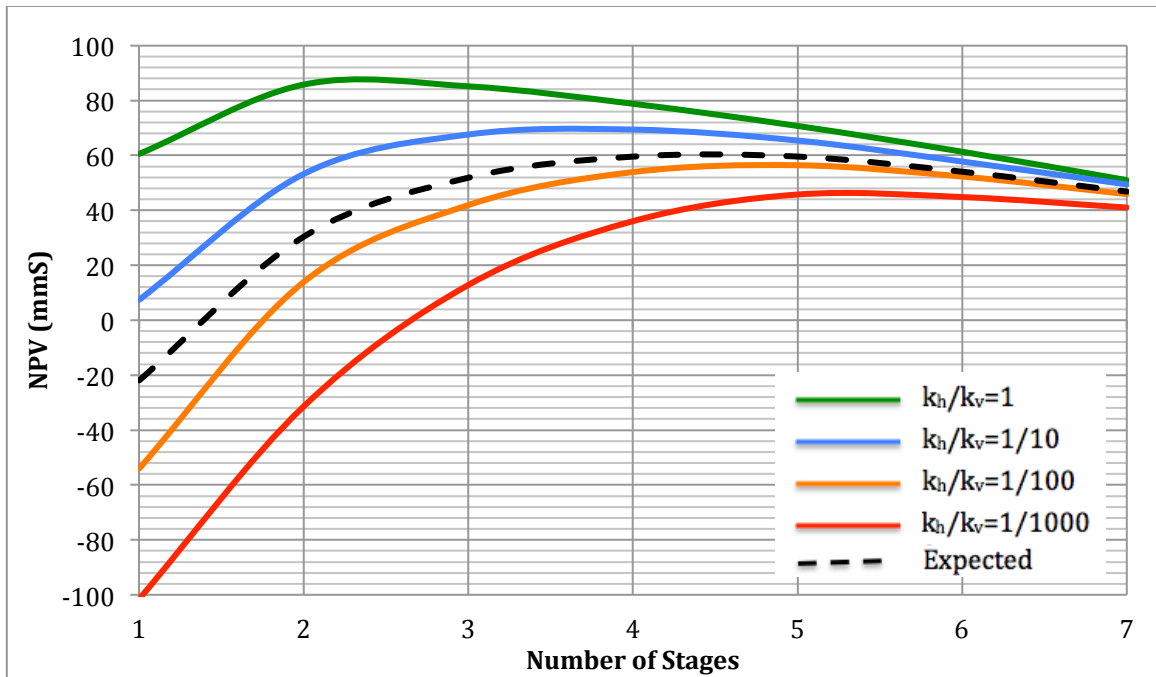
Fig. 5.26. Expected NPV versus number of stages to fracture for fracture height uncertainty

Table 5.15 Optimization Results, Fracture Height Uncertainty: NPV

# of Fracture	Exp. NPV (mm$) $k_h/k_v=1$	Exp. NPV (mm$) $k_h/k_v=10$	Exp. NPV (mm$) $k_h/k_v=100$	Exp. NPV (mm$) $k_h/k_v=1000$
1	60.45	7.325	-54	-101.5
2	**85.77**	53.22	13.87	-31.42
3	85.14	67.595	41.9	12.8
4	78.79	**69.4**	53.925	36.05
5	70.71	65.4175	**56.41**	**45.75**
6	61.33	57.76	52.3	44.825
7	51.33	49.4342	45.9	41

Table 5.16. Optimization Results Fracture Height Uncertainty: Expected NPV

# of Fracture	Condition Expected NPV(mm$)
1	-21.93
2	30.36
3	51.86
4	**59.67**
5	59.52
6	54.05
7	46.83

Considering the uncertainties in fracture height and vertical permeability, each realization

of permeability results in an expected NPV based on the fracture height realizations. Each

permeability realization determined an optimal number of stages. The conditional

expectation was then taken over all permeability realizations to determine the optimal

number stages for both height and permeability uncertainty. The optimal number of stages

for conditional expectation is 4. Interestingly, this is only slightly better than the NPV for

5 stages, but it has more variation. Again, to account for the risk, the utility theory is

applied as show in Fig. 5.27 and Table 5.17.
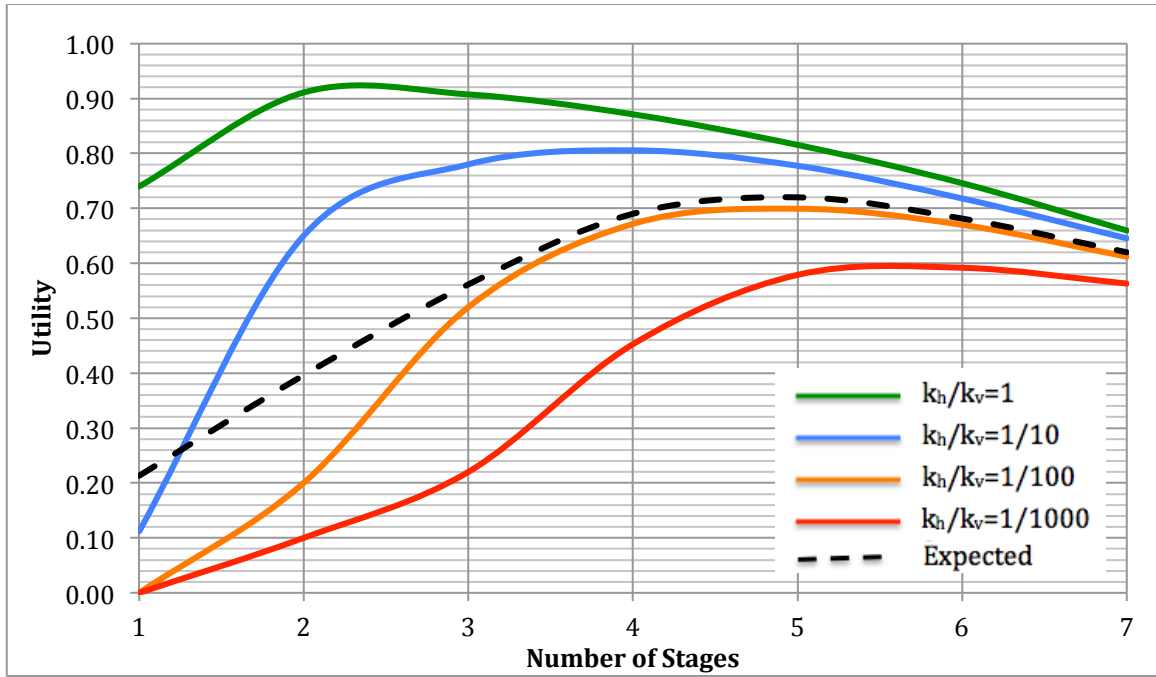
Fig. 5.27. Reservoir and fracture height utility versus number of stages to fracture

Table 5.17. Optimization Results, Fracture Height Uncertainty: Expected Utility

# of Fracture	Utility $k_h/k_v=1$	Utility $k_h/k_v=10$	Utility $k_h/k_v=100$	Utility $k_h/k_v=1000$	Utility Expected
1	0.74	0.11	0.00	0.00	0.21
2	**0.92**	0.65	0.20	0.10	0.40
3	0.91	0.78	0.52	0.22	0.56
4	0.87	**0.81**	0.67	0.45	0.69
5	0.82	0.78	**0.70**	0.58	**0.72**
6	0.75	0.72	0.67	**0.59**	0.68
7	0.66	0.65	0.61	0.56	0.62

Systematically accounting for risk in the cases of both reservoir and fracture height

uncertainty results in a new optimal number of stages. By no surprise, the optimum is 6.

Increasing the number of stages mostly compensated for the reservoir risk and tightened the range of outcomes .

Remarks

This analysis provided interesting insights. When reservoir permeability was a risk, the design favored more stages to fracture, but when completion cost was a risk, the design favored fewer stages to fracture. When fracture height growth was a risk, there was no general trend; in some cases the design favored more stages, in some other cases, less.

The analysis also hinted at a more general aspect of design under uncertainty, which is how decisions we make affect overall uncertainty. When the reservoir permeability was the risk, adding more stages reduced and even eliminated it. The economic risk, although seemingly out of the grasp of engineering, can be managed with best practices such as detailed "practice runs" in test facilities. The same cannot be said for fracture height-growth risk. No matter what decision is made, there is no way of eliminating that risk; the uncertainty exists in nature, and all that can be done is to design for the best-expected outcome or use more "out-of-box" thinking such as spending more resources on information that can reduce the particular uncertainty.

In essence, this analysis allows for specific quantification for associating a dollar value with specific geology and rock mechanics information. The differences in outcome (NPV) of the possible realizations can be directly used quantify the value of information and

whether further information gathering is warranted. It comes as no surprise that such

information is more valuable (or the lack of it is more detrimental) in an offshore

development than in traditional, onshore development.

Tables 5.18 to 5.20 summarize the results of these quantifications.

Table 5.18. Aspect Ratio 2

	Aspect Ratio 2	# of fractures
	Expected NPV k_h/k_v =1	3
	Expected NPV k_h/k_v =10	4
	Expected NPV k_h/k_v =100	6
Deterministic	Expected NPV k_h/k_v =1000	7
	Expected NPV Reservoir Risk	5
	Expected Utility Reservoir Risk	6
	Expected Utility Completion Cost Risk k_h/k_v =1	2
	Expected Utility Completion Cost Risk k_h/k_v =10	3
	Expected Utility Completion Cost Risk k_h/k_v =100	5
Stochastic	Expected Utility Completion Cost Risk k_h/k_v =1000	7
	Expected Utility Completion Cost and Reservoir Risk	5

Table 5.19. Aspect Ratio 1

	Aspect Ratio 1	#of fractures
	Expected NPV k_h/k_v =1	2
	Expected NPV k_h/k_v =10	3
	Expected NPV k_h/k_v =100	4
Deterministic	Expected NPV k_h/k_v =1000	5
Stochastic		
	NPV -Reservoir Risk	4

Table 5.20. Fracture Height Uncertainty

	Aspect Ratio Uncertainty	#of fractures
	Expected NPV k_h/k_v =1	2
	Expected NPV k_h/k_v =10	4
	Expected NPV k_h/k_v =100	5
Stochastic	Expected NPV k_h/k_v =1000	5
	Conditional NPV –Reservoir Risk	4
	Expected Utility k_h/k_v =1	2
	Expected Utility k_h/k_v =10	4
	Expected Utility k_h/k_v =100	5
	Expected Utility k_h/k_v =1000	6
	Conditional Expected Utility –Reservoir Risk	5

CHAPTER VI

HYDRAULIC FRACTURE OPTIMIZATION: HORIZONTAL WELLS

The optimization of a horizontal well with multiple transverse fractures was next

formulated as a mixed-integer, nonlinear, two-stage stochastic program with full recourse.

The well length, number of fractures, and fracture dimensions were used as decision

variables. The well length was a continuous variable while the number of fractures was an

integer value. The first-stage decision was the length of the horizontal well. The second-

stage decisions were the number and dimensions of multiple transverse fractures. There

was initial uncertainty in the permeability before the well was drilled. After the well was

drilled, but before it was fractured, the uncertainty was revealed. This assumption is

natural, as during the drilling process core samples may be collected and well logs may be

run to deduce permeability. The objective was to maximize the expected NPV and

subsequently the expected utility.

Deterministic Problem

Before solving the stochastic program it is imperative to formulate the underlying

deterministic program. In this case it consisted of the optimization of a horizontal well

with multiple transverse fractures with certainty in all parameters and constraints. For this

analysis, we assumed that there was a constant budget constraint linking the drilling and

completion costs. The premise of this problem was to find the optimum tradeoff between

horizontal well length, number of fractures, and fracture dimensions, all coupled under

economic constraints. We hypothesized that resources (money) spent on drilling longer laterals can be better allocated on fracturing and vice versa. At the extreme, it was possible that all the resources could be spent on drilling—leaving no capital for fracturing—or almost all resources could be spent on fracturing.

This problem falls under the larger category of mixed integer nonlinear programming (MINLP). *Mixed integer* comes from the fact that decision variables are mixed (some have continuous values, others integer values). For this case, the well length was continuous in a given interval. Although this may not be entirely true as drillpipe length and production tubing may be discrete values, for all practical purposes this assumption is valid. However, the number of fractures has an integer value. The problem is considered nonlinear as the objective function and constraints contain nonlinear functions with respect to the decision variables. This is true both for the productivity of the well/fracture configuration and the associated costs.

Generally, the solutions of mixed-integer, nonlinear programs are complex and require numerical optimization. Analytical gradient approaches cannot be applied as the integer variables impose nondifferentiability in the objective function. Purely probabilistic methods such as genetic algorithms, particle swarm algorithms, or simulated annealing optimizations do not guarantee global optimization and may require unnecessary calculations. Direct-search methods such as the Nelder-Mead simplex method seem attractive, but they may have computational issues. However, instead of relying on pre-

coded, standard optimization packages, this problem can be readily solved by the *branch-and-bound* technique.

The branch-and-bound technique is a nonheuristic global optimization method that uses bounding to constrain the search space where local optimization or enumerations can be employed. The branch-and-bound method revolves around partitioning the feasible region into mutually exclusive sets (branching), determining provable upper and lower bounds (bounding) on the objective function for each set, and then terminating (fathoming) suboptimal solution sets based on the upper and lower bounds. No further calculations are done on sets that have been fathomed, vastly reducing the search space and, correspondingly, the actual evaluation burden. The strength of the branch-and-bound method is the ability to remove en masse large sets of suboptimal solutions. The weakness in the method is that it can lead to complete enumeration if the bounding fails.

Constraints

For any mixed-integer problem where enumeration (at some point) is required, additional constraints actually improve algorithmic performance by reducing the feasible domain. For this purpose economic, operational, and physical constraints were considered for the dual purpose of achieving a more realistic design and to reduce the computational burden.

Economic Constraints

For this optimization, as mentioned above the total capital available for drilling and completing was directly connected: the total capital less the capital spent on drilling was spent on completing. No leftover capital was allowed. This constraints ensured convexity in the objective function.

Operational Constraints

The main operational constraint in this optimization was the proppant mass per stage allowed. At high injection velocity the proppant (especially bauxite) exhibits abrasive behavior, damaging the service tools and completion hardware. Currently,[1] there is a mechanical limit on the amount of proppant that is pumped through the tool as well as the frac sleeve. This limit is estimated at a 750,000- to 1 million-lbm/sleeve. For this work, no more than 1 million lbm of proppant was allowed per stage.

Physical Constraints

Fracture Height Growth

For vertical fractures extending from a horizontal wellbore, radial (penny shape) fractures can be reasonable assumed. This leads to an aspect ratio constraint of

$$w_x = w_z \quad \text{..} \quad (6.1)$$

---

[1] Private Conservation with Haliburton Completion Engineer

Although this assumption is a simplification of the actual fracture propagation profile, in practice fracture design engineers everywhere use it, either explicitly or implicitly (in the form of "model calibration" for a given area).

Minimum Fracture Spacing:

During the process of hydraulic fracturing there is a reorientation of the in situ stress around the propped fracture. This occurs because the imposed stress perpendicular to the fracture is larger then the imposed stress parallel to the fracture. This phenomenon may directly affect the growth of subsequent hydraulic fractures. Experience shows that the integrity of the individual fractures cannot be assured if they are placed too close.

Preliminary Analysis

Partial Penetration and Choke Skin

The productivity of a horizontal well with transverse fractures is significantly different from the productivity of a fractured vertical well. For a horizontal well with a transverse fracture the flow inside the fracture will not be linear. The flow will converges radially in the x-z plane to the wellbore. This radial convergence is a strong function of fracture geometry, particularly the fracture height. As the fracture height grows, the pressure drop due to convergence increases. Effectively this results in a non-productive part of the fracture.

The main parameter affecting fracture performance is the conductivity. Generally the fracture conductivity is defined with respect to the fracture half-length. However, for a transverse fracture, the vertical fracture conductivity must also be considered.

$$C_{fd,V} = \frac{2\,k_f\,w_{ave}}{k\,h_f}$$ .... (6.2)

As the fracture height increases, the vertical conductivity decreases, impeding productivity. This effect is exacerbated in higher-permeability reservoirs.

In chapter 5, full penetration was almost always favored over partial penetration for its effect of on productivity in vertical wells. Now, since the fracture experiences additional convergence pressure drop, the same cannot be said. As the fracture height increases, the effect of partial penetration is reduced, but the effect of convergence flow is increased. This phenomenon sets a limit on the expected productivity of a transverse fracture in a horizontal well. The productivity of a transverse fracture cannot ever reach the productivity of a fracture in a vertical well, if the same amount of proppant is used. In some cases it can be orders of magnitude less.

Dimensionless productivity versus vertical penetration ratio is given in Figs. 6.1 and 6.2 for several cases. Note the change in scale on the vertical axes.
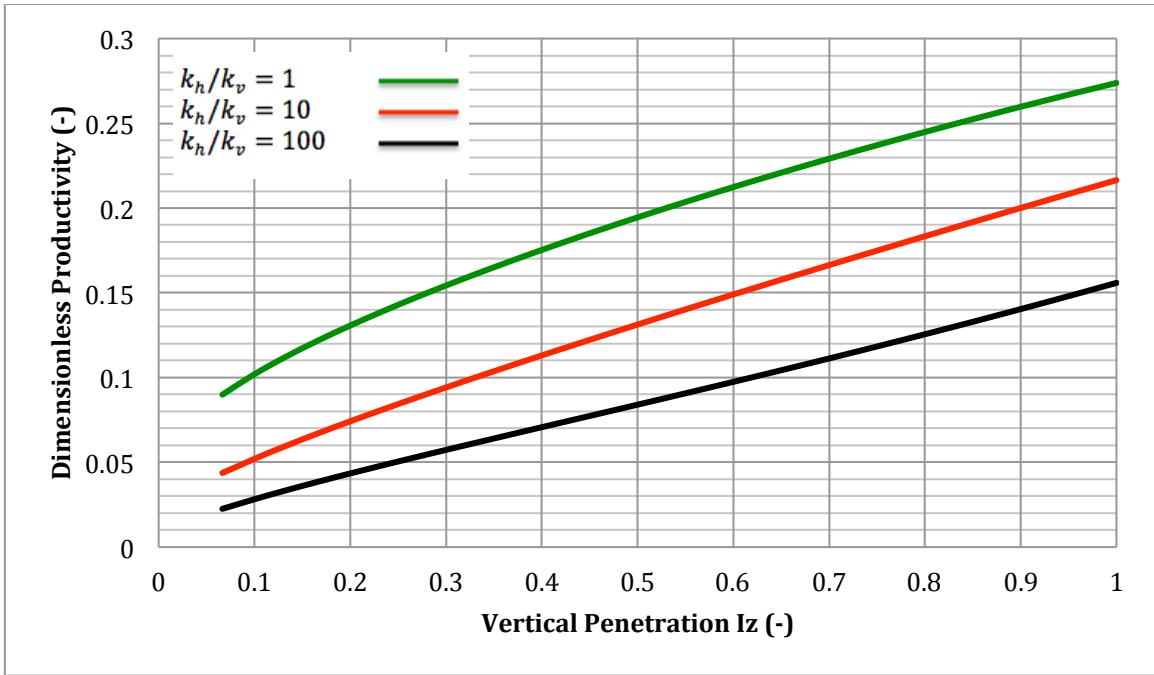
Fig. 6.1. Dimensionless productivity versus vertical penetration ratio for k_h=1 md
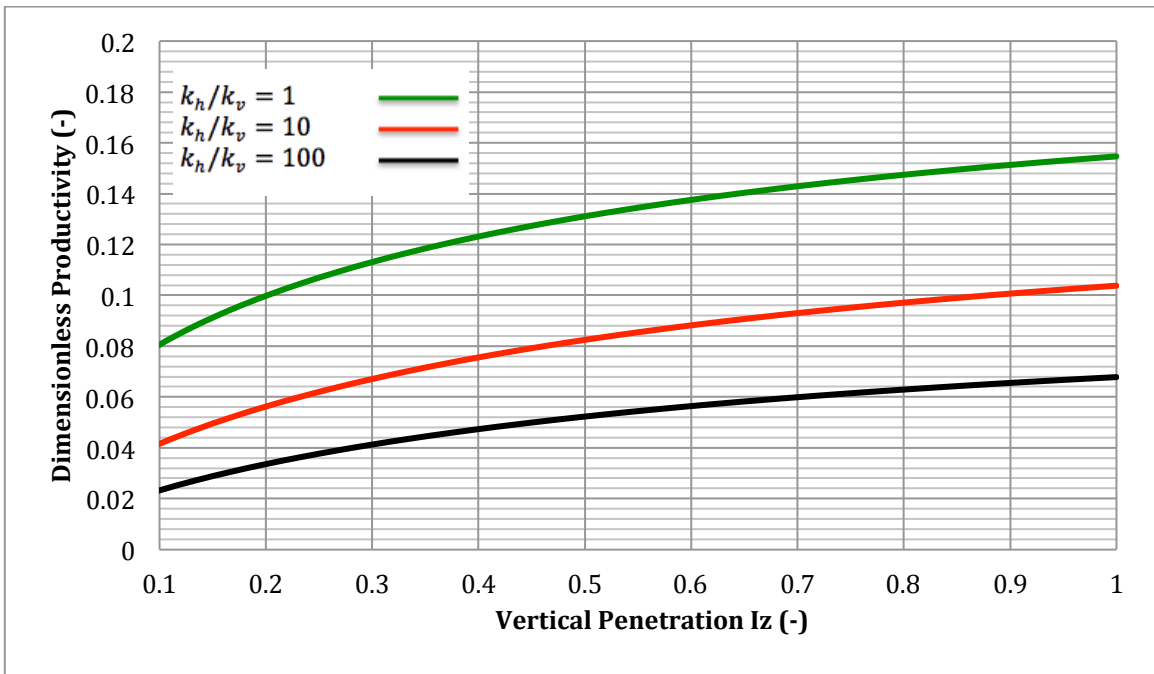
Fig. 6.2. Dimensionless productivity versus vertical penetration ratio for k_h=10 md

119

For the case of lower horizontal permeability $k_h = 1$ md, the productivity increases nearly linearly with vertical penetration. The fracture exhibits relatively high conductivity and the convergence pressure drop is rather small. However, for the higher horizontal permeability case $k_h = 10$ md, the fracture conductivity is lower, resulting in higher pressure loss due to convergence. Therefore, the increase in productivity for larger fracture heights is only moderate.

This effect is given in Fig. 6.3, which displays the dimensionless productivity versus vertical penetration ratio parametrically, for different horizontal permeabilities.
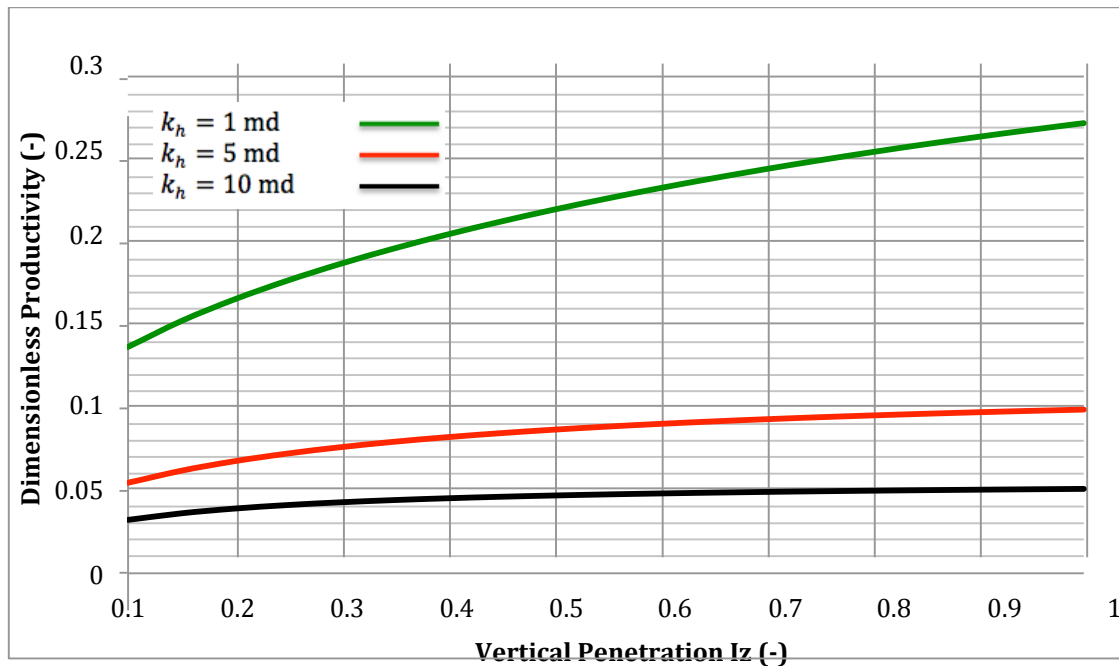
Fig. 6.3. Dimensionless productivity versus vertical penetration ratio for various permeabilities

For $k_h = 10$ md, the productivity increase with more penetration is minuscule. Note that for the above comparison, the fracture width and half-length remained constant. In terms of amount of proppant required, the difference between a vertical penetration of 1/10 and 1 is 10-fold. Injecting 10 times more proppant, solely for height growth, the relative productivity increased 2, 1.8, and 1.6-fold for $k_h = 10$ md, $k_h = 5$md, and $k_h = 1$ md, respectively. These increases with respect to the base case, $I_z = 0.1$, is given in Fig. 6.4. The fold of increase is defined as:

$$F = \frac{J_{dT,iz}}{J_{dT,iz=1/10}} \qquad\qquad\qquad\qquad\qquad\qquad\qquad\qquad\qquad (6.3)$$
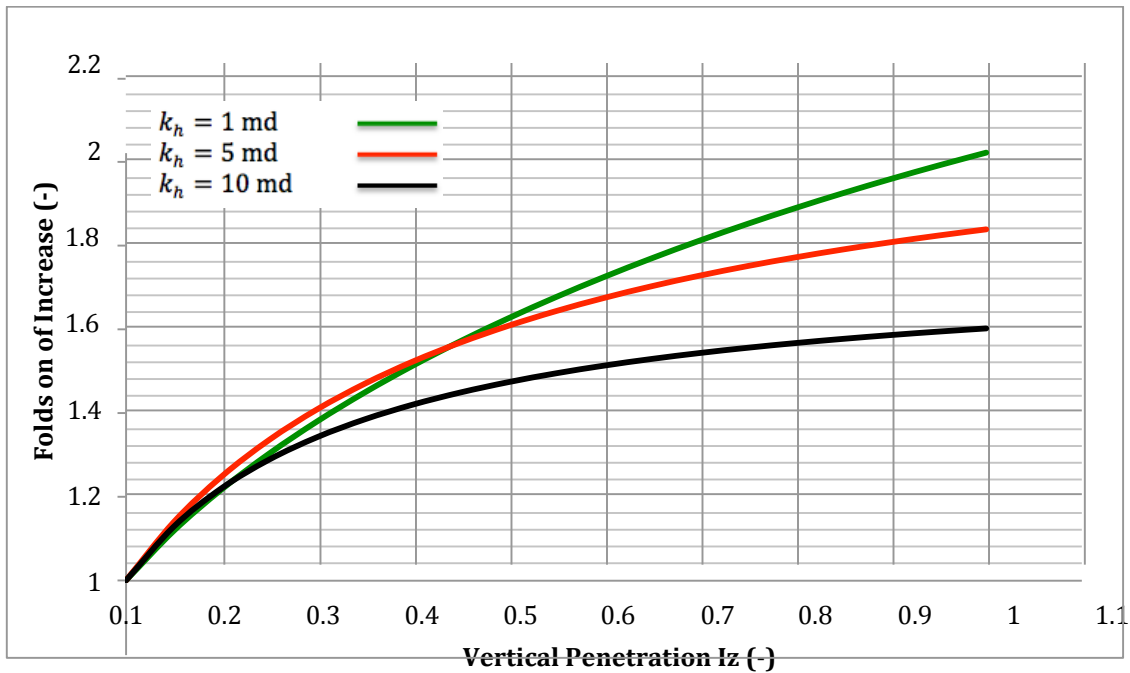
Fig. 6.4. Folds of increase versus vertical penetration ratio for various permeabilities

The lower permeability case experiences the greatest productivity increase with respect to fracture height penetration.

Constant Aspect Ratio

For fracture growth that follows an aspect ratio of one, the previous analysis was repeated with $I_z = I_x$ (Fig. 6.5).
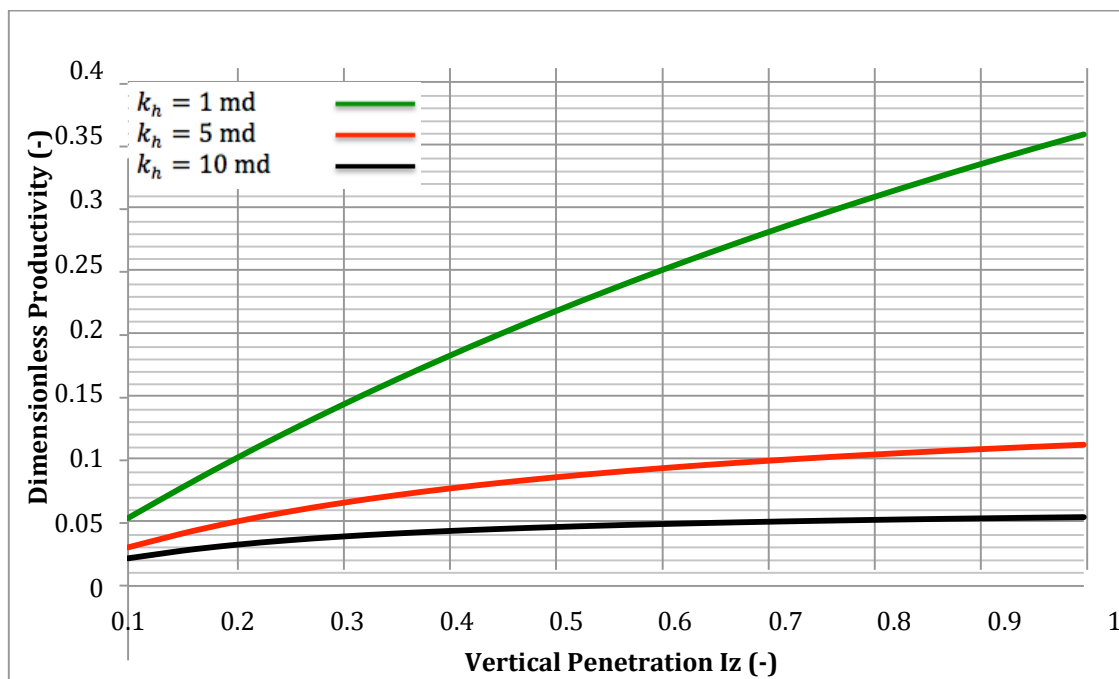
Fig. 6.5. Dimensionless productivity versus vertical penetration ratio for various permeabilities and *Ar*=1

Considering finite conductivity and convergence inside the fracture results in significantly different profiles of productivity vs. fracture penetration. For the case of lower

permeability, the productivity increases more rapidly and gains significantly more folds

on increase (Fig. 6.6). The folds of increase are given below and defined as

$$F = \frac{J_{dT,iz}}{J_{dT,iz=1/10}} \dots\dots\dots\dots\dots\dots\dots\dots\dots\dots\dots\dots\dots\dots\dots\dots\dots\dots\dots\dots\dots (6.4)$$
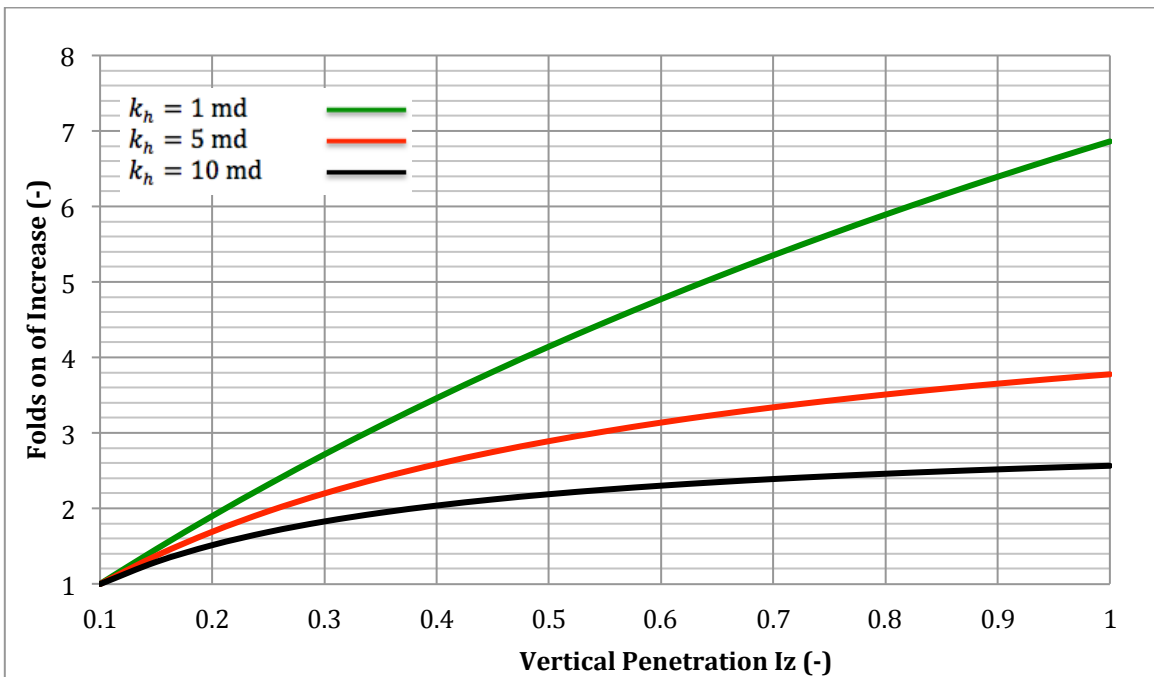
Fig. 6.6. Folds of increase versus vertical penetration ratio for various permeabilities and *Ar*=1

 The effect is more pronounced when fracture growth follows a fixed aspect ratio. The

lowest permeability formation gains the most productivity.

Number of Fractures

The next step in the analysis was to investigate how the number of fractures affects total productivity. For this analysis, we assumed that each fracture drains a uniform individual area. We also assumed that the fracture dimensions are constant. For a horizontal well with transverse fractures, the cumulative well productivity is the sum of the individual fracture productivities. For constant fracture dimensions and equal drainage area, the total well productivity is

$$J_{dT} = J_{dF} n_f \quad\text{...} (6.5)$$

For the case of a partially penetrating horizontal well, the fractures at the ends of the well will have a different drainage area and fracture location. The total well productivity can be expressed as a sum of the inner and outer fracture productivities.

$$J_{dT} = J_{dF,inner}(n_f - 2) + 2J_{dF,outer}(n_f - 2) \quad\text{...} (6.6)$$

For clarity, the first case investigated was the fully penetrating horizontal well with fully penetrating (both horizontal and vertical) uniform flux fracture. Fig. 6.7 displays the individual and total dimensionless productivity.
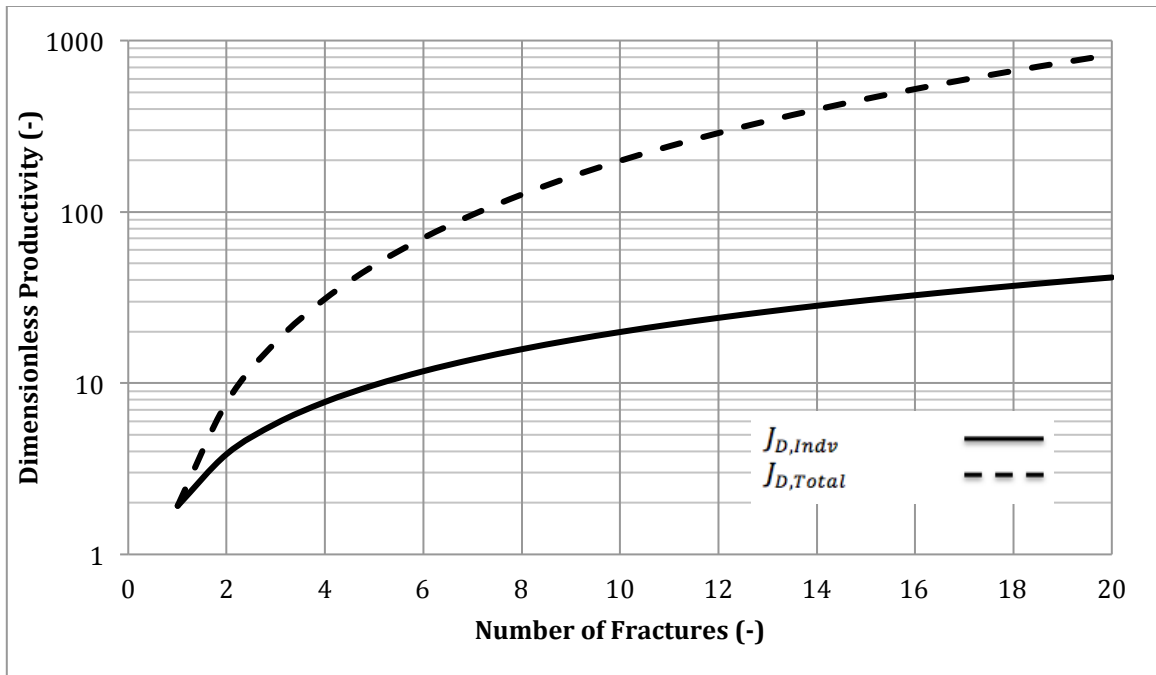
Fig. 6.7. Dimensionless productivity versus number of fractures for fully penetrating uniform flux fractures

As expected, the individual productivity increased linearly with number of fractures and the total productivity increased exponentially with number of fractures.

The next case investigated a fully penetrating horizontal well with partial-penetrating uniform flux fractures. Vertical penetration I_z and horizontal penetration I_x of the fractures were both set to ½.
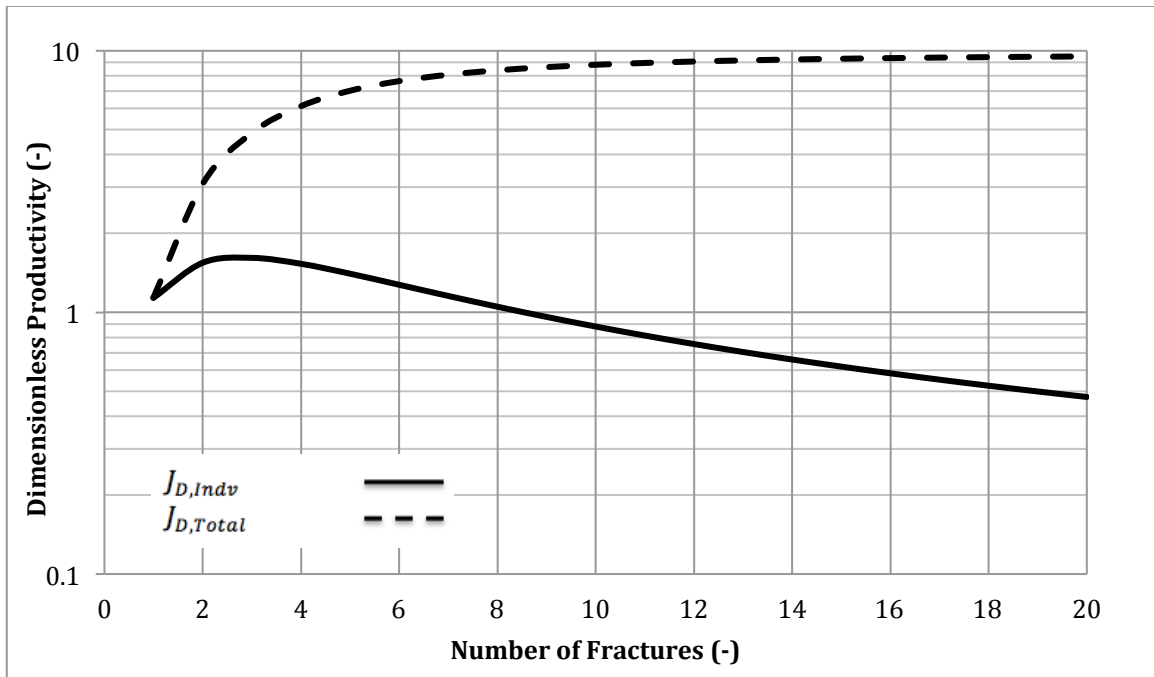
Fig. 6.8. Dimensionless productivity versus number of fractures for partially penetrating uniform flux fractures

As seen, the individual fracture productivity finds an optimum. The total productivity increases rapidly at first and then flattens, signifying diminishing returns on productivity. This result is very different from the uniform flux fully penetrating fracture case, in that the marginal return on increasing the number of fractures rapidly diminishes.

The above case provides insight but is still unrealistic for the Lower Tertiary. First, due to the high well cost, the expected drainage area must be large (on the order of 500 acres, if not more.) Furthermore, the vertical penetration is significant, as the formation thickness is estimated to be 1,000 ft to 1,500 ft and the vertical connectivity is limited by heavy

126

layering. For a 250-ft fracture with an aspect ratio of 1, the horizontal penetration is approximately I_x=1/8 and the vertical penetration is I_z=1/3. Additionally, due to the relatively large reservoir permeability, the fracture conductivity is crucial. Fig. 6.9 shows the results, for this situation, in which fracture conductivity and partial penetration were both considered.
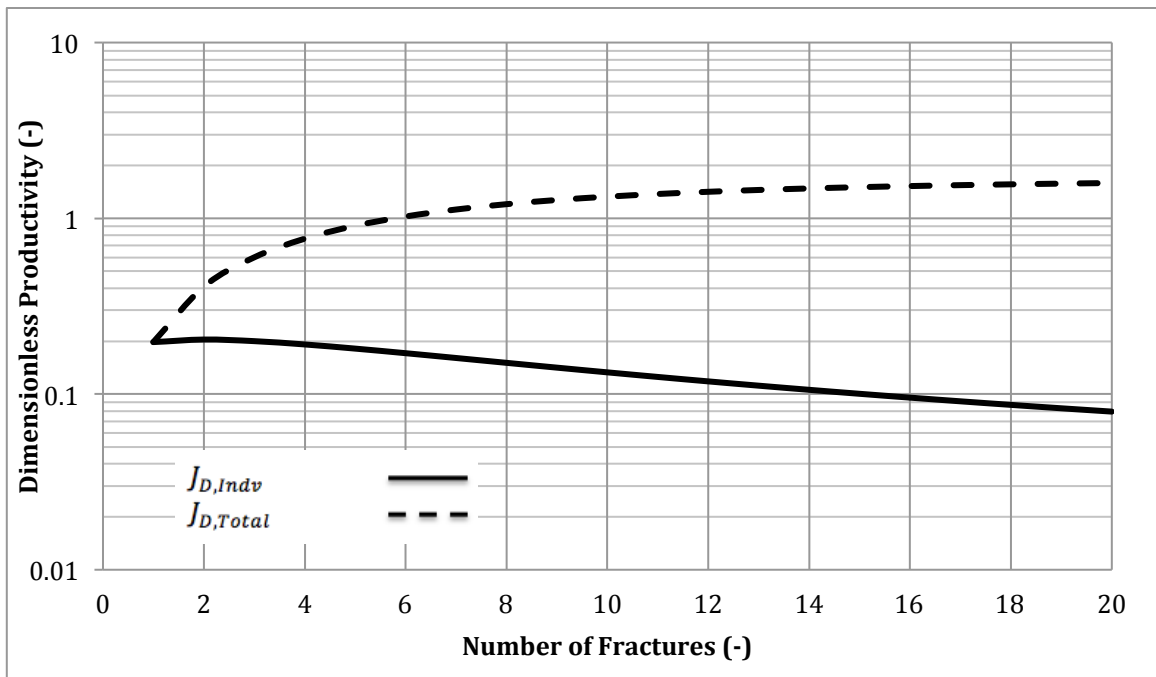
Fig. 6.9. Dimensionless productivity versus number of fractures for partially penetrating finite conductivity transverse fractures

As seen, the individual fracture productivity finds an optimum at 2 fractures. After this point, the individual productivity of the individual fractures diminishes. This time, however, the effect of finite conductivity and radial convergence are more pronounced, leading to a steeper decrease in fracture performance. Again, the total well productivity

127

quickly flattens with increasing number of fractures. The total productivity is an order of

magnitude less than in the previous case.

Fig. 6.10 shows the productivity versus number of fractures for different horizontal
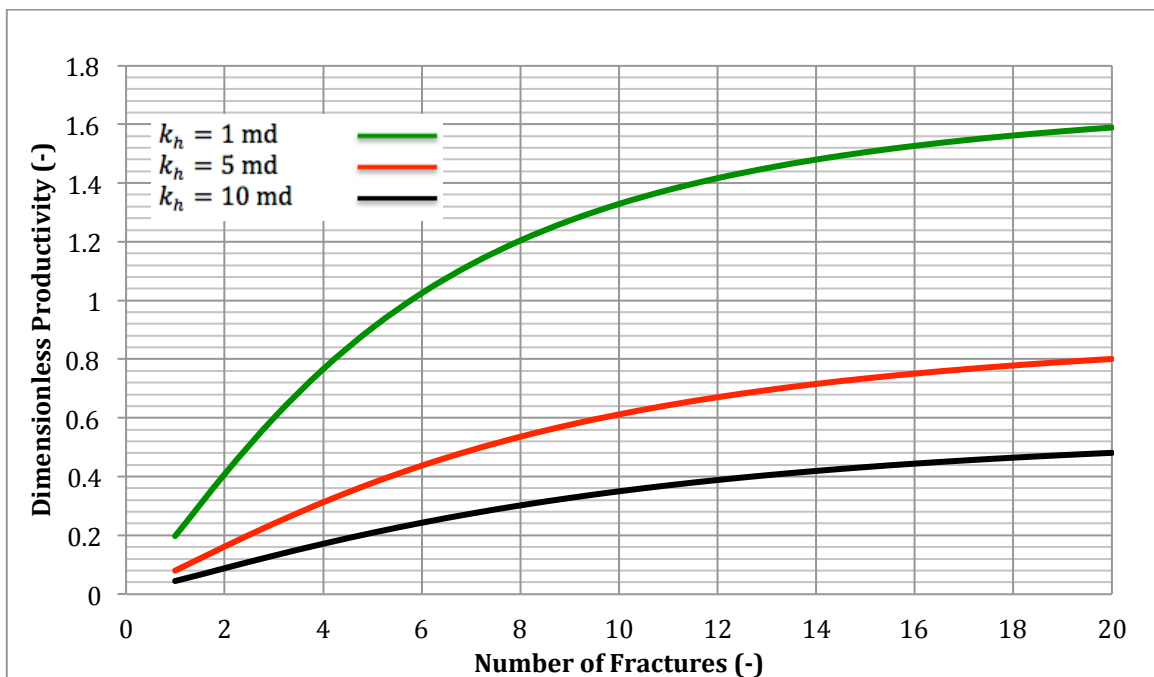
permeabilities.

Fig. 6.10. Dimensionless productivity versus number of fractures for partially penetrating finite conductivity transverse fractures for various permeabilities

As seen, in the case of lower horizontal permeability the total productivity is higher, but

the effect diminishes more rapidly than in the case of higher horizontal permeability.

Fig. 6.11 shows the folds of increase versus number of fractures for different horizontal permeabilities. The folds of increase are defined with respect to a single fracture.

$$F = \frac{J_{dT,n}}{J_{dT,1}} \quad \text{...} \quad (6.7)$$
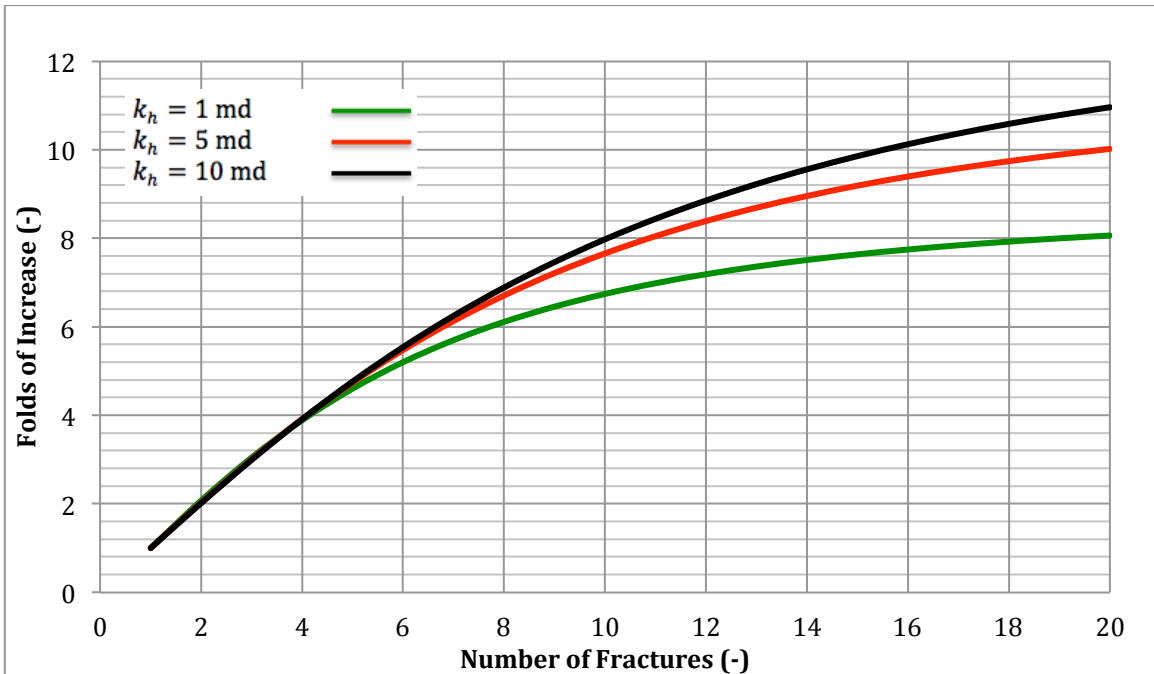
Fig. 6.11. Folds of increase versus number of fractures for partially penetrating finite conductivity transverse fractures for various permeabilities

Interestingly, while overall productivity is lower, the folds of increase are better when the horizontal permeability is higher.

Combining the above analysis of fracture performance versus fracture dimensions and fracture performance versus number of stages determines the total productivity of fracture performance for a given well length . In practical terms, this analysis determines how to

distribute a fixed proppant mass in terms of number of stages and dimensions of each fracture. In the extremes, it is possible to create a single large fracture or an infinite number of small fractures. The optimum design will depend on reservoir properties, on proppant properties, and on constraints.

Fig. 6.12 shows the total wellbore productivity versus number of fractures. However, the number of fractures is directly linked to proppant mass available, and thus the number of stages sets the fractures dimensions.

$$M_{p,\text{per fracture}}= \frac{M_{p,\text{total}}}{N_f} \quad\text{..}\quad (6.8)$$

$$M_{p,\text{per fracture}}= 2x_f w_f h_f \ (1-\phi_p)\rho_p \quad\text{..}\quad (6.9)$$

$$M_{p,\text{total}} = N_f 2x_f w_f h_f \ (1-\phi_p)\rho_p \quad\text{..}\quad (6.10)$$

Various horizontal permeabilities result in distinct optimum configurations with respect to number of fractures and dimensions of the individual fractures. For the $k_h = 1$ md case, the optimum number of fractures is $N_f = 8$ with $2x_f = h_f = 275$ ft. For the $k_h = 5$ md case, the optimum number of fractures is $N_f = 16$ with $2x_f = h_f = 175$ ft. For the $k_h = 10$ md case, the optimum number of fractures is $N_f = 23$ with $2x_f = h_f = 135$ ft.
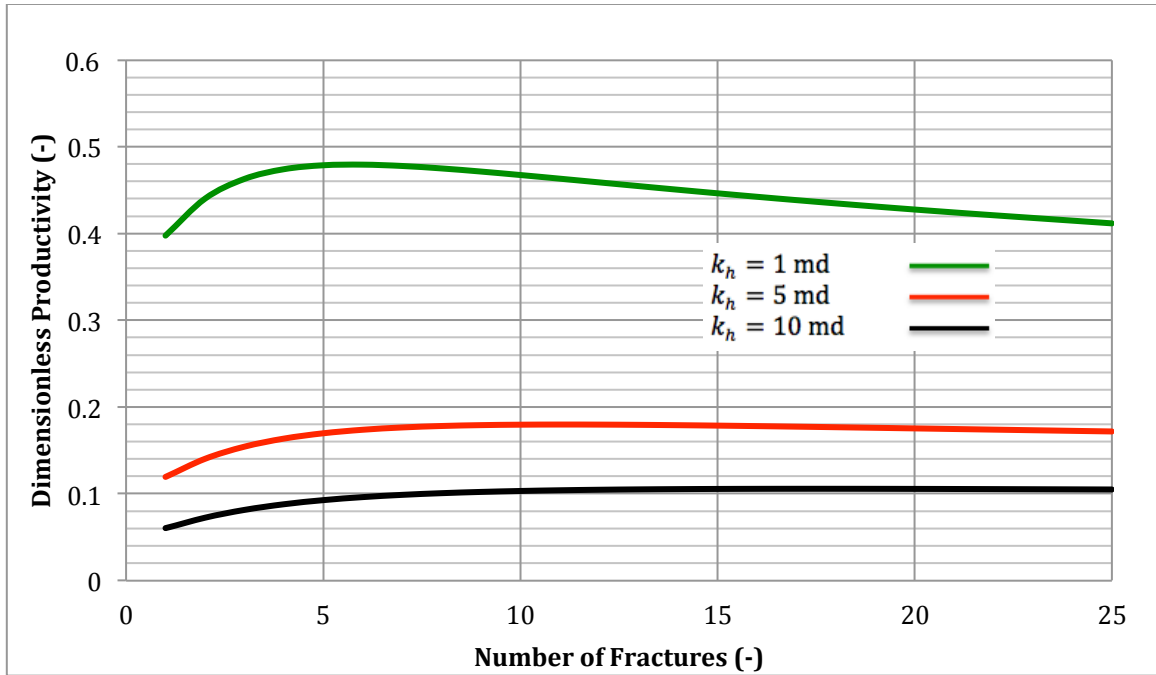
Fig. 6.12. Dimensionless productivity versus number of fractures and fracture penetration ratio for partially penetrating finite-conductivity transverse fractures for various permeabilities

Due to the difference in total productivity, the scale in Fig. 6.12 does not easily portray the optimum values for the cases $k_h = 5$ md and $k_h = 10$ md. Fig. 6.13 shows the folds of increase with respect to number of fractures and the optimums are easier to recognize. The folds of increase are defined as

$$F = \frac{J_{dT,n}}{J_{dT,1}} \quad \text{...} \quad (6.11)$$
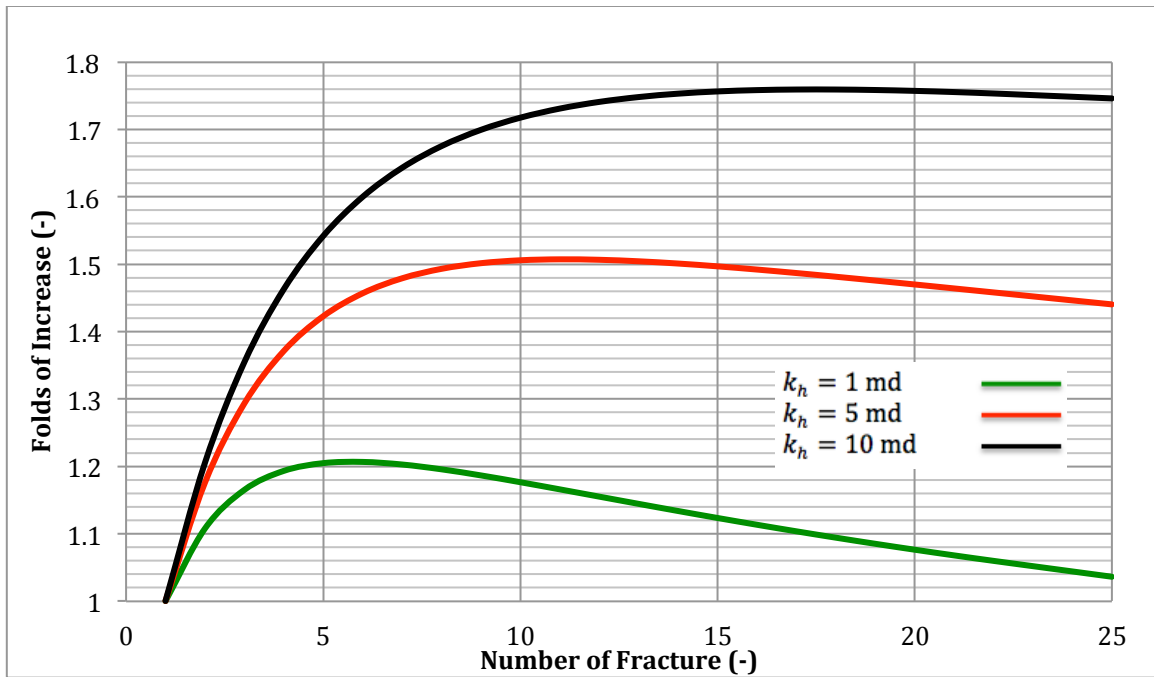
Fig. 6.13. Folds of increase versus number of fractures and fracture penetration ratio for partially penetrating finite-conductivity transverse fractures for various permeabilities

This analysis provides the primary insight for optimal design in terms of the number and dimensions of individual fractures. In summary some general remarks can be made:

- Increasing fracture dimensions: lower-permeability formations experience greater folds of increase

- Increasing number of stages: higher-permeability formations experience greater folds

Wellbore Length and Fracture Configuration Optimization

The next step in the analysis was to add the effect of wellbore length. For this analysis, we assumed that the wellbore length and fracture costs are directly linked. In other words, resources (capital) are spent on a combination of drilling and completing. Thus, the drilling cost is a function of wellbore length and increases with length. Similarly, the fracturing cost is a function of the mass of proppant injected into the formation and increases with proppant mass.

Furthermore, the drilling cost increases linearly with wellbore length. Admittedly, this is a simplification, but it captures the main effect. This assumption also implies a discount in drilling rig cost from multiwell contracting.

The fracturing cost also increases linearly with the proppant mass. Again, this assumption may not be entirely valid, as individual stimulation vessels have a certain capacity resulting in a piecewise behavior in terms of cost. Also, hydraulic horsepower and fracturing fluid requirements tend to bias the overall cost behavior toward exponential dependence on injected proppant mass. These issues can be handled easily by considering piecewise linear cost functions if the detailed information is at hand.

Mathematically the optimization follows:

$$\max NPV[W_L, N_f, w_x, w_y, w_z]$$

$$\frac{W_L}{N_f} = C_1$$

$$w_x w_z = C_2$$

$$w_y = C_3$$

$$w_x w_y w_z = C_4$$

$$c_1 W_L + c_2 N_f w_x w_y w_z = C_5 \quad ....(6.12)$$

Example: Budget 500 Million

In this analysis the budget was set to \$500 million (including allocated platform capital expenditure, CAPEX). Figs. 6.14 to 6.17 show wellbore length versus NPV for various permeability cases. Tables 6.3 and 6.4 report the well length, optimum number of fractures, half-length, inner fracture spacing, and NPV.

For various permeabilities there is a clear optimum combination of wellbore length, number of fractures, and fracture dimensions. A general trend is observed: increasing the well length results in an increasing number of fractures. For the low-permeability case ($k_h = 1$ md), the optimum NPV corresponds to a well length of 3,989 ft with 8 fractures.
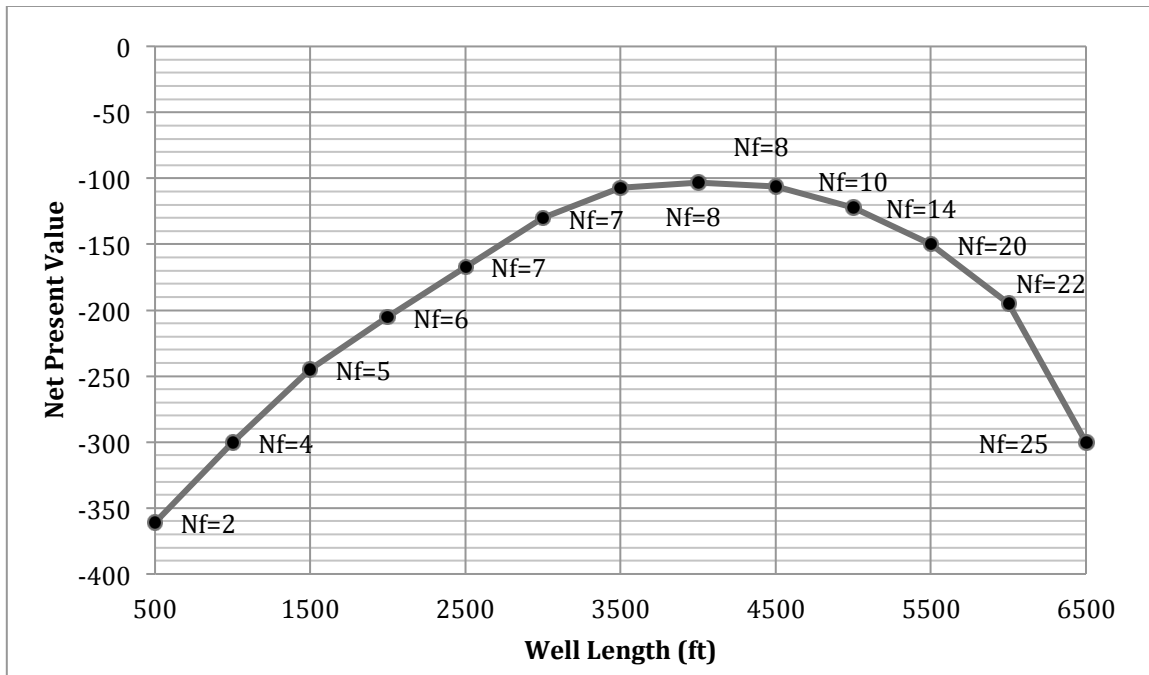
Fig. 6.14. NPV versus number of fractures and well length for k_h=1 md

Table 6.1. Optimization Results k_h=1 md: Well Length, Number of Fractures, and NPV

Well Length (ft)	Opt # of Fractures	Half Length(ft)	Fracture Spacing (ft)	NPV ($mm)
500	2	377	500	-361
1000	4	377	500	-300
1500	4	377	500	-245
2000	5	377	500	-205
2500	6	377	500	-167
3000	7	377	500	-130
3500	7	359	583	-107
4000	8	308	571	**-103**
4500	8	278	642	-106
5000	10	218	555	-122
5500	14	166	423	-150
6000	20	195	315	-195
6500	25	43	254	-300
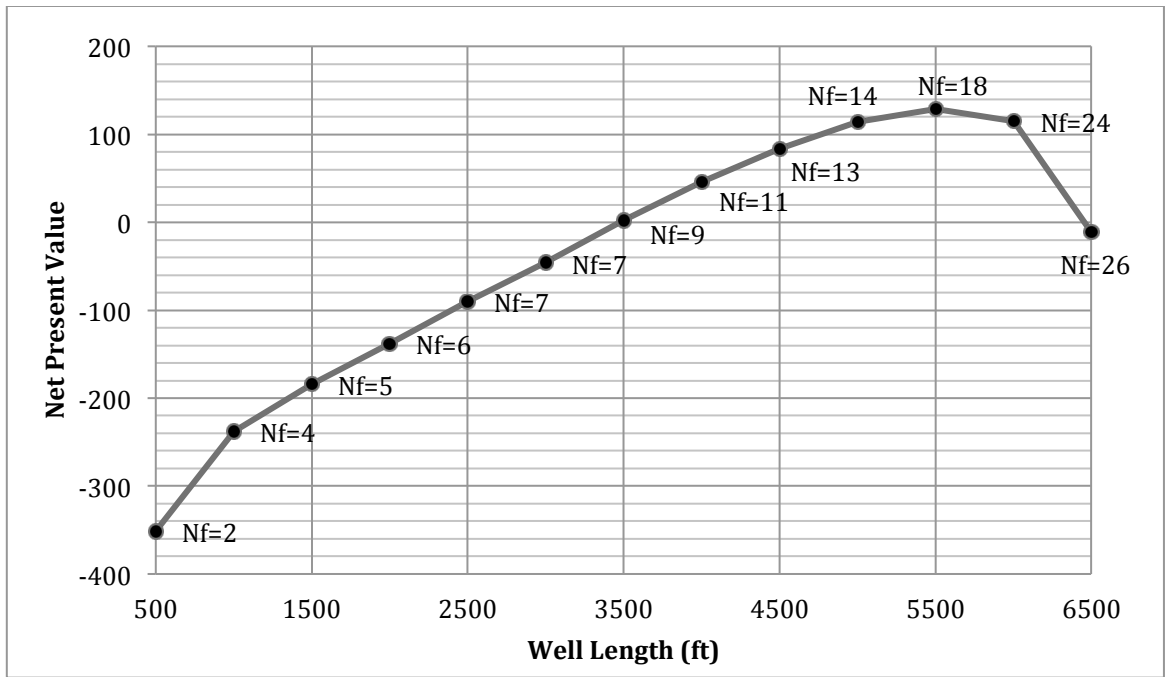
Fig. 6.15. NPV versus number of fractures and well length for k_h=5 md

Table 6.2. Optimization Results, k_h=5 md: Well Length, Number of Fractures, and NPV

Well Length (ft)	Opt # of Fractures	Half Length (ft)	Fracture Spacing (ft)	NPV ($mm)
500	2	377	500	-351
1000	4	377	500	-238
1500	4	377	500	-184
2000	5	377	500	-138
2500	6	377	500	-90
3000	7	377	500	-46
3500	9	317	437	1.9
4000	11	263	400	46
4500	13	218	375	84
5000	15	178	357	114
5500	18	126	323	**129**
6000	24	89	315	115
6500	26	43	254	-11
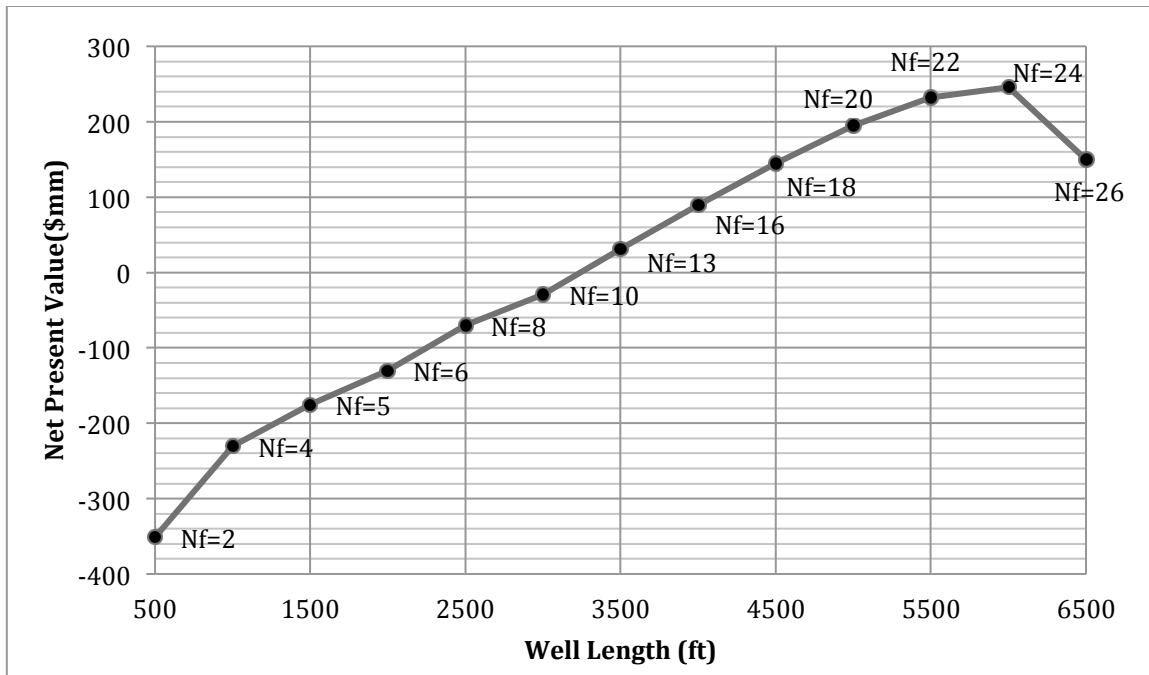
Fig. 6.16. NPV versus number of fractures and well length for k_h=10 md

Table 6.3. Optimization Results, k_h=10 md: Well Length, Number of Fractures, and NPV

Well Length (ft)	Opt # of Fractures	Half Length (ft)	Fracture Spacing (ft)	NPV ($mm)
500	2	377	500	-345
1000	4	377	500	-230
1500	5	377	500	-175
2000	6	377	500	-130
2500	8	377	500	-70
3000	10	377	500	-29
3500	13	263	291	31
4000	16	218	266	90
4500	18	185	266	145
5000	20	254	264	195
5500	22	123	261	232
6000	24	89	260	**246**
6500	26	43	254	155

Table 6.4. Deterministic Optimization Results

Permeability (md)	Opt. Well Length	Opt # of Fractures	Opt Half Length (ft.)	NPV ($mm)
1	3989	8	328	-100
5	5580	19	124	130
10	5921	23	97	246

Increasing permeability shifts the optimal values to longer wellbore lengths and more but smaller fractures. For $k_h = 5$ md and $k_h = 10$ md, the optimal well length and number of stages are 5,580 ft. and 5,921 ft, and the number of fractures is 19 and 23, respectively. These observations are consistent with the preliminary analysis in that the lower-permeability formation benefits more from increasing fracture size while the higher-permeability formation benefits more from increasing the number of fractures. However, from the preliminary analysis alone, the effect of wellbore length couldn't be deduced. This analysis indicated that the optimal number of fractures and well length are inherently linked. This result warrants further investigation.

Recalling the constraint of minimum fracture spacing of 250 ft, we observed that the optimal number of fractures is well below the admissible number for $k_h = 1$ md. However, for the case of $k_h = 10$ md, the optimal number of fractures is limited by the imposed constraint (the constraint becomes sharp.) If rock mechanical constraints were ignored, this effect would shift the optimal scenario towards even more but smaller fractures. The horizontal well with transverse fractures starts to "look" like a horizontal well with a larger wellbore. This effect is the result of the relatively low fracture

conductivity and radial convergence in higher-permeability formations. When the horizontal permeability is reduced, the fracture conductivity is higher and the number of fracture stages and fracture dimensions call for a unique optimum configuration where the constraints are not sharp.

The effect of the maximum proppant per stage is also interesting. The maximum proppant per stage corresponds to a fracture half-length of 377 ft. This, combined with the minimum fracture spacing constraint, severely limits the NPV of short wellbores, and a situation arises when not all the proppant is used but the budget is already spent. In these situations, the actual NPV may be a bit higher (if some of the costs could be saved). Nevertheless, such phenomena usually signify an unfavorable set of conditions, questioning the rationale for the whole project.

Branch-and-Bound Algorithm

To efficiently determine optimal wellbore length and fracture configurations, a branch and bound scheme was developed. The method revolves around maintaining upper and lower bounds for the number of fractures and well length. A modified golden-section search algorithm was implemented as the one-dimensional subspace search technique. The scheme works as follows:

- Prescreen phase 1: This prescreen phase eliminates wellbore and fracture configurations that do not meet the system constraints. This is used to eliminate wellbore fracture configurations in which the number of fractures exceeds the

minimum spacing requirement or the proppant mass per fracture is larger than the specified constraint.

- Prescreen phase 2: This prescreen phase eliminates wellbore and fracture configurations that can be determined as suboptimal without a production forecast. For instance, there is no need to test configurations with n-1 fractures for a given wellbore length, if at least n full fractures will exhaust the available budget.

- Main Phase: After the prescreening has determined a feasible set of solutions, the golden-search algorithm is implemented with respect to well length. For each well length, a suboptimization for number and dimensions of the fractures is undertaken. To increase the optimization efficiency (by applying petroleum engineering considerations), the bound on the numbers of fractures is simultaneously updated, as the well length is. In general, longer well lengths require a higher number of fractures if they are considered to be optimal candidates. If the lower bound on the well length is increased, the lower bound on number of fractures is simultaneously increased to the latest suboptimal number of fractures. If the upper bound on the well length is decreased, then the upper bound on the number of fractures is simultaneously decreased in a similar manner. To ensure no candidates are eliminated light handedly, fuzzy logic is implemented and, depending on the exact well length, the bounds are slightly relaxed with regard to the existing best suboptimum.

Stochastic Optimization Reservoir Uncertainty

In the stochastic optimization, the objective function was the maximization of expected NPV. The random variable in this optimization is the horizontal permeability. For this optimization, two different scenarios were analyzed. The first scenario was simple recourse, in that the uncertainty in permeability was only revealed after all decisions had been made. This scenario was similar to the optimization of the vertical well. The second scenario was full recourse, in that after the first-stage decisions had been made, the uncertainty was revealed, and second stage could be optimized. In this case, the first stage decisions corresponded to well length and the second stage decisions were the number of fractures. Uncertainty in permeability was revealed after the first stage (well drilling), but before the second stage (well fracturing). The goal was to find the optimal well length and number of fractures to optimize expected NPV.

$$\max E_{kh}[NPV(W_L, N_f, w_x, w_y, w_z)]$$

$$\frac{W_L}{N_f} = C_1$$

$$w_x w_z = C_2$$

$$w_y = C_3$$

$$w_x w_y w_z = C_4$$

$$c_1 W_L + c_2 N_f w_x w_y w_z = C_5$$

$$k_h(\omega) = \{1, 5, 10\}$$

$$\omega = \{\tfrac{1}{3}, \tfrac{1}{3}, \tfrac{1}{3}\} \quad \dotfill (6.13)$$

The permeability values and associated probabilities are given in Table 6.5.

Table 6.5. Probabilistic Inputs

Permeability (md)	Probabilities
1	1/3
5	1/3
10	1/3

The first step in stochastic programming is to calculate the *expected value of perfect information*, which is a metric to judge the (negative) value of uncertainty. For this case, the expectation of the optimal NPVs (determined above) were used to determine the EVPI (Table 6.6).

Table 6.6. Optimization Results: Expected Value of Perfect Information

Permeability (md)	1	5	10	Expected
NPV	-100	130	246	91

The next step in the analysis is to determine the mean-value solution. The mean value of permeability corresponds to 5.33 md. Performing a deterministic optimization (similar to the procedure above) results in an NPV of $138 million, approximately 1.5x higher than the expected value associated with perfect information (Table 6.7).

Table 6.7 Optimization Results: Mean Value Solution

Permeability (md)	Opt Well Length	Opt # of Fractures	Opt Half Length (ft)	NPV ($mm)
5.33	5580	19	126	138

However, the NPV calculated above may not be realistic. The key idea of stochastic

programming is that the deterministic NPV corresponding to the average permeability

always overestimates the expected value. Using the same design parameters, the NPV for

each permeability realization was calculated and the expected NPV was found.

Table 6.8. Optimization Results: Expected NPV

Permeability (md)	Well Length	# of Fractures	Half Length (ft)	NPV ($mm)
1	5580	19	126	-158
5	5580	19	126	129
10	5580	19	126	232
Expected				67.6

The NPV of $67.6 million represents the *mean-value solution*. This value is substantially

lower than the NPV calculated using the mean value of permeability and is lower than the

expected value of perfect information.

For the simple recourse optimization, the solution involved determining a *single* best set

of wellbore length, number of fractures, and fracture dimensions that will maximize

expected NPV. The optimal solutions and expected NPVs are given below. For simple

recourse, there was no change in design throughout the entire procedure; that is, the well

length and number of fractures were kept the same for all designs (Table 6.9).

Table 6.9. Optimization Results: Simple Recourse Solution

Permeability (md)	Well Length	# of Fractures	Half Length (ft)	NPV ($mm)
1	5510	20	120	-155
5	5510	20	120	129
10	5510	20	120	232
Expected				68.7

As shown, the expected NPV increases to $68.7 million, approximately1.5%.
Interestingly, the design favors a wellbore length that is less than the corresponding length
of the mean value solution, but has more fractures. The range of possible outcomes is
reduced by this method, decreasing the worst-case scenario by almost $3 million. Note
that for the simple recourse optimization, the design parameters are a single set.

Although the above design improved expected NPV, it did not address the realization of
uncertainty. For the full recourse solution, we took into account, that after a well is drilled
the permeability is known to a better extent, and the design can be altered. The goal was
to determine the optimal well length that accounts for the future realization of uncertainty.
The results are given in Table 6.10.

Table 6.10 Optimization Results: Full Recourse Solution

Permeability (md)	Well Length	# of Fractures	Half Length (ft)	NPV ($mm)
1	5490	*13*	218	-149
5	5490	*19*	124	129
10	5490	*22*	119	233
Expected				71.1

As seen, the optimal well length is 5,490 ft, which is less than the corresponding number

in the mean-value solution and in the simple recourse solution. However, note that now

the number of fractures varies for each realization. The expected NPV from this result is

$71.1 million , which is approximately 5% better than the mean-value solution and 3%

better than the simple recourse solution. Furthermore, the range of possible outcomes is

reduced, limiting risk and improving expectations. The expected NPV less the mean-value

solution is the *value of the stochastic solution* representing the improvement of applying

stochastic programming; in this case, it amounts to $3.5 million (Table 6.11).

Table 6.11. Optimization Results: Summary

Solution	Mean Value	Simple Recourse	Full Recourse	EVPI	VSS
NPV (mm$)	67.6	68.7	71.1	91	3.5

Remarks

Applying the stochastic programming methodology will systematically increase expected

NPV when uncertainty exists. For this example, the stochastic methodology increased

expected NPV by 5%. Although not glamorous, consistently improving project

expectations by 5% might be the key to success. Furthermore, a by-product of this

analysis is that a dollar value can be associated to the specific information. The expected

value of perfect information is significantly higher than the mean-value and full recourse

solution. This difference represents the value that we could gain by eliminating

uncertainty. For this case, the value of uncertainty is nearly $24 million. The higher this

value, the more warranted are further exploration and appraisal. This value can be used

directly to quantify the benefit of risk reduction and may justify budget for further investigations (of geological, petrophysical, rock-mechanics, and similar nature.)

Another aspect emerging from this work is that of the benefit of flexible design. This is shown by the difference in the simple and full recourse results. By adapting the design as new information is revealed, better outcomes can be expected. In the simple recourse there was no realization of uncertainty (or it wasn't acted on), while in the full recourse there was. In this analysis, we assumed that the permeability became known after the well was drilled. Of course, this might not always be the case. But in general, there will be a significant *narrowing* of the probability distribution. The monetary difference between these two solutions (in the example, $2.4 million) may be used to justify the budget for gathering more data (from sources such as cores and logs) after the well has been drilled. The stochastic programming approach also appears to assign a *shadow value* to any information involved.

This methodology shows the importance of uncertainty analysis. In some cases the mean value solution will yield design parameters similar to the stochastic optimum; at other times, they will be significantly different. However, this can only be known after the stochastic analysis has been undertaken. A good start in any case is to determine the mean value and the expected value of perfect information. If the difference is small, no stochastic programming is needed. If the difference is large and the full recourse solution can significantly increase expectations, then no additional steps need to be taken. On the

other hand, if the difference is large, but the full recourse does not significantly improve

expectations, more information gathering might be the key to success.

CHAPTER VII

SUMMARY AND CONCLUSIONS

Summary

The primary purpose of this work was to develop a methodology for completion design under uncertainty in reservoir and economic parameters. In particular, this work focused on offshore hydraulic fracturing completions for thick, anisotropic reservoirs in the deepwater Gulf of Mexico Lower Tertiary play.

In this work we performed the following tasks:

- Confirmed and applied the method of distributed volumetric sources (DVS) for transient and pseudosteady-state production forecasts for various well-fracture configurations in an anisotropic formation.

- Applied the stochastic programming framework to hydraulic fracture design under physical (reservoir) and economic uncertainty.

- Formulated systematic risk analysis by application of utility theory.

- Formulated and solved the corresponding mixed-integer nonlinear optimization problem, in particular for horizontal wells, in regards to well length, number, and dimensions of transverse fractures.

- Developed a branch-and bound type technique to effectively find the optimum solution.

- Demonstrated the value of the stochastic solution and value of the perfect information in a high-risk offshore environment.

Conclusions

The application of the distributed volumetric source method, stochastic programming, and utility framework presented here systematically allows the completion engineer to optimally design wellbores, accounting for reservoir, physical, and economic risks.

- The distributed volumetric source is a fast, accurate, and consistent method to determine the transient and pseudosteady-state wellbore productivity and production profiles for a large number of fracture/well configurations pertinent to industry applications.
- Stochastic programming, with emphases on recourse, provides a powerful decision-making framework, yielding designs with higher expected value and quantifying the value of information (or loss of value due to the lack of information).
- The branch-and-bound algorithm can be adopted to solve the resulting optimization problems in an effective way, allowing the use of petroleum engineering knowledge to reduce computations.

Specific findings from this work follow:

- Fracture configuration optimization that considers both the transient and pseudosteady-state flow regimes and material balance will ultimately lead to better economic decisions than the original (simplified) unified fracture design approach.

- For a fractured vertical well:

    o When designing under reservoir uncertainty, more stages are favored.

    o When designing under cost uncertainty, fewer stages are favored.

- For a fractured horizontal well:

    o There is an optimal well length, number of fractures, and fracture geometry for a given budget.

    o Lower-permeability formations generally exhibit larger folds of productivity increase by increasing individual fracture dimensions.

    o Higher-permeability formations generally exhibit larger folds of productivity increase by increasing the number of stages.

Recommendations for Future Work

This work focused largely on proppant management and completion risks in the offshore environment. Water treatment, logistical, and surface facility constraints should be investigated in terms of offshore hydraulic fracturing.

Future work in stochastic programming for petroleum engineering should continue in the area of hydraulic fracturing. Multistage recourse optimization should be examined. One

150

possible extension is to use additional data (seismic monitoring and pressure fall off from previous stages of hydraulic fracturing treatment) to re-design upcoming stages.

Risk analysis for the horizontal well should be continued. More representative probability characterization for drilling and completion of the horizontal well must be obtained. Utility theory should be applied to economic, reservoir, fracture-height growth, and numerous other uncertainties.

The branch-and-bound algorithm (especially the bounding procedures within it) should be mathematically proven and improved upon. Applying basic petroleum engineering insight, instead of just relaying on computational power, may be more efficient in improving optimization robustness.

REFERENCES

Amini, Shahram, Peter P. Valkó. 2010. Using Distributed Volumetric Sources To Predict

    Production From Multiple-Fractured Horizontal Wells Under Non-Darcy-Flow

    Conditions (in English). *SPE Journal* **15** (1): pp. 105-115.

Begg, S.H., R.B. Bratvold, J.M. Campbell. 2001. Improving Investment Decisions Using

    a Stochastic Integrated Asset Model. Proc., SPE Annual Technical Conference and

    Exhibition, New Orleans, Louisiana.

Birchenko, Vasily M, Vasily Demyanov, Michael R. Konopczynski et al. 2008. Impact of

    Reservoir Uncertainty on Selection of Advanced Completion Type. Proc., SPE

    Annual Technical Conference and Exhibition, Denver, Colorado, USA.

Birge, J. R. 1982. The Value of the Stochastic Solution in Stochastic Linear-Programs

    with Fixed Recourse (in English). *Mathematical Programming* **24** (3): 314-325.

Birge, John R., François Louveaux. 2011. *Introduction to stochastic programming*, 2nd

    edition. New York: Springer series in operations research and financial

    engineering,, Springer.

Bratvold, Reidar B., J. Eric Bickel, Hans P. Lohne. 2009. Value of Information in the Oil

    and Gas Industry: Past, Present, and Future (in English). *SPE Reservoir*

    Evaluation & Engineering **12** (4): pp. 630-638.

Campbell, J. M., Robert A. Campbell, Stewart Brown. 1999. Measuring Strategic

    Investment Value. Proc., SPE Annual Technical Conference and Exhibition,

    Houston, Texas.

Cinco, H., F. Samaniego, N. Dominguez. 1978. Transient Pressure Behavior for a Well with a Finite-Conductivity Vertical Fracture (in English). *Society of Petroleum Engineers Journal* **18** (4): 253-264..

Cozzolino, John M. 1977. A Simplified Utility Framework For the Analysis of Financial Risk. Proc., SPE Economics and Evaluation Symposium, Dallas, Texas.

Cunha, Jose C S, Oswaldo M Mayer Moreira, Gabriel Henrique Azevedo et al. 2009. Challenges on Drilling and Completion Operations of Deep Wells in Ultra-Deepwater Zones in the Gulf of Mexico. Proc., SPE Annual Technical Conference and Exhibition, New Orleans, Louisiana.

Dantzig, G. B. 1955. Linear Programming under Uncertainty (in English). *Management Science* **1** (3-4): 197-206..

Dear III, S.F., R.D. Beasley, K.P. Barr. 1995. Use of a Decision Tree To Select the Mud System for the Oso Field, Nigeria (in English). *Journal of Petroleum Technology* **47** (10): 909-912.

Dietz, D. 1965. Determination of Average Reservoir Pressure From Build-Up Surveys *Journal of Petroleum Technology* **17**(8): 955-959

Dong, Zhenzhen, Stephen Holditch, Duane McVay. 2013. Resource Evaluation for Shale Gas Reservoirs. *SPE Economics & Management* **5** (1): 5-16.

Dusterhoft, Ronald Glen, Marshal Allen Strobel, Michael Szatny. 2012. An Automated Software Workflow To Optimize Gulf of Mexico Lower Tertiary Wilcox Sand Reservoirs. Proc., SPE International Symposium and Exhibition on Formation Damage Control, Lafayette, Louisiana, USA.

Esmaiel, Talal Ebraheem, Joost Clemens Heeremans. 2006. Optimization of the WAG Process Under Uncertainty in a Smart Wells Environment: Utility Theory Approach. Proc., Intelligent Energy Conference and Exhibition, Amsterdam, The Netherlands.

Ettehadtavakkol, Amin, Christopher J. Jablonowski, Larry Wayne Lake. 2011. Stochastic Optimization and Uncertainty Analysis for E&P Projects: A Case in Offshore Gas Field Development. Proc., Offshore Technology Conference, Houston, Texas, USA.

Everitt, R., W. T. Ziemba. 1979. 2-Period Stochastic Programs with Simple Recourse. *Operations Research* **27** (3): 485-502.

Goel, V., I. E. Grossmann. 2004. A stochastic programming approach to planning of offshore gas field developments under uncertainty in reserves. *Computers & Chemical Engineering* **28** (8): 1409-1429.

Gringarten,A.C, H. J. Ramey, R. Raghavan. 1974. Unsteady-State Pressure Distributions Created by a Well with a Single Infinite Conductivity Vertical Fracture (in English). *Society of Petroleum Engineers Journal* **14** (4): 347-360.

Guyaguler, B., R. N. Horne. 2004. Uncertainty assessment of well-placement optimization (in English). *Spe Reservoir Evaluation & Engineering* **7** (1): 24-32.

Haddad, Ziad, Michael B. Smith, Flavio Dias De Moraes. 2012. Designing Multistage Frac Packs in the Lower Tertiary Formation--Cascade and Chinook Project (in English). *SPE Drilling & Completion* **27** (1): pp. 50-64.

154

Haldorsen, Helge H., Elvind Damsleth. 1990. Stochastic Modeling (includes associated
 papers 21255 and 21299) (in English). *Journal of Petroleum Technology* **42** (4):
 404-412.

Hansotia, B. J. 1980. Stochastic Linear-Programs with Simple Recourse - the Equivalent
 Deterministic Convex Program for the Normal, Exponential, and Erlang Cases (in
 English). *Naval Research Logistics* **27** (2): 257-272.

Harrison, C. Glenn. 1982. Fishing Decisions Under Uncertainty (in English). *Journal of
 Petroleum Technology* **34** (2): 299-300.

Haugland, D., A. Hallefjord, H. Asheim. 1988. Models for Petroleum Field Exploitation
 (in English). *European Journal of Operational Research* **37** (1): 58-72.

Hughes, D.S., P. Murphy. 1988. Use of a Monte Carlo Method To Simulate Unstable
 Miscible and Immiscible Flow Through Porous Media. *SPE Reservoir
 Engineering* **3** (4): 1129-1136.

Jensen, J. L. W. V. 1906. On the convex functions and inequalities between mean values
 (in French). *Acta Mathematica* **30** (2): 175-193.

Jonsbraten, T. W. 1998. Oil field optimization under price uncertainty. *Journal of the
 Operational Research Society* **49** (8): 811-818. <Go to

Kabir, C. Shah, Sheldon B. Gorell, Maria E. Portillo et al. 2007. Decision Making With
 Uncertainty While Developing Multiple Gas/Condensate Reservoirs: Well Count
 and Pipeline Optimization (in English). *SPE Reservoir Evaluation & Engineering*
 10 (3): pp. 251-259.

Lach, Joseph R, Gavin Longmuir. 2010. Can IOR in Deepwater Gulf of Mexico Secure
        Energy for America? Proc., Offshore Technology Conference, Houston, Texas,
        USA.

Lewis, Jennifer, Simon Clinch, Dave Meyer et al. Exploration and appraisal challenges in
        the Gulf of Mexico deep-water Wilcox: Part 1—exploration overview, reservoir
        quality, and seismic imaging. Proc., 27th Gulf Coast Section SEPM , Houston,
        Texas, USA

Madansky, A. 1960. Inequalities for Stochastic Linear-Programming Problems (in
        English). *Management Science* **6** (2): 197-204.

Mangasarian, O. L. 1964. Nonlinear-Programming Problems with Stochastic Objective
        Functions (in English). *Management Science* **10** (2): 353-359.

Mangasarian, O. L., J. B. Rosen. 1964. Inequalities for Stochastic Nonlinear-
        Programming Problems (in English). *Operations Research* **12** (1): 143-&.

Mathur, Vinod. 2008. The Emerging Paleogene Play: Deepwater Gulf of Mexico. Proc.,
        Offshore Technology Conference, Houston, Texas, USA.

McKenna, C. J. 1986. *The economics of uncertainty*. New York, Oxford University Press.

Meyer, Bruce Roman, Robert Henry Jacot. 2005. Pseudosteady-State Analysis of Finite-
        Conductivity Vertical Fractures. Proc., SPE Annual Technical Conference and
        Exhibition, Dallas, Texas.

Mian, M. A. 2011. *Project economics and decision analysis*, 2nd edition. Tulsa, Okla.,
        PennWell Corp.

Mukherjee, Hemanta, Michael J. Economides. 1991. A Parametric Comparison of

    Horizontal and Vertical Well Performance (in English). *SPE Formation*

    Evaluation **6** (2): 209-216.

Newendor.Pd, P. J. Root. 1967. Risk Analysis in Drilling Investment Decisions (in

    English). *Journal of Petroleum Technology* **19** (9): 1168-&.

Newendorp, Paul D. 1978. *Petroleum economics and risk analysis*. London: Geological

    Society miscellaneous paper, Geological Society.

Newendorp, Paul D., John Schuyler. 2000. *Decision analysis for petroleum exploration*,

    2nd edition. Aurora, Colo., Planning Press.

Newman, A. B. 1936. Heating and cooling rectangular and cylindrical solids (in English).

    Industrial and Engineering Chemistry **28**: 545-548.

Ogier, Kenneth Scott, Ziad A Haddad, Oswaldo M Mayer Moreira et al. 2011. The

    World's Deepest Frac-Pack Completions Utilizing a Single-Trip, Multi-Zone

    System: A Gulf of Mexico Case Study in the Lower Tertiary Formation. Proc.,

    SPE Annual Technical Conference and Exhibition, Denver, Colorado, USA.

Ouyang, Liang-Biao. 2007. Uncertainty Assessment on Well Performance Prediction for

    an Oil Well Equipped With Selected Completions. Proc., Production and

    Operations Symposium, Oklahoma City, Oklahoma, U.S.A.

Ozdogan, U., R. N. Horne. 2006. Optimization of well placement under time-dependent

    uncertainty (in English). *Spe Reservoir Evaluation & Engineering* **9** (2): 135-145.

Prats, M. 1961. Effect of Vertical Fractures on Reservoir Behavior - Incompressible Fluid.

    Transactions of the Society of Petroleum Engineers of Aime **222** (2): 105-118.

Pratt, J. W. 1964. Risk-Aversion in the Small and in the Large (in English). *Econometrica* **32** (1-2): 122-136.

Raghavan, Rajagopal S., Chih-Cheng Chen, Bijan Agarwal. 1997. An Analysis of Horizontal Wells Intercepted by Multiple Fractures (in English). *SPE Journal* **2** (3): 235-245.

Raiffa, Howard, Robert Schlaifer. 1961. *Applied statistical decision theory*. Boston,: Studies in managerial economics, Division of Research, Graduate School of Business Adminitration, Harvard University.

Ramey,H.J., William M. Cobb. 1971. A General Pressure Buildup Theory for a Well in a Closed Drainage Area (includes associated paper 6563) (in English). *Journal of Petroleum Technology* **23** (12): 1493-1505.

Reed, Ronald L. 1972. A Monte Carlo Approach to Optimal Drilling (in English). *Society of Petroleum Engineers Journal* **12** (5): 423-438.

Romero, Diego J., Peter P. Valko, Michael J. Economides. 2002. The Optimization Of The Productivity Index And The Fracture Geometry Of A Stimulated Well With Fracture Face And Choke Skins. Proc., International Symposium and Exhibition on Formation Damage Control, Lafayette, Louisiana.

Shapiro, Alexander, Darinka Dentcheva, Andrzej P. Ruszczyński. 2009. *Lectures on stochastic programming : modeling and theory*. Philadelphia: MPS-SIAM series on optimization, Society for Industrial and Applied Mathematics : Mathematical Programming Society.

Tarhan, B., I. E. Grossmann, V. Goel. 2009. Stochastic Programming Approach for the Planning of Offshore Oil or Gas Field Infrastructure under Decision-Dependent Uncertainty (in English). *Industrial & Engineering Chemistry Research* **48** (6): 3078-3097..

Thambynayagam, R. K. Michael. 2011. *The diffusion handbook : applied solutions for engineers*. New York, McGraw-Hill.

Valko, P.P., S. Amini. 2007. The Method of Distributed Volumetric Sources for Calculating the Transient and Pseudosteady-State Productivity of Complex Well-Fracture Configurations. Proc., SPE Hydraulic Fracturing Technology Conference, College Station, Texas USA.

Valko, Peter P., Michael J. Economides. 1998. Heavy Crude Production from Shallow Formations: Long Horizontal Wells Versus Horizontal Fractures. Proc., SPE International Conference on Horizontal Well Technology, Calgary, Alberta, Canada.

Walls, Michael R. 1995. Corporate Risk Tolerance and Capital Allocation: A Practical Approach to Implementing an Exploration Risk Policy. *Journal of Petroleum Technology* **47** (4): 307-311.

Wattenbarger, Robert A., Ahmed H. El-Banbi, Mauricio E. Villegas et al. 1998. Production Analysis of Linear Flow Into Fractured Tight Gas Wells. Proc., SPE Rocky Mountain Regional/Low-Permeability Reservoirs Symposium, Denver, Colorado.

Wehunt, C. D. 2006. Well performance with operating limits under reservoir and completion uncertainties. *Spe Drilling & Completion* **21** (3): 200-211..

Wiltgen, Nick A. 2008. The Contradiction in the Lower Tertiary Deepwater GoM. Proc., SPE Annual Technical Conference and Exhibition, Denver, Colorado, USA.

Yarus, Jeffrey M., R. L. Chambers. 1994. *Stochastic modeling and geostatistics : principles, methods, and case studies*. Tulsa, Okla.: AAPG computer applications in geology, American Association of Petroleum Geologists.

Yu, O. Y., S. D. Guikema, J. L. Briaud et al. 2011. Quantitative decision tools for system selection in environmentally friendly drilling. *Civil Engineering and Environmental Systems* **28** (3): 185-208.

Zhang, Y., S. Srinivasan. 2005. Markov Chain Monte Carlo for Modelling Permeability Variations in Reservoirs. *Journal of Canadian Petroleum Technology* **44** (3).

APPENDIX

Table A.1. Economic Inputs for Horizontal Well:

Fixed CAPEX per well:	$250,000,000
Vertical Drilling Segment &Upper Completion	$150,000,000
Horizontal Drilling Segment	$15,000/ ft
Fracture Cost	$7.5/lbm proppant
Rig Rate	$1,000,000/day

Note that the fracture cost and drilling cost are all-inclusive, representing the entire

process and equipment.

Table A.2. Cost Calculation Factors

Corporate Tax Rate	35%
Royalty Rate	15%
Discount Rate	10%